MODELING BUILDING HEIGHT ERRORS IN

3D URBAN ENVIRONMENTS

A THESIS SUBMITTED TO

THE GRADUATE SCHOOL OF NATURAL AND APPLIED SCIENCES

OF

MIDDLE EAST TECHNICAL UNIVERSITY

BY

ÖZGE ERGİN

IN PARTIAL FULFILLMENT OF THE REQUIREMENTS

FOR

THE DEGREE OF MASTER OF SCIENCE

IN

GEODETIC AND GEOGRAPHIC INFORMATION TECHNOLOGIES

DECEMBER 2007

Approval of the thesis:

**MODELING BUILDING HEIGHT ERRORS IN
3D URBAN ENVIRONMENTS**

Submitted by **ÖZGE ERGİN** in partial fulfillment of the requirements for the degree of **Master of Science in Geodetic and Geographic Information Technologies Department, Middle East Technical University by,**

Prof Dr. Canan Özgen   _____
Dean, Graduate School of **Natural and Applied Sciences**

Assoc. Prof Dr. Şebnem Düzgün   _____
Head of Department, **Geodetic and Geographic Information Technologies Department**

Assoc. Prof Dr. Şebnem Düzgün   _____
Supervisor, **Geodetic and Geographic Information Technologies Department, METU**

Examining Committee Members:

Assoc. Prof. Nurünnisa Usul   _____
Civil Engineering Dept., METU

Assoc. Prof. Şebnem Düzgün   _____
Mining Engineering Dept., METU

Assoc. Prof. Zuhal Akyürek   _____
Civil Engineering Dept., METU

Assoc. Prof. Ayşegül Aksoy   _____
Environment Engineering Dept., METU

Assoc. Prof. Mahmut Onur Karslıoğlu   _____
Civil Engineering Dept., METU

Date: (06 December 2007)

I hereby declare that all information in this document has been obtained and presented in accordance with academic rules and ethical conduct. I also declare that, as required by these rules and conduct, I have fully cited and referenced all material and results that are not original to this work.

Name, Last name   : Özge Ergin

Signature   :

ABSTRACT

MODELING BUILDING HEIGHT ERRORS IN
3D URBAN ENVIRONMENTS

Özge Ergin

M.S. , Geodetic and Geographic Information Technologies

Supervisor   : Prof. Dr. Şebnem Düzgün

December 2007, 166 pages

A great interest in 3-D modeling in Geographic Information Technologies (GIS) has emerged in recent years, because many GIS related implementations, ranging from urban area design to environmental analysis require 3-D models. Especially the need for 3-D models is quite urgent in urban areas.

However, numerous applications in GIS only represent two-dimensional information. The GIS community has been struggling with solving complex problems dealing with 3-D objects using a 2-D approach. This research focused on finding most accurate method which is used for getting height information that is used in 3D modeling of man made structures in urban areas. The first method is estimating height information from floor numbers of the buildings data from municipal database systems. The second method is deriving heights of buildings from Digital Elevation Model (DEM) that is generated from stereo satellite images. The third method is measuring height values of the buildings

from 3D view of stereo IKONOS satellite images by operators. The comparisons between these three methods are done with respect to height data collected from field study, and according to these comparisons, the amount of the error is determined. The error is classified according to floor numbers of buildings, so that, the quantified errors can be applied for similar works in future. Lastly, the third method is utilized by the assistance of 10 people who have different experience level about 3D viewing, in order to see the error amount changes according to different operators. Several results are presented with a discussion of evaluation of the methods applied. It is found that, if there is an updated floor number database, obtaining building height is the most accurate way from this database. The second most accurate method is found to be getting height information by using 3D view of stereo IKONOS images through experienced users.

Keywords: Measurement Error, GIS, Getting Height Information, 3D City Models, Modeling Error

ÖZ

3 BOYUTLU KENT MODELLERİNDE BİNA YÜKSEKLİĞİNDEKİ
HATALARIN MODELLENMESİ

Özge Ergin

Y.L, Jeodezi ve Coğrafi Bilgi Teknolojileri

Tez Yöneticisi : Prof. Dr. Şebnem Düzgün

Aralık 2007, 166 sayfa

Coğrafi Bilgi Sistemlerinde (CBS) üç boyutlu modellere olan ilgi son yıllarda oldukça artmıştır, çünkü kentsel tasarımdan çevresel analize kadar pek çok çeşitli CBS uygulamalarında üç boyutlu modellere ihtiyaç duyulmaktadır. Özellikle de kentsel alanlarda bu ihtiyaç çok önemlidir.

Fakat, CBS'deki uygulamaların pek çoğu 2 boyutlu veriyi gösterir. CBS dünyası 2 boyutlu yaklaşımları kullanan 3 boyutlu nesnelerin neden olduğu karmaşık problemlere çözüm bulmak için uğraş vermektedir. Bu çalışma, 3 boyutlu kent modellerinde kullanılan bina yükseklik verilerinin elde edilmesinde kullanılan metodların hangisinin ya da hangilerinin daha doğru olduğunu bulmaya yöneliktir. Uygulanan metodlardan ilki belediye veri tabanındaki kat yükseklik verilerinden bina yüksekliğinin tahmin edilmesidir. İkinci yöntem stereo uydu görüntülerinden elde edilmiş Sayısal Yükseklik Modeli'nden yükseklik verisinin bulunmasıdır. Üçüncüsü ise IKONOS stereo uydu görüntüleri ile sağlanan 3 boyutlu görüntüden bina yüksekliklerinin operatörler tarafından ölçülmesidir. Bu üç metodun karşılaştırılması, saha çalışmasında toplanan yükseklik verisi ile yapılmış

ve hata miktarı tespit edilmiştir. Hata değerleri binaların kat sayılarına göre sınıflandırılarak bulunan hatalar benzer uygulamalarda kullanılanılabilecek hale dönüştürülmüştür. Son olarak, uygulanan üçüncü metod, hata miktarının kullanıcıya bağlı olarak nasıl değiştiğini görmek için farklı deneyim seviyelerine sahip 10 operatörün yardımıyla tamamlanmıştır. Metodların değerlendirilmesine ait tartışmalarla birlikte muhtelif sonuçlar verilmiştir. Sonuç olarak, eğer güncel bir kat yüksekliği veritabanı varsa, bina yüksekliklerinin bu veritabanından bakılması en doğru sonucu vermektedir. İkinci en doğru sonuç, bina yüksekliklerinin stereo uydu görüntülerinin deneyimli operatörler ile görsellenmesinden elde edilmiştir.

Anahtar Kelimeler: Ölçüm Hatası, CBS, Yükseklik Verisi Elde Etmek, 3 Boyutlu Kent Modeli, Hata Modelleme

To My Love

and

To My Family

ACKNOWLEDGEMENTS

TABLE OF CONTENTS

LIST OF TABLES

LIST OF FIGURES

CHAPTER 1

INTRODUCTION

In urban environments, height information of human made structures has been gaining emphasis, because in the last decades urban development in vertical direction has increased exponentially. Traditionally, cadastral registration is applied by using 2D parcels in many countries, since the individualization of the property started initially with the division of land using 2D boundaries (Stoter et al., 2004). However, in the case of 3D environments, with regard to providing true principles of property rights, and ability to control the development vertically, the structures of urbanized areas has to be considered in three dimensions (Akçın and Yüceer, 2005). Consequently, the demand for 3D city models is growing and expanding rapidly especially in urban planning and various kinds of fields such as environmental studies, microclimate controls and simulation (pollution, noise), military, tourism, facility management, and telecommunication network design, etc. This demand is demonstrated by The European Organization for Experimental Photogrammetric Research (OEEPE) survey on 3D City Models (Fuchs et al., 1998). Fifty-five institutions – users and producers – from 17 European countries took an active part in the OEEPE survey on 3D city models. Applications mentioned in the survey included architecture, tourist information systems, the telecommunication, and the computer game industry; 95 % of the participants mention 3D building data to be of most interest within city models, followed by information about traffic networks (about 85%) and about 71% of the users are concerned with vegetation (Fuchs et al., 1998).

In order to satisfy the demand, many methods have been developed for generation of 3D city models that are using 2D digital maps, aerial photographs, high-resolution satellite images, and laser scanning data. Especially, automatic and semi-automatic 3D generation methods which are using high-resolution satellite images developed rapidly with the commercial availability of IKONOS satellite images. In addition to offering high-resolution and multispectral data, these systems provide a short revisit time (2.9 days) and the capability to perform stereo mapping (Di et al., 2002). Moreover, stereo pairs can be formed in near real time due to a very flexible pointing mechanism (Di et al., 2002). These characteristics make the IKONOS imagery very popular for generation of 3D city models.

However, accuracy of the IKONOS achieved is still being discussed. Authors are mostly interested in positional accuracy in 3D city models, which are more popular research topics and the height of buildings often is just taken as an attribute, which of course is the necessity in establishing a 3D city model (Förstner, 1999). Additionally, the vertical accuracy is an important issue that should be given crucial attention, since; accuracy of the height data plays a critical role in many cases in urban environments.

In this study, modeling error of the selected three methods for getting height information was studied with special emphasis on vertical accuracy of the satellite imagery. The first method is estimating height information from floor numbers of the building data from municipal database system. The second method is obtaining heights of buildings from Digital Elevation Model (DEM) that is generated from stereo satellite images. The third method is measuring height values of the buildings from 3D view of stereo IKONOS satellite images by operators. The comparisons between these three methods are done with respect to height data collected from field study, and according to these comparisons, the amount of the error is determined. The error is classified according to floor numbers of buildings, so that, the quantified

error can be applied for similar areas in the future works. Finally, the third method is investigated in order to determine error amounts for different users who have different experience level in 3D viewing.

In the following subsections, the usage of 3D urban models in various fields and their relation to acquiring height information is reviewed.

1.1 Role of Building Height in 3D Models

Applications for 3D Urban Models can be classified in four different categories, (1) Urban Planning and Design, (2) Infrastructure and facility services, (3) Commercial sector, (4) Promotion and Learning of Information on Cities (Shiode, 2001).

In urban planning, the structure of urbanized area has to be considered in three dimensions. The problems about site planning, community planning and public participation in offer to provide legal security should be solved by 3D visualization (Akçın and Yüceer, 2005). For example, planning of the infrastructure and vertical development of built areas, 3D ownership has been gaining an importance (Akçın and Yüceer, 2005). On the other hand, aesthetics considerations of landscape as well as daylight and line-of-sight are also key issues that often need 3D models. Visual representation of environmental impact is also widely supported by 3D models, especially in hazard and disaster management issues (Shiode, 2001). In many of these applications obtaining accurate building height information is directly related to the analyses performed.

The second category for 3D model applications concerns with the urban infrastructure and mobile communications. Local services like water, sewerage, and electricity provision as well as road network require detailed 2D and 3D data for their improvement and maintenance. In communication works, line of sight analysis is very important for mobile and fixed telecommunication devices in the high-urbanized areas, which

are dominated by high buildings to be sure about clearance reception of signals (Shiode, 2001). They are used to define shadowed areas while simulating the propagation of electromagnetic waves in order to determine optimal positions for transmitter stations (Haala and Brenner, 1999). In such applications, predicting accurate building height values has crucial importance. In traffic planning, city models are used to simulate the impact of noise to the surrounding buildings while planning new traffic routes (Haala and Brenner, 1999). Finally, in residential areas, analysis and visualization of access route to locations by the police, fire, ambulance, and other emergency services are crucial for maintaining a safe environment.

3D models are also effective for visualizing the locations of related uses, spatial distribution of the clients and market demands for specific economic activities such as the availability of space for development (Shiode, 2001). Additionally, it is also available to make queries on the 3D city models, and these 3D city models can be accessed from internet by civilian users (Zlatanova and Tempfli, 2000).

3D visualization offers an easy way to learn many things about cities for users who are from different levels of education.

1.2 Factors to be Considered in 3D Model Generation

In the generation of 3D city models, there are a number of factors to be considered for effective usage of the models.

According to Shiode (2001), there are at least three elements in the generation of the models; the degree of reality, types of data input, and the degree of functionality. Shiode (2001) explains the degree of reality as the amount of detail captured and reproduced within the model and summarizes model typology in terms of the difference in geometrical details.

According to degree of the reality, six modeling methods can be developed. These methods are listed in the order of low geometric content to high geometric content:

• *2D digital maps and ortho-photographs* generate 3D models from conventional 2D GIS maps. They do not have capability of giving detailed spatial information for any analyses (Shiode, 2001).

• *Image based rendering,* is the method, which uses panoramic images. It is an inexpensive method, although the number of shots taken will limit its viewpoints and it would not incorporate spatial analysis functions (Shiode, 2001).

• *Prismatic building block models,* use techniques of block extrusion by a fusion of 2D building footprints with airborne survey data and other height resource. They lack the architectural detail but are sufficient for analyzing view sheds and the shortest path (Shiode, 2001).

• *Block modeling with image-based texture mapping,* is similar to prismatic building block models but with image-based facades. The building textures are most commonly generated form either oblique aerial or terrestrial images which, in most cases, successfully used for the simplification of the outline of building geometry (Shiode, 2001).

• *Models with architectural details and roof morphology,* enables an efficient recovery of 3D surface details (Shiode, 2001). To identify the corresponding locations as points, edges and regions automated search techniques are used and overlapping images are used to generate a number of possible geometries. However, it is still require significant manual intervention for architecturally rich contents (Shiode, 2001).

• *Full volumetric CAD models* are frequently undertaken by a combination of measured building survey and terrestrial photogrammetry (Shiode,

2001). Such methods provide wide range of complexity from the simplest in which images are rectified and combined to remove perspective effects to the full architectural details. Conversely, the cost would be expensive for full city coverage (Shiode, 2001).

The data availability also affects the final output of the model. It can be classified into five groups according to data acquiring methods that are commonly used;

• *Terrestrial Images* are still widely used to provide surface information. Images of building facades and video recordings of streetscapes are widely used to provide surface information. Because of the problems of helicopter flight paths or access to rooftops for obtaining suitable viewpoints for image acquisition in a city centre, building textures are mostly generated from ground level photographs. So it results often in failure (Shiode, 2001).

• *Panoramic Photograph* provides a highly realistic visualization to all angles from static viewpoints in the area. It is possible to provide a very detailed representation of an urban area with people, vehicles and street furniture, if captured with sufficient density (Shiode, 2001).

• *Aerial Photographs* provides a rapid and efficient method for the coverage of a wide city area. The most common source of data are 2D images which lack direct 3D information. There are many kinds of aerial images, which may differ from each other with respect to scale, spectral range of recording, sensor geometry, image quality, imaging conditions (whether, lighting) etc. (Grün, 2000). However, in order to have detailed building facades, oblique aerial images must be preferred rather than the conventional, near vertical aerial images (Shiode, 2001). Human made structures like buildings can be very complex with many architectural details; moreover, they may be surrounded by other disturbing human made and natural objects. Solving building detection and reconstruction problem under these conditions not only is of great practical importance

but also requires an excellent developed image understanding techniques (Grün, 2000).

• *High Resolution Satellite Images* capture very detailed information of the terrain. Especially, images such as IKONOS and Quickbird are at the resolution close to that of small-scale aerial photographs (Kocaman, et.al, 2005). IKONOS is now commercially available at a spatial resolution of 1 m and Quickbird at 0.6 m. In recent years, large amount of research has been completed about accuracy assessment of generated outputs of high-resolution imagery data. Examples for these studies are discussed in the third chapter.

• *Range Imaging,* The LIDAR (Light Detection and Ranging) imaging techniques are based on camera systems that use a pulsed laser device to record the distance from the camera to each point in the image. Common applications use ground based or airborne sensors, the former being suitable for architectural surveys and the latter for small-scale surveys including city models (Shiode, 2001).

The last factor is the functionality, which is the most crucial one. Some of the models are often less functional, where as GIS-based models provide ability of making many spatial and non-spatial analyses. It is obviously clear to understand that the models, which have a potential of extensive and alternative use in GIS, are more powerful. The groups are divided into three as aesthetic models, proprietary models with limited analytical capabilities, full analytical features and hybrid models and related techniques (Shiode, 2001)

1.3 Problem Definition

3D city models are used in various kinds of applications, and recently various 3D model generation methods are developed. With the commercial availability of IKONOS Imagery, there have been

fundamental changes in this technology. High-resolution IKONOS Satellite images provide potentially useful information for the identification of surface objects like buildings in the urban areas (Kim and Muller, 2002).

However, the detailed structure of buildings and height information in 3D city models are still uncertain, because of the various reasons emerged from image acquisition process such as existence of strong shadows due to the large oblique angles and the local time of overpass (Kim and Muller, 2002), reasons originated from urban structure of the area and users in semi-automatic methods. In recent years, many authors give special attention to accuracy assessments of the high-resolution imagery data. Examples about accuracy assessments according to sensor modeling and image orientation (Baltsavias et al., 2001; Fraser et al., 2002), automatic DTM/DSM generation (Jacobsen, 2004; Toutin, 2004; Zhang and Gruen, 2004), feature extraction (Lee et al., 2002; Hu and Tao, 2003; Di et al., 2004) and multi channel color processing can be found out (Hong and Zhang, 2004).

On the other hand, there isn't any study about accuracy assessment of 3D city modeling that is applied for the cities of Turkey, where highly concentrated and mixed urban structure makes harder to distinguish buildings in satellite images.

1.4 Objectives

While the overall purpose of this study is to find the most accurate method for determining height values of the buildings in residential areas, to be used for generating 3D city models, it also aims at answering the following key questions to gain a comprehensive understanding of the 3D building extraction and its visualization.

• What is the amount of error in the applied three methods?

• What is the spatial distribution of measurement errors in these methods?

• How is the distribution of measurement error changes according to number of floors and spatial arrangement of the buildings?

1.5 Organization of the Thesis

The organization of the thesis is as follows;

In Chapter 2, general information about error and uncertainty definitions and error sources are presented.

In the third chapter, commonly used methods in 3D urban area generation are discussed, with special emphasis on the accuracy of height value in 3D data.

In the forth chapter, developed methodology in the thesis is explained. Firstly, data collection from field study is mentioned. Then used methods for data acquisition from Stereo Satellite images and performed analysis like automatic Digital Terrain Model (DTM) and Digital Surface Model (DSM) generations are given in this chapter.

The fifth chapter contains implementation of the case study. How to perform data collection in the study field and how to use that collected data in the comparison with other analysis about prediction height value of features in urban areas are explained. It is mainly focused on the analysis of the measurements of height values, which are done with using satellite stereo images manually by different users. The results of these measurements are compared with the user-based statistics and floor numbers of the measured buildings based statistics. This method is also compared with other height value getting methods like automatic

generation of DTM from satellite image and calculating heights by multiplying floor numbers of the buildings with constant standard floor height value.

In the Conclusion chapter, an evaluation is made, regarding the aim, objective of the study and analysis for these objectives. Finally, recommendations and conclusion of the study were discussed and some ideas are given about the future studies.

CHAPTER 2

LITERATURE REVIEW

This section covers descriptions terms and basic concepts related with measurement error, uncertainty and accuracy, error sources studied in the literature.

2.1 Error, Uncertainty and Accuracy

The terms of error, uncertainty and accuracy are related concepts and sometimes they can be used interchangeably. However, these three terms all have different meanings.

The error in a quantitative attribute can be described as the difference between reality and our representation of reality (Heuvelink, 1998). It includes not only "mistakes", or "faults" but also the statistical concept of error i.e. "variation" (Burrough, 1986). The data collected in the field have been classified, interpreted, estimated naturally and so contain a certain amount of error. Errors can also be emerged from measurements (Heuvelink, 1998).

According to the definition of error, the value of it is never exactly known, because the true value is mostly unknown. However, uncertainties, which are described as likely errors, can be estimated. The uncertainty is an estimate of errors as a possible range of errors. In other words, error in geographic data produces data uncertainty. Spatial data quality depends on the level of uncertainty, or how well the data represents reality. For example, categorical coverage map data quality is

measured by how consistently the category labeled at points in the database matches what is actually there in the real world (Ehlschlaeger and Goodchild 1994).

Uncertainty can be defined as "knowledge of possible deviation from a 'true' value, but without precise knowledge of the magnitude" (Davis and Keller 1997). Evans (1997) also described uncertainty as the potential variance from the truth, or the condition of being variable or questionable. Accuracy is "the freedom from error or deviation from a model within acceptable limits…" (Evans, 1997).

Data accuracy in spatial information is an extensive term that can be divided into positional accuracy, which is checking whether objects are in their correct positions, or not, geometric accuracy like size or length of linear objects, and interrelationship accuracy that can be called as topological accuracy that describes the relationships between objects, attribute accuracy, and temporal accuracy (Cai, 2003).

Positional accuracy can be divided into absolute positional accuracy and relative positional accuracy (ISO, 2003). Absolute positional accuracy examines how closely all positions on a map or data layer match to corresponding positions of features represented on the ground in a desired map projection system (Chong, 1997). Relative positional accuracy considers how closely all the positions on a map or data layer represent their corresponding geometrical relationships on the ground (Chong 1997). In other words, relative positional accuracy is concerned with the accuracy of the geographic relationships between entities on a map and absolute positional accuracy deals with how well the coordinates of a location on the map correspond to the true location on the ground.

Geometric accuracy means the accuracy of geometric properties of spatial objects. For example, height, length, direction, and orientation of linear objects, and area and perimeter of area object.

Interrelationship accuracy refers to the accuracy of topology, which describes the spatial relationship between spatial objects including connectivity, adjacency, and proximity.

Attribute accuracy, temporal accuracy, precision, logical consistency or completeness, and lineage are the other aspects of data quality. Attribute accuracies can be defined as accuracy of the attributes (Evans 1997). Temporal accuracy is defined as that part of the data's error that arises due to the temporary nature of the data. It is affected by the interaction between the duration of the recording interval and the rate of change in the event (Cai, 2003). Precision is the exactness with which a classification or measurement is made. Logical consistency or completeness is the fidelity of relationships between points, lines, and areas. Lineage is related to the date when the data were collected, and what kinds of processing they were subjected to (Davis and Keller 1997, Kraak and Ormerling 1996).

It is impossible to eliminate all the errors in spatial data. A certain error tolerance may be fully acceptable (Rasdorf et al., 2001). However, errors are by no means desirable. Knowledge about how errors and uncertainties occur would be very helpful in controlling and possibly reducing them. Finally, a thorough understanding of errors and error propagation can be used to improve our understanding of spatial patterns and processes (Cai, 2003).

In summary, a variety of different kinds of errors and uncertainties contribute to spatial data inaccuracy and these need to be well understood and carefully controlled in any GIS applications. They will occur even with the recent advances in technologies to more accurately acquire raw data and in improved computer hardware and GIS software, which process and analyze data (Rasdorf et al. 2001). It is an important goal to provide a quantified approach to give users, analysts, and decision-makers information about the quality and accuracy of the data being provided, analyzed, and used.

2.2 Error Sources in GIS

The production of a geographic database is often a complex, and undocumented, process involving many different people, different sets of measurements, stages of interpretation and manipulation that confuse the relationship between original measurements and the final database contents (Heuvelink 1998). The Geographic Information Systems world tries to complete with the discussions of the reasons for data error.

By definition, a model is an approximation of the reality. Some models describe reality better than others; however, each model has some errors. There are two main types of errors; the systematic error, which happens consistently as a constant difference between the measurement and the true value and the random error, which is random and uncontrollable. All of the measurements have random errors. Furthermore random errors cannot be eliminated; the easiest way to reduce random errors is to take more measurements. The systematic errors can be determined, and reduced by comparing the measurement instruments against a known value.

The spatial data inherits errors and uncertainties. These errors and uncertainties contribute to the inaccuracy in spatial models and thus, must be understood and controlled in spatial analyses.

Some researchers tried to identify error sources and error ranges. Amrhein and Schut (1990) discussed the range of errors that can accompany any datasets, and made comprehensive statements about data quality that is needed by users. The error and quality issues in the spatial data are studied in a series of publications by Goodchild (1991a, b, 1998).

Rasdorf et al. (2001) summarized all the error sources that could be encountered in data collection phase. It is not uncommon to find summarized error source information from GIS books, for example, Burrough and McDonnell (1998) identified 7 factors that affect the quality of spatial data. The findings from these research efforts are summarized in the following paragraphs.

Errors encountered in primary methods of data collection (data collected directly by aerial and terrestrial surveying and satellite imagery) include:

• Personal errors (biases introduced by the personnel who carry out the task of data collection)

• Instrumental errors (errors in instrument calibration, biased instruments, variations in instruments due to external factors)

• Environmental errors (solar illumination, clouds, wind, etc.)

Errors encountered in secondary methods of data collections (data are collected from images, charts, maps, graphs, etc.) include:

• All errors encountered in primary methods of data collection

• Compilation errors

• Errors in drawing

• Errors in map generalization and reproduction

• Errors due to material deformation

• Errors due to feature exaggeration

• Errors introduced due to the use of wrong scale

• Errors in digitizing or scanning

• Errors due to the uncertainties in the definition of a feature

Derived data are data generated by certain operations (functions or models) upon the input data. Errors in the derived data can be attributed to the errors in the input data, the quality of the operations, and the way the input data and the operations interact. In this thesis, the height information is obtained from secondary data, error in this category are investigated. Moreover, as the building height in the study region is measured by using a range finder, the error analyses related to the primary methods are also considered.

CHAPTER 3

METHODS OF BUILDING HEIGHT EXTRACTION FOR 3D CITY MODELING

This chapter contains examples of methods for extraction height information for 3D city models. The 3D city modeling tasks may differ in terms of required resolution of models (level of detail), type of product (vector model, hybrid model, including mapped texture, attributed model with integrated thematic information), size of dataset, sensor platform (satellite, aerial, and terrestrial), sensor and data type (images in various forms, laserscans, scanned maps, etc.) (Grün, 2000). Additionally, the authors have been developing new methods which are using combinations of different data sources, in order to increase accuracy and overcome the complexity of the reconstruction of the buildings. In this chapter, these methods are examined according to achieved accuracy in height information extraction.

3.1 Getting Height Information from Shadow Analysis

Heights of the objects have been able to extract from aerial photographs using parallax in stereo-pair photographs. The lengths of the shadows cast by the objects are also used to determine heights (Huertas and Nevatia, 1988; Liow and Pavlidis, 1990). If the sun and sensor geometry are known, it is fairly simple to establish a relationship between shadow lengths and the heights of objects. The above usages, however, are confined to high resolution photographs, with pixel resolutions much better than the object heights being measured (Shettigara and Sumerling, 1998).

The first example for this method is estimating building heights by using a set of single-look SPOT pancromathic and multispectral images taken from the same satellite simultaneously. Shettigara and Sumerling (1998) have applied this technique and they used shadows cast by rows of trees in SPOT images were in order to estimate mean heights of trees. Then, calibration lines were constructed to relate the actual mean heights of rows of trees to the estimated heights. Using these calibration lines, heights of some industrial buildings in the image were estimated using their shadows with sub-pixel accuracy. The accuracy achieved is better than 3 meters (RMSE – Root Mean Square Error), or one-third the pixel size of the SPOT panchromatic image. One of the important challenges involved in the process was to determine an appropriate threshold for outlining shadow zones in the images. The technique is also useful for estimating heights of extended objects situated in flat terrains. The type of resampling used for overlaying a multispectral image over a panchromatic image changes the accuracy of height estimation. However, the change is tolerable if the heights to be estimated are within the ground-truth data range used for deriving calibration lines (Shettigara and Sumerling, 1998).

This method can be also applied with high resolution satellite images that provide metadata such as scene geometry, acquisition time, geolocation, etc. The scene geometry metadata contains azimuth angle of the sun and those angles of the satellite when satellite image data is acquired. Since, sun elevation and azimuth angles as well as sensor elevation and azimuth angles are mostly given in satellite metadata, it is possible to detect vertical lines and shadow lines automatically. Then by measuring the length of vertical lines or shadow lines, it can be estimated the height of the buildings (Lee and Kim, 2005).

Lee and Kim (2005) have used IKONOS as high resolution satellite images, in order to reconstruct accurate 3D building structures. They proposed an algorithm that used metadata of the satellite which indicate

18

the direction of vertical lines of a building and the direction of building shadows within the image space. As a result, they found the total RMSE (Root Mean Square Error) was 1,48431 m, the maximum error was 2,5493 and 0,7360 as minimum in the heights of buildings (Lee and Kim, 2005).

To sum up, getting height information from shadow analysis is an efficient and accurate method, but it should be applied on the plane surfaces which have small relief differences and also not containing small objects.

3.2 Combining 2D Digital Maps and Aerial Images

Various kinds of techniques for feature extraction from aerial photographs are available in the literature. Since the technologies have changed several times fundamentally, today the issue of the reconstruction of buildings using only aerial images as data source has been proven to be a very difficult problem (Suveg and Vosselman, 2003). The complexity of this problem can be overcome by combining the aerial images with other data sources.

Suveg and Vosselman (2003) described a 3D building reconstruction method that integrates the aerial image analysis with information from large-scale 2D GIS databases and domain knowledge. In the first stage of their proposed method, the buildings are localized in the images based on the information from the ground plans of the buildings contained in the GIS database. Then, they applied the approach of modeling buildings using a set of basic buildings and a set of basic primitives (flat roof, gable roof, and hip roof building). In this way, a complex building can be seen as a Constructive Solid Geometry (CSG) tree, where the leaf nodes contain primitive building models, and the internal nodes contain Boolean operations such as union, intersection, and difference. According to Suveg and Vosselman (2003), the CSG tree representing a building is

given by the best fit of the building models corresponding to the building partitions. In the final verification step, the complete CSG tree is fitted to the image data. As a result the root mean square error (RMSE) obtained from this method is 0.38 m in height, and they commented as the deviations are less then 10 cm, for the length, width, and gable height, but the deviation for the height is quite large, which is due to the fact that the roof base edges are difficult to detect because of the low contrast (Suveg and Vosselman, 2003).

3.3 Using Light Detection and Ranging Data with Other Sources

Light Detection and Ranging (LIDAR) is defined as an optical remote sensing technology that measures properties of scattered light to find range and/or other information of a distant target (Web4). It is also referred to as 'Airborne Laser Mapping', 'Laser Altimetry', 'LIDAR mapping' or 'Airborne Laser scanning' (Web7).

LIDAR technology has many applications such as archaeology, geography, geology, seismology, remote sensing, atmospheric physics etc. The distance between the sender and an object is measured as follows; a narrow laser beam is send towards the object and the time taken by the laser to be reflected off the target and returned to the sender is measured and multiplied by the speed of the laser beam. Laser scanners are mounted on aircraft and apply a laser beam (infrared light) to measure the distance from points located on the ground to the aircraft. This distance measurement is then integrated with exact information on the aircraft's position to calculate the height of the Earth's surface. Laser scanning is used to produce high resolution Digital Terrain Models (DTM) and also to provide height data for generating three-dimensional building and city models (METU, 2003).

A number of authors have shown approaches for the generation of 3D building models mainly or solely based on laser altimetry data.

For example, Maas and Vosselman (1999) proposed two techniques for the determination of the building models from laser altimetry data. The first approach is based on the analysis of invariant moments of standard gable roof house types which are derived from 0th, 1st, and 2nd order moments, and asymmetries such as dorms on the roof house types. The second approach is a data driven technique and based on the intersection of planar faces in triangulated points. The common point of these two approaches is the fact that they use the original 3D data points rather than data interpolation. They applied these techniques to a laser altimetry dataset containing 51 buildings, with a point density of 1 point / m^2. They found accuracy as standard deviation of 0,11 m for the first approach and 0,07 m for the second.

The laser scanning data is one of the most functional data sources for city modeling for a number of reasons. Firstly, LIDAR is an active remote sensing technique, in which pulses of it are directed towards the ground and the period for these pulses to return to the sensor is measured and processed in order to determine the distance between sensor and the object or surface (Smith, 2003). Recently, it provides very high resolutions. Moreover, Lawless (2001) argues that the Digital Surface Model (DSM), which is created by LIDAR, are the most suitable for the generation of 3D city models (Lawless, 2001). Due to the advantages of time consuming error prone matching techniques, airborne laser scanning has meanwhile become a rather important source of information for the generation of 3D city models (Maas and Voselman, 1999). However, the point densities delivered by most of the systems in standard operation mode are still too small (often in the order of 1 point/10 m^2) (Maas and Voselman, 1999). Another disadvantage of LIDAR is its inability to penetrate heavily canopied forests without breaks, thus preventing creation of accurate DEM. Therefore, in some cases it needs calculations through mathematical modeling and filtering

of the data set. LIDAR operators are required to have a sound understanding of LIDAR, GPS and INS systems, making them more expensive to produce. However, there are no published policies or international protocols for LIDAR calibration and operation (Web6).

Haala and Brenner (1997) are one of the earliest researchers who have significant works with airborne laser scanners. Haala and Brenner (1997) employed a DSM segmentation technique based on local surface normals. The normal direction from a Lidar DEM was approximated using the derivatives of a local bivariate polynomial fit. The direction of the unit normal vector of a possible roof plane emerging from the ground plan is used as perpendicular to the segment of it (Kim and Muller, 2002). Therefore, the accurate extent of heights can be determined and segmentation carried out within the building outline (Haala and Brenner, 1997).

Haala and Walter (1999) proposed another way to generate 3D city models. They used the combination of Digital Surface Model (DSM) that was generated from airborne laser scanning and color aerial imagery for landuse classification in urban environments (Haala and Walter, 1999). This kind of external data such as maps and digital maps can also be used, but such additional data is not always available (Kim and Muller, 2002).

Tao and Yasuoka (2002) described another method which is applied by using Lidar and very high resolution airborne SAR. The researches initially used some ground seed points starting at low resolution. The height points of the objects were detected by their height difference and the SAR amplitude information (Tao and Yasuoka, 2002).

3.4 Using High Resolution Satellite Images (HRSI)

With the commercially availability of the high resolution satellite images, they have been widely used as data sources for building extraction in 3D city modeling. The two most relevant in terms of urban feature extraction are IKONOS and Quickbird images (Smith, 2003) with spatial resolution of 1 m and 0,6 m. These data have been used in variety of studies as a single image or stereo images.

3.4.1 Single Image HRSI Data

An example for extracting height information from single high resolution satellite images can be given from the studies of Wilneff et al. (2005). They extract metric information by using IKONOS and QuickBird imagery which has camera replacement models such as rational polynomial coefficients (RPCs) or alternative models such as the affine projection model. With the sensor orientation determined, accurate metric 3D information can be extracted from HRSI through multi-image processing as well as from single images via monoplotting (Wilneff et al. 2005). The monoplotting operation determines the object point corresponding to the measured image point via an iterative process of intersecting the imaging ray with the underlying DEM surface. Wilneff et al. (2005) found lower height accuracies of approximately 6m for RPCs and 3m for the affine model from IKONOS near-nadir images. On the other hand, they achieved 1 m accuracy with QuickBird imagery for both the RPC and affine models (Wilneff et al. 2005).

Although, it has been demonstrated that monoplotting from HRSI imagery with the RPC and affine models is an accurate method for producing 3D information, it has some limitations. For example, at least one building point at ground level should be visible and can be measured in regular monoplotting mode and it is assumed that roof cornerpoints are at the same height.

3.4.2 Stereo Image HRSI Data

Fraser et al. (2002) examined the potential of IKONOS imagery for sub-metre level, namely Geo images, coupled with alternative computational schemes for mono-stereo and multi-image positioning. They examine according to three aspects; the geometric accuracy of geopositioning from stereo and multi-image coverage; the radiometric quality, with emphasis on characteristics to support automatic feature extraction; and attributes of the imagery for the special applications of building extraction and visual reconstruction are examined. As a result, they found that within the stereo triangulation, the rational functions (RFCs-which provide a mechanism for object-to-image space transformation and 3D point determination) have RMS accuracies of 0,7 m in planimetry and 0,9 m in height after removal of the bias in object space using the known GCP (Ground Control Points) coordinates. This corresponds to accuracy estimates resulting from the 19 checkpoints for the affine and Direct Linear Transformation (DLT) models with 6 GCPs with at least 0,6 m, and at most 1,0 m for planimetry and height (Fraser et al. 2002).

Kim and Muller (2002) tested using IKONOS stereo pairs and Lidar Data as an alternative source. They use algorithm of using a Digital Terrain Model (DTM) derived from Lidar and a geometrically corrected IKONOS stereo images. They apply segmentation of DSMs (Digital Surface Model) in focusing strategy to reduce the search space of machine vision algorithms and large size (11x11 km) into more manageable discrete units. In addition, they have tested two solutions in order to decrease the positioning error of IKONOS Geo product. The first is to exploit secondary information such as Lidar and the second is to update the positioning accuracy and DEM quality of IKONOS stereo (Kim and Muller, 2002). In order to do positional accuracy assessment, they use 24 static GCP measurements. As a result, they found positional accuracy of 3-4 m and vertical accuracy of 3 meters (Kim and Muller, 2002). These results are

updated with a rational polynomial coefficients (RPC) analysis. Additionally, they claimed that with 2-meter resolution Lidar data and IKONOS Precision images excellent results can be obtained mainly because of the good delineations of building outline (Kim and Muller, 2002).

Poon et al. (2006) performed a detailed study on the accuracy and performance of height information extraction from different kinds of commercial-off-the-shelf (COTS) software, with emphasis on DSMs generated from IKONOS stereo pairs. They selected three systems in order to make comparisons of their achieved accuracy in height information extraction. The selected systems were the Softcopy Exploitation Tool (SOCET SET) Automatic Terrain Extraction (ATE) version 5.2, Z/I Imaging's ImageStation Automatic Elevation (ISAE) version 4.4 and ERDAS Imagine OrthoBASE Pro version 8.6 (BAE Systems, 2005). The comparisons of these three COTS were done against an InSAR (Interferomatetric Satellite Aperture Radar images) DEM of lower, accuracy. As a result, they found vertical accuracy of 9,25 m with SOCET SET ATE, 9,48 m with Z/I Imaging ISAE and 6,09 m with OrthoBASE Pro systems (Poon et al., 2006).

Another study with IKONOS is a detailed accuracy evaluation of a DSM generated with a geo stereopair, derived firstly using an intensity based matching method embedded in commercial software and, secondly, via a hybrid image matching algorithm by Poon et al. (2005). The accuracy assessment which is based on comparisons against a first pulse laser DSM, encompasses diverse land cover types from urban high-rise buildings to rural forest areas. In the first method, ISAE software was used for height generation by utilizing image and feature pyramids to match homologous points in a hierarchical structure. Overall, the RMS discrepancy (RMSE) was 4,0 m and the regions with the greatest error were, not surprisingly, in areas of large topographic variability, namely the CBD (Central Building District) and forest regions with RMSE values of 4,3 m and 4,5 m respectively (Poon et al, 2005). The second method,

the hybrid image matching DSM procedure has an overall RMSE of 2,7 m in height. This evaluation shows that the generated DSM is indeed a good representation of the actual terrain with accuracies of 1,7 m and 2,2 m RMSE values in low rise and sparse vegetation areas (Poon et al, 2005).

3.5 Comparisons of the Methods

The selected example methods, their data sources and accuracies achieved in heights of the buildings are summarized in the Table 3-1

Table 3-1: Comparisons of the height information extraction methods

Method	Data Source	Vertical Accuracy
Getting Height Information from Shadow Analysis	Single IKONOS High Resolution Satellite Image	1,48431 m (RMS) (Lee and Kim, 2005)
	SPOT	Better than 3 m (RMS) (Lee and Kim, 2005)
Integrating the aerial image analysis with information from large-scale 2D GIS databases and domain knowledge	High-resolution aerial Image (The Scale of1:3000 and are scanned at 600 dpi)	0.38 m (RMS) (Suveg and Vosselman, 2003)
Using Sensor Orientation Model as RPCs	IKONOS	6, 59 m (RMS) (Wilneff et al. 2005)
	QuickBird	3,05 m (RMS) (Wilneff et al. 2005)
Using Sensor Orientation Model	IKONOS	1 m (RMS) (Wilneff et al. 2005)

Table 3-1: Comparisons of the height information extraction methods

Method	Data Source	Vertical Accuracy
as Affine Models	QuickBird	1,34 m (RMS) (Wilneff et al. 2005)
Analysis of Moments with raw laser altimetry data	Raw Laser Altimetry Data (High Density with 1 point/m^2)	0,11 m (Standard Deviation) (Maas and Vosselman, 1999)
Intersection of Planar Faces Method	Raw Laser Altimetry Data (High Density with 1 point/m^2)	0,07 m (Standard Deviation) (Maas and Vosselman, 1999)
Getting Height Information from Digital Terrain Model (DTM) derived from Lidar and a geometrically corrected IKONOS	LIDAR and IKONOS Stereo	3 m (RMS) (Kim and Muller, 2002)
Using IKONOS stereo Images and stereo triangulation with the rational functions	IKONOS Geo Stereo Images	0,9 m (RMS) (Fraser et al., 2002)
Using IKONOS stereo Images and 19 checkpoints for the affine and Direct Linear Transformation (DLT) models	IKONOS Geo Stereo Image	0,6 m to 1,0 m (RMS) (Fraser et al., 2002)
Getting Height Information from DSM	IKONOS and SOCET SET ATE System	9,25 m (RMS) (Poon et al., 2006)
	IKONOS and Z/I Imaging ISAE System	9,48 (RMS) (Poon et al., 2006)

Table 3-1: Comparisons of the height information extraction methods

Method	Data Source	Vertical Accuracy
	IKONOS and OrthoBASE Pro System	6,09 m (RMS) (Poon et al., 2006)
Getting Height Information from DSM which is generated by using commercial software (Imaging ISAE)	Overal: 4,0 m CBD : 4,5 m Residential : 3,1 m University : 3,3 m Forest : 4,3 m (Poon et al., 2005)	
Getting Height Information from DSM which is generated with the method of hybrid image matching	Overal: 2,7 m CBD : 3,4 m Residential : 2,0 m University : 2,2 m Forest : 3,2 m (Poon et al., 2005)	

CHAPTER 4

METHODOLOGY

The proposed methodology of the study has four main steps: Data Collection, Methods, Analyses and Results. Flow chart of the study is illustrated in Figure 4-1. These steps are explained in the following subsections.

4.1 Data Collection

The first step of the methodology is data collection (Figure 4-1), which is divided into three parts; Data collection in the field study, gathering ground plan of the study area and getting IKONOS Satellite Stereo Images.

For the purposes of finding errors of the methods, first an accurate and precise set of building height values had to be gathered from field study. For this purpose, building height values are measured with a laser range finder measurement instrument, which has an accuracy of 30 cm in distance and 0,25 degrees in inclination in the range up to one kilometer. In order to find the accuracy of the height measurements "Error Propagation Law" is applied by using the defined vertical distance and angle accuracy specifications of the instruments. The laser height measurement are considered to be the most accurate height measurement method and used in comparison of other methodologies. The measurements are repeated 6 times for each building in the study area, to reduce the random errors.

Data Collection

Field Study
- ❖ **394** buildings is measured in the study area (Cumhuriye Neighborhood, in Eskisehir)
- ❖ Measurements were repeated **6** times for each building
- ❖ **Range Finder** used for measurement instrument

Ground Plan
- ❖ The shape file of the study area obtained from

IKONOS Satellite Images
- ❖ Precision Stereo (1 meter horizontal (RMSE) and 2 meter vertical (RMSE) accuracy)
- ❖ Acquisition Date: 2002-05-03
- ❖ Taken along the city of Eskişehir

METHOD: 1
- ❖ Getting height values of buildings by multiplying constant floor height value with **floor numbers.**

METHOD: 2
- ❖ Generating DSM
- ❖ Generating DEM
- ❖ Raster Calculation; substraction DEM from DSM
- ❖ Get height values of the buildings by zonal analysis

METHOD: 3
- ❖ Getting height values by measuring from stereo images manually.
- ❖ Repeated **10** times by **10** operators.

Uncertainty Analysis of measured height values (Application of Error Propagation Law)

Error Analyses for METHOD: 1
- ☑ Calculated:
  - ☑ Error mean
  - ☑ Standard Error
  - ☑ 95% Confidence Interval
- ☑ Classified statistics according to number of floors.

Error Analyses for METHOD: 2
- ☑ Calculated:
  - ☑ Error mean
  - ☑ Standard Error
  - ☑ 95% Confidence Interval
- ☑ Classified statistics according to number of floors.

Error Analyses for METHOD: 3
- ☑ Calculated:
  - ☑ Error mean
  - ☑ Standard Error
  - ☑ 95% Confidence Interval
- ☑ Classified statistics according to number of floors.
- ☑ Classified statistics according to operators.

Comparison of Applied Analysis Results

Comparison of Applied Analysis Results of Users

Visualization

Results & Discussion

Data Collection

Methods

Analysis

Results

Figure 4-1: Flow chart of the methodology used in this study

The second and the third part of the data collection steps are completed with the support of the Department of Geodetic and Geographic Information Technologies of METU. Ground plan was requested from municipality of Eskişehir and IKONOS satellite images were purchased by the department for ongoing research studies. The specifications of these two datasets were detailed in Section 5.2.1.

4.2 Applied Methods for Prediction of Height

As stated in the third chapter, there are many ways to get 3D models in urban areas. Using LIDAR, Stereo Satellite Images, generating DEM and combinations of these data sources are the most common ones. Beside finding positional accuracy, knowing vertical accuracy of 3D features is also very important topic in 3D city models. Three methods are selected for predicting height values of 3D features in urban areas; using number of floors obtained from municipality database and updated in the field study, automatic generation of DTM and DSM from stereo satellite images and manual measuring from stereo satellite images. Detailed explanations of these methods are described in the following sections.

4.2.1 Method 1: Using Number of Floors

The first method is the most simple and easy way to get height values of the buildings in urban areas. In this method, building height values are determined using number of floors of buildings. The number of floors for the buildings were obtained from the database of Municipality of Tepebaşı in Eskişehir and updated in the field study. In order to get height values of the buildings the number of floors are multiplied with a constant height value which is defined by municipal zone regulations (Eskişehir Büyükşehir Belediyesi İmar Yönetmeliği, 2004). According to regulations

about structure of buildings, the height of the buildings should be calculated by using Equation 4-1:

$$h = 0,5 + n \times 3,00 \qquad \qquad \textbf{(4-1)}$$

Where;
h : Building height
n : Floor Number

Additionally, during the data collection process in the study area, the characteristics of the buildings were considered such as if there are shops or garages at their basement or not. The buildings that have shops at their basements were defined and checked with floor numbers data in the municipality database. As a result, it is seen that these buildings have extra 2 floors, which is explained in detail in section 5.3.

4.2.2 Method 2: DSM Segmentation

In the second method, height values of the buildings are obtained from Digital Terrain Model (DTM) and Digital Elevation Model (DEM), which are automatically generated from IKONOS Precision stereo images.

A digital terrain model (DTM) is a 3D digital representation of the Earth's terrain or topography. Automatic DTM extraction involves the automatic extraction of elevation information from imagery and the subsequent creation of a 3D digital representation of the Earth's surface. A DTM represents the elevation associated with the Earth's topography and not necessarily the human-made (e.g., buildings) or natural (e.g., trees) features located on the Earth's surface.

A digital surface model (DSM), also called a digital elevation model (DEM), represents the elevation associated with the Earth's surface including topography and all natural or human-made features located on

the Earth's surface. The primary difference between a DSM and a DTM is that the DTM represents the Earth's terrain whereas a DSM represents the Earth's surface (OrthoBASE Pro User's Guide, 2003).

While a DSM may be useful for landscape modeling, city modeling and visualization applications, a DTM is often required for flood or drainage modeling, land-use studies, geological applications, etc (Web3).

Terrain points which have 3D information are used in the DTM generation. Terrain points collection for DSM generation is developed with the help of ERDAS Stereo Analyst Module. A hundred and twenty four 3D features, which are distributed homogeneously in the study area, have been collected as point type. Inverse Distance Weighted method is used as raster interpolation method.

For automatic generation of Digital Surface Model (DSM) from satellite stereo images, Leica Photogrammetry OrthoBASE Pro software is used and fifty tie points have been selected on the overlapping images. Tie points are the common points in overlapping areas of two or more images. They connect the images in the block to each other and are necessary input for the triangulation. Tie points are necessary for accuracy checking of the generated DSM. Stereo Imagery serves as the primary source of data input for the automatic extraction of DSMs for OrthoBASE Pro. DSMs can only be extracted if two or more overlapping images are available. Prior to the automatic extraction of DSMs, sensor model information associated with an image must be available. The IKONOS sensor model supports IKONOS imagery and its associated rational polynomial coefficient (RPC) and metadata files. The metadata files contain information regarding the images in the data set. RPC files contain the necessary information to determine interior and exterior orientation.

In order to get height values of the buildings, raster calculation should be performed over generated DTM and DSM data. As seen in the profile

graphics in Figure 4-2 of these two models, building heights should be calculated by subtracting DTM raster data from DSM raster. The difference (DSM-DTM) is called normalized DSM (nDSM) (Equation 4-2) (Clode, 2005). Eventhough objects rising from the terrain can be detected quiet well from the height data, discrimination between buildings can be difficult (Haala and Brenner, 1999).

nDSM = DSM – DTM   **(4-2)**
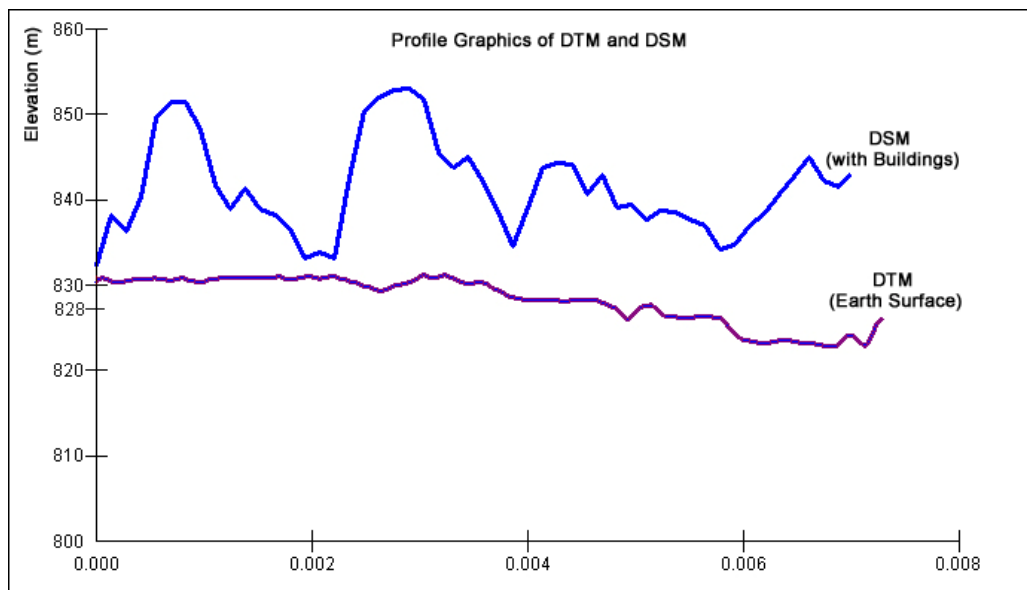
Figure 4-2: Profile analysis of DSM and DTM

Then, the calculated raster data is used as an input for zonal analysis, to find the height value for each building. Zonal functions take a value as an input and for each cell a statistic is calculated. Zonal statistical functions perform operations on a per-zone basis; a single output value is computed for every zone in the input zone dataset. The following statistics can be computed within each zone: Maximum, Mean, Median, Minimum, Range, Standard Deviation, and Sum. The zonal functions are grouped by how the zones are specified, and by the number of input value.

34

Using zonal statistics, a statistic is calculated for each zone defined by building polygons in shape data, based on the values from calculated DSM. In the case study, it is essential to obtain mean zonal statistic in nDSM to obtain average building height value is obtained.

4.2.3 Method 3: Manual Measurement from Stereo Pairs

In the third method, the height values are measured from stereo images, which are performed by 10 users who have different levels of experiences in 3D viewing. They are asked to determine height (Z) values of the buildings from a 3D image, which is displayed by using the stereo image, a shutter glass, and a computer with a special hardware for 3D image display. A shape file, which contains the polygon zones of each building, is overlaid by the 3D image, to make it easier to distinguish the buildings in the study area. The users are asked to add points to the inside of these polygons, which determined the height value of the buildings. After completing the building height point's users are asked to enter point to the low-level areas, such as parks, playgrounds. Those low-level points are used to generate a bottom layer for determining building height. Since the study area is nearly flat, these low level points are decided to be sufficient in determining the building height. Figure 4-3 shows a user performing measurement with shutter glasses and a computer equipped with special hardware.

Figure 4-3: A user using the shutter glass

Each user entered 359 points for building heights and 14 points for low level ground, for each user a feature project consisting of only points is generated. The snapshot of the feature project is displayed in Figure 4-4.
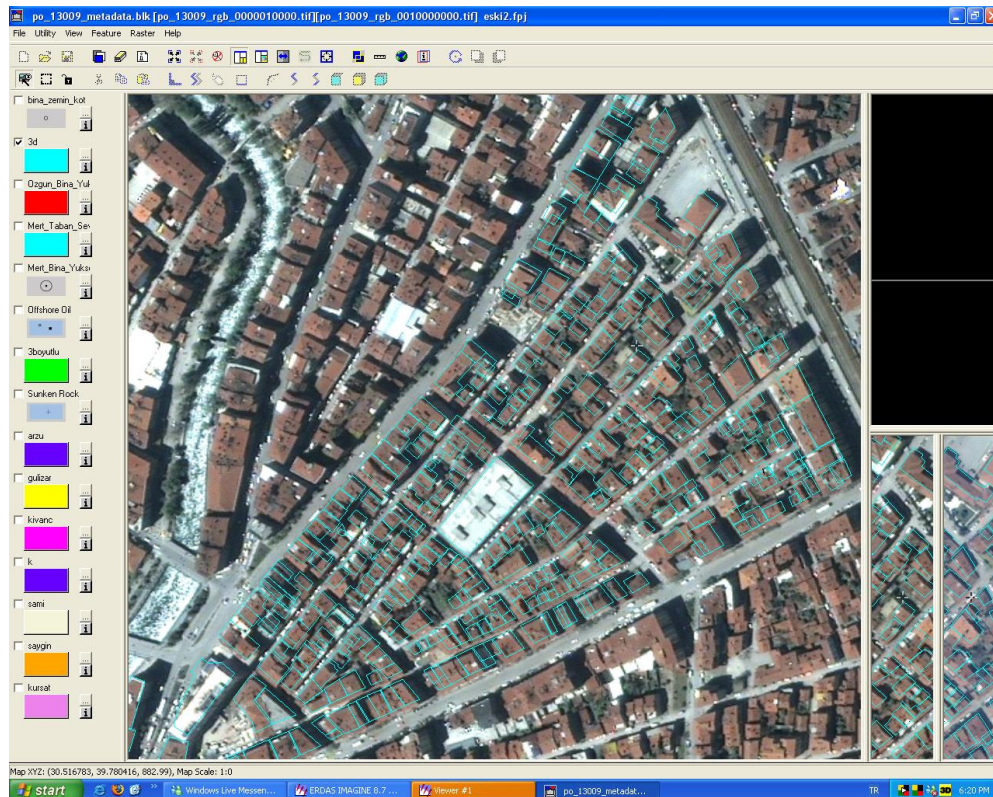
Figure 4-4: Snapshot of the feature project

Users were selected from three different ranges:

1. The first group is well-experienced users, who have advanced knowledge about height measurement from stereo images. These users used stereo images several times, either in their jobs, or during perpetration of a study.

2. The second group is moderately experienced users, who have knowledge of height measurement from stereo images. These users have taken lecture on the subject and at least measured height a few times.

3. The last group is inexperienced users, who do not have any idea about 3D viewing from stereo images. These users measured height values for the first time.

Users are requested to perform their measurements at the corners or the edges of the buildings as illustrated in the Figure 4-5. The reason is that the data collected in the field study consists of height measurements from the terrain and the top of the roofs.

Measurement Points on the Satellite Imagery (They are put down on the edges of the roofs).	Measurements in the field study with range finder measurement instrument.
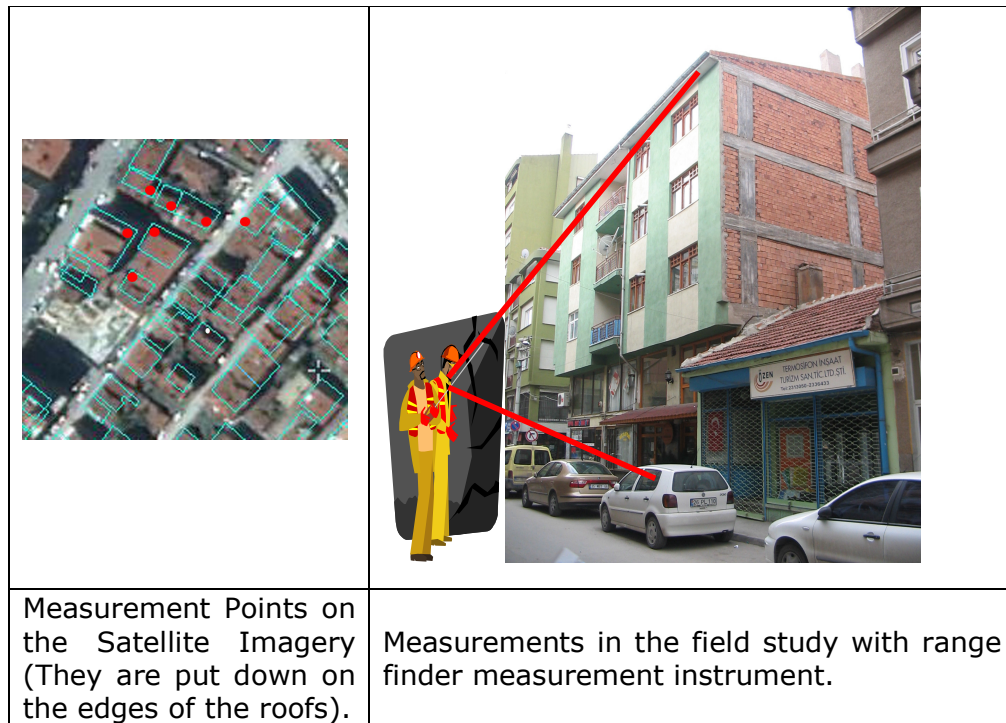
Figure 4-5: Measurement technique from satellite image and in the field study

4.3 Analyses

As seen in the Figure 4-1, analyses part of the methodology has different steps. The first analysis is related with the data that were collected in the field study. Measurements are evaluated in terms of the "Error Propagation Law" in accordance with accuracy specifications of used measurement instrument. The second, the third and the fourth parts of the analyses are statistical calculations related with applied methods in order to make comparisons. Three methods are compared with each other; also, the third method is evaluated separately according to the skills of the users. In addition to that spatial distribution of errors from each method is investigated. In order for the results to be applicable to similar areas, errors in each method are classified according to floor numbers. Furthermore, errors of the three methods are analyzed by considering the number of floors.

4.3.1 Statistical Analyses

The second, the third and the fourth parts of the analyses steps are performed after making error calculations. In order to find error in the height values retrieved in the three methods, they are subtracted from the mean value of building height values obtained from the field study. Descriptive statistics are calculated for error values of each method.

If a large number of samples are taken from the same population, each of these will have a different mean and standard deviation. A distribution of such sample statistics is known as sampling distribution. If all possible samples of size n were taken from a population, then the statistical distribution of those sample means would approximately be normally distributed about the population mean (Central limit theorem), whatever

the character of the population, provided the samples are fairly large (n>30) (METU 2007).

The standard deviation of a sampling distribution is called the standard error of the sample statistic or in short standard error. If all possible samples of size n were drawn, then the mean of these sample means ($\mu_{\bar{x}}$) would equal to population mean (μ).

The standard deviation of the sampling distribution of the means is:

$$\sigma_{\bar{x}} = \frac{s}{\sqrt{n}}$$
(4-3)

Where;

$\sigma_{\bar{x}}$: Standard error of sample means

S : Standard deviation of sample

N : Sample size

The mean of the population can be estimated by using confidence limits. Confidence limit is a range where the population mean is expected to be within a certain level of probability called confidence level (METU 2007). The confidence limits can be found for a selected confidence levels as:

$$\bar{x} \pm z_c \sigma_{\bar{x}}$$
(4-4)

Where;

$\bar{x}$: Sample mean

z_c: Critical z value for selected confidence level

$\sigma_{\bar{x}}$: Standard error of sample means

The central limit theorem only applies to large samples (n > 30). When the sample is small (n < 30) the shape of the sampling distribution depends on the shape of the background population. For small samples, the sampling distribution has a form known as "t-distribution". Unlike normal distribution, the shape of the t-distribution depends on the sample size (METU 2007).

The confidence limit for small samples is:

$$\bar{x} \pm t_c \sigma_{\bar{x}}$$

(4-5)

4.4 Results

This is the last step of the methodology. Results step contains comparisons of applied methods, comparisons of the users' results in third method and interpretations according to these results. Results of applied analysis are mostly explained with tables, graphs and illustrated in maps.

CHAPTER 5

CASE STUDY

This chapter describes the case study designed in the context of error modeling in height measurements of human made structures in urban areas by utilizing three different methods. In this chapter, detailed information regarding the definition of the case study, data sources, errors in the data source, the steps taken to carry out error modeling are provided.

In order to obtain height values of the buildings for 3D modeling, three methods are selected and applied to a case study. The first method is calculating height values according to number of floor, which is obtained from city information section of the municipality and updated according to field study. The second method is segmentation of Digital Surface Model (DSM) which is generated from stereo satellite images. The last one is user based measurement method. In this method, the height values of the buildings are measured from the stereo satellite images of IKONOS by different users. The results of these three methods are compared with the height values of the buildings acquired from the field study, which are considered to be the most accurate, in order to discover the more accurate method. Additionally, accuracy results for each method are evaluated by classifying the errors according to the number of floors. By this way, it is tried to generalize the results so that they can be applied to similar studies.

5.1 Selection of the Study Area

The scope of this study is determined based on the availability of required dataset of a district called Cumhuriye Neighborhood in Eskişehir, which is one of the cities of Turkey and in 39°47'N latitude and 30°31'E longitude of geographic coordinates. Cumhuriye Neighborhood lays down approximately 123.000 m^2 area and has 394 buildings in it.
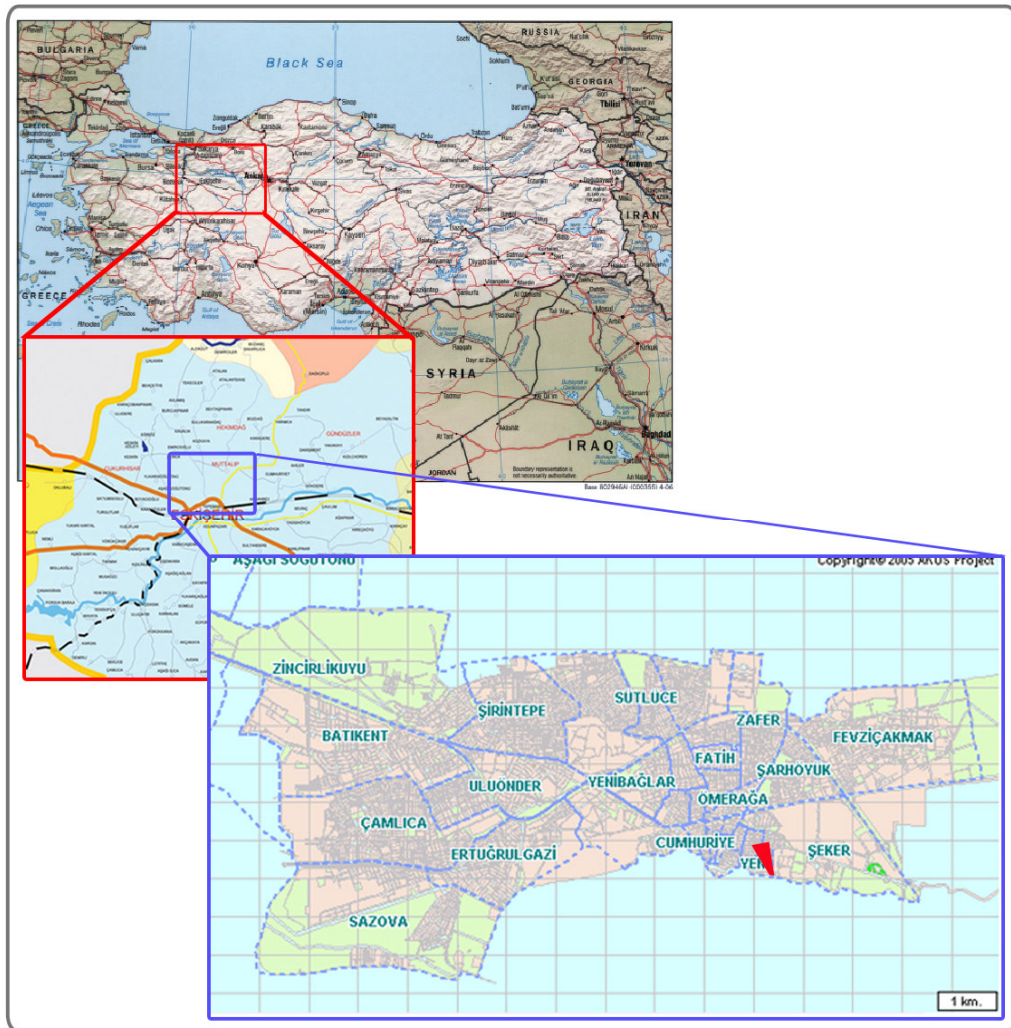
Figure 5-1: Location of the study area

Figure 5-2: Satellite image of the study area

Figure 5-1 shows the location of it in Eskişehir and in Turkey map and Figure 5-2 represents satellite image of Cumhuriye Neighborhood.

This study area is selected based on the following factors:

- Data availability, especially, the availability of IKONOS Precision Stereo Satellite Images: The Satellite images were purchased to be used for an ongoing research study in the department of Geodetic and Geographic Information Technologies of METU.

- The diversity of buildings' heights in the area: The area is a good representation of typical urban areas of Turkish cities, mixture of low and high building heights.

- Sample size or the numbers of buildings that exist in the field are suitable for applying error modeling.

5.2 Description of Data

5.2.1 IKONOS Satellite Stereo Images

The IKONOS precision stereo images were taken along the city of Eskişehir and two stereo pairs of 1 m IKONOS images of the study area were acquired on 2002, which are displayed in Figure 5-3. The two stereo pairs were 8796x7900 pixels and 8708x7480 pixels respectively. The Satellite images were purchased to be used for an ongoing research study in the department of Geodetic and Geographic Information Technologies of METU.

Acquisition parameters for the precision stereo images are indicated in Table 5-1.

Table 5-1: Parameters of IKONOS precision stereo images

Parameters	Left Stereo	Right Stereo
Acquisition data & time (GMT)	2002-05-03 09:05	2002-05-03 09:06
Nominal Collection Azimuth (θ)	349.1478 degrees	246.7747 degrees
Nominal Collection Elevation (α)	65.43637 degrees	76.24377 degrees
Cross Scan (GSD)	0.98 meters	0.85 meters
Along Scan (GSD)	0.90 meters	0.86 meters
Scan Azimuth	270.04 degrees	270.04 degrees
Scan Direction	Reverse	Reverse
Sun Angle Azimuth	152.0464 degrees	152.4692 degrees
Sun Angle Elevation	63.70996 degrees	63.78503 degrees

IKONOS Stereo pairs are collected in the same orbital pass, minimizing changes in lighting or scene content. Images are epipolar projected and

resampled to a 1-meter increment for ease of display. The stereo images are provided with Rational Polynomial Coefficients (RPC) or Image Geometry Model (IGM), which describe the relationship between image pixels and ground positions (Web 1).

IKONOS Stereo products are provided in two different metric accuracies as Standard Stereo and Precision Stereo. In the case study precision stereo was selected which having 1 meter horizontal (RMSE) and 2 meter vertical (RMSE) accuracy.

| Right Stereo | Left Stereo |
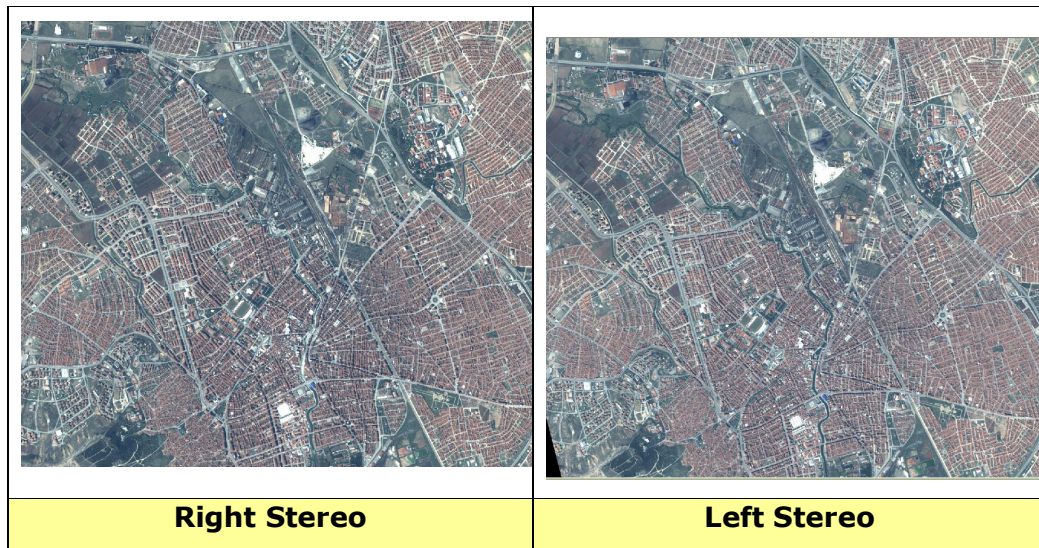
Figure 5-3: IKONOS precision stereo images

5.2.2 Definition of Ground Plan

The measured height values were stored in the ground plan of the study area, which has a format file of ESRI shape file data. It was requested from municipality of Eskişehir. The preparation year of the data was 2002.
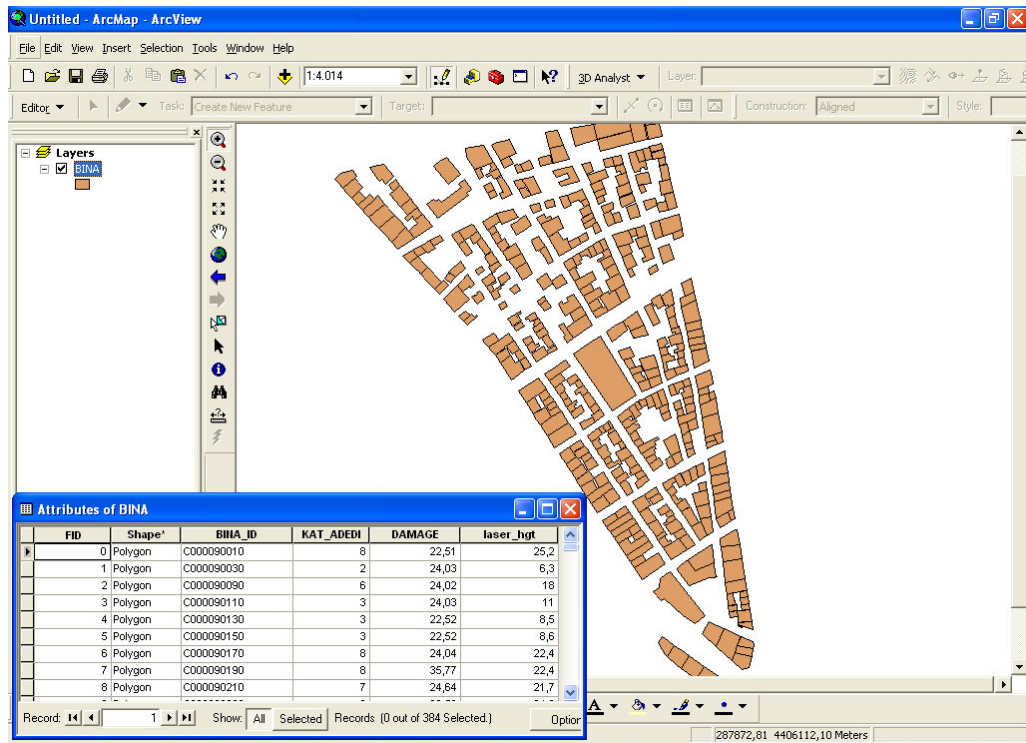
Figure 5-4: Esri shape data

It consists of only building layer, which has 387 entries and 5 attributes for each entry. As seen in the Figure 5-4, the attributes are FID as object ID type, Shape field as Polygon type, BINA_ID as string, KAT_ ADEDI field as short which gives number of floors of the building, and DAMAGE as a double which gives the information of percentage of the damages in the building.

5.2.3 Data Collection in the Field

The data collection in the field study is performed for obtaining more precise height values of buildings. This section describes how measurements are made and analyzed.

The height measurements are repeated 6 times in ground surveying for each building and completed in a week. The measurements have been

46

carried out by using range finder instrument. The collected measurements were recorded into the attribute tables of ESRI shape data that contains a layer of buildings of the study area.

TruPulse 200 Laser Range Finder is used to obtain height values of the buildings. Range finders have advanced digital technology designed for many applications requiring measurement of horizontal and vertical distance and other values such as speed, slope and angle. A laser range finder is a device, which uses a laser beam in order to determine the distance to an opaque object with high accuracy. Similar to a police radar gun, a laser range finder works by sending a laser pulse in a narrow beam towards the object and then measuring how long it takes for the pulse to bounce off the target and return to the sender. The laser range finders measure line-of-sight distance using eye-safe laser and precision electronics. The measurement range of the range finder is up to 3280 ft (1000 m) in distance and +/- 90 degrees as inclination. It has an accuracy of +/- 1 ft (+/- 30 cm) in distance and +/- 0.25 degrees as an inclination. The range finders need Pythagorean Function when distances cannot be measured directly e.g., if a target point is missing such as with a flat roof. (Figure 5-5).
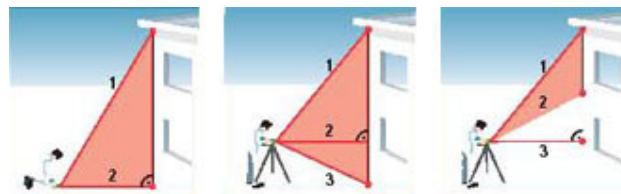
Figure 5-5: Pythagorean function

Six attributes for the measurements, which have field names as LASER1, LASER2, LASER3, LASER4, LASER5 and LASER6 has been added to shape file. Laser measurement results for each building are presented in Table A-1 in Appendix A.

Moreover the floor numbers which were obtained from municipality and dated 2002 were updated during the field study.

In order to insert acquired measured height values from range finder into computer systems, a mobile device and ESRI ArcPad as a software product has been used. An example interface of the software is displayed in Figure 5-6. Arcpad is software for mobile GIS and field mapping applications, which uses handheld or mobile devices. ArcPad provides field-based personnel with the ability to capture, analyze, and display geographic information. It is a thin client application that provides basic functions as loading data, displaying and making simple editing while in the field.

Additionally, a mobile device, which satisfies the software system requirements of ArcPad, has been used.
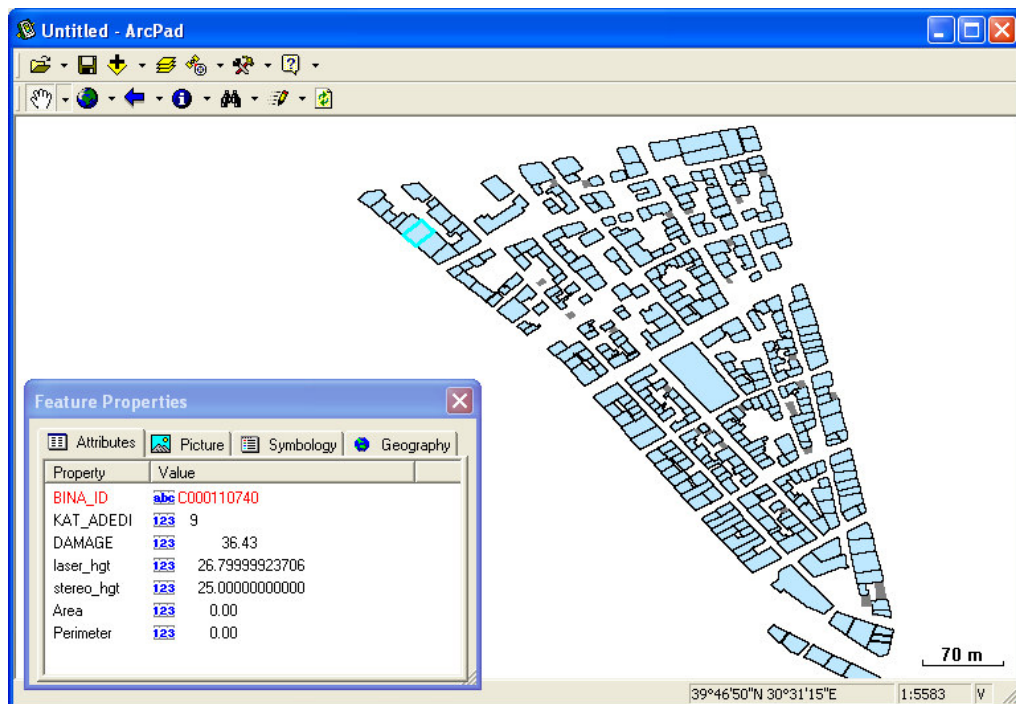
Figure 5-6: Snapshot of ESRI ArcPad software

5.3 Obtaining Building Heights

In this section obtaining building heights for each method are explained.

5.3.1 Obtaining Building Heights in Method 1

In Method 1, building height values are calculated by using number of floors. Equation 4-1 is used for the height calculations as defined in municipality regulations (Eskişehir Büyükşehir Belediyesi İmar Yönetmeliği, 2004). Therefore, floor numbers are multiplied by 3.00 m and summed with 0,5 m for finding each building height value. For the buildings which have shops at their basements extra floor numbers are added in the database.

The numbers of floors for the buildings are acquired as an attribute of a shape data from database of municipality and updated according to today's situation in field study. The creation year of the data is 2002. The distribution of the number of buildings according to the number of floors is displayed in the Table 5-2, which also contains number of buildings, used in the statistical analyses. Some buildings are not included in the analyses, because not all of the collected data is taken into account in the analysis. The reasons for exclusions will be explained in the following chapters, Figure 5-7 illustrates the distribution of buildings with their floor number in the study area.

Table 5-2: The Distribution of buildings according to floor numbers

Number of Floors	Number of Buildings	Number of Buildings Used in Statistical Analysis
0	6	0
2	81	70
3	76	73
4	90	90
5	40	35
6	25	25

7	10	10
8	25	24
9	37	37
10	4	4
Total:	**394**	**359**

LEGEND

(Floor Numbers of Buildings)

- 2
- 3
- 4
- 5
- 6
- 7
- 8
- 9
- 10

Figure 5-7: Floor numbers map of the buildings used in statistical analysis

The characteristics of the buildings are also considered. During the data collection in the field study, the information about existence of shops or

garages in the basements is added to databases as an additional attribute. Figure 5-8 represents buildings which have shops in their basements with dark color. The buildings that have shops in their basements were defined and checked with floor numbers data in the municipality database. As a result, it is found that these buildings have been entered with extra 2 floors to the database.

Figure 5-8: Buildings with or without Shops

For example the buildings labeled in Zone A of the Figure 5-8, has 9 floors according to database of the municipality. However, as it seen in the Figure 5-9, it has 7 floors and a shop floor in its basement. The building in Figure 5-9b and labeled Zone B in the Figure 5-8 has 5 floors according to database of the municipality, but in fact it has 3 floors and a shop as seen in the Figure 5-10. The building labeled as C has also same specification, it is 4 floored building and has a shop, but it is seen 6 floored building in the database as illustrated in the Figure 5-11.

These examples can be increased. Therefore, as the height of the shops are already included in the database, they are also included in the height computations of method 1.

Figure 5-9: An example building with shop at their basements in zone A

Figure 5-10: An example building with shop at their basements in zone B

Figure 5-11: An example building with shop at their basements in zone C

5.3.2 Obtaining Building Height in Method 2

IKONOS Precision Stereo Images are used for automatic generation of DEM and DSM. DEM generation is utilized with spatial analyst module of ARCView. Additionally, feature collection for DEM generation is developed with the help of ERDAS Stereo Analyst Module. A hundred and twenty four 3D features have been collected as point type. They are selected homogenously in the study area. Figure 5-12 shows the distribution of the selected point features, which are used in raster conversion. Inverse Distance Weighted method is selected as raster interpolation method.

FID	Shape	FID_1	Avg_Z
0	Point	1	827,09
1	Point	2	827,1
2	Point	3	827,1
3	Point	4	827,11
4	Point	5	827,11
5	Point	6	827,11
6	Point	7	827,1
7	Point	8	827,1
8	Point	9	827,09
9	Point	10	827,08
10	Point	11	826,39
11	Point	12	826,38
12	Point	13	826,38
13	Point	14	826,38
14	Point	15	827,08
15	Point	16	827,07
16	Point	17	827,07
17	Point	18	827,07
18	Point	19	827,07
19	Point	20	827,07
20	Point	21	827,08
21	Point	22	827,07
22	Point	23	827,77
23	Point	24	827,77
24	Point	25	827,77
25	Point	26	827,76
26	Point	27	827,76
27	Point	28	827,76
28	Point	29	827,75

Figure 5-12: Selected points used for DEM generation

For automatic generation of Digital Surface Model (DSM) from satellite stereo images, fifty tie points has been selected on the overlapping images. Tie points are the common points in overlapping areas of two or more images. They connect the images in the block to each other and are necessary input for the triangulation. Tie points are necessary for accuracy checking of the generated DSM.

Once DSM has been successfully extracted, a corresponding DSM ASCII report is created which gives information about general information such as processing time, size of DSM, type of DSM, strategy parameters used and their settings, RMS errors associated with each set of 3D reference information and global quality of the output DSM. Table 5-3 shows vertical and global accuracy information of generated DSM.

Table 5-3: DSM generation report

Parameters	Vertical Accuracy	Block Tie Point to DTM Vertical Accuracy
Total # of 3D Reference Points Used:	49	49
Minimum, Maximum Error:	-1.9601, 4.6346	-1.9601, 4.6346
Mean Error:	0.1059	0.1059
Mean Absolute Error:	1.0093	1.0093
Root Mean Square Error (RMSE):	1.3373	1.3373
Absolute Linear Error 90 (LE90):	1.9601	1.9601
NIMA Absolute Linear Error 90:	+/- 1.4441	+/- 1.4441

In order to evaluate Method 2, the first Digital Elevation Model (DEM) is generated. Then Digital Surface Model (DSM) is created, which contains building features on it. Afterwards raster calculation is performed, which is subtraction of DSM raster from DEM raster for acquiring building heights. Lastly zonal statistical analyses are performed, which is calculation of height of each zone defined in building shape data, based on values from resultant raster found in raster calculation.

Digital Terrain Model (DTM) is generated for the study with the aid of 124 points which are selected from IKONOS Precision Stereo Images. They are selected homogenously in the study area. In Figure 5-13, generated DEM is illustrated. As seen from the Figure 5-13, the selected study area is almost flat area that the maximum difference of the height is 2,62 m.

In order to generate DSM from precision stereo images, ERDAS IMAGINE / Leica Photogrammetry Suite OrthoBASE & OrthoBASE Pro, is used as a

software tool, which constitutes a comprehensive software packet for analysis and processing of spatial data. (Leica Photogrammetry Suite OrthoBASE & OrthoBASE Pro User's Guide, 2003) In Figure 5-14 the generated DSM with shape file of buildings polygons is illustrated.
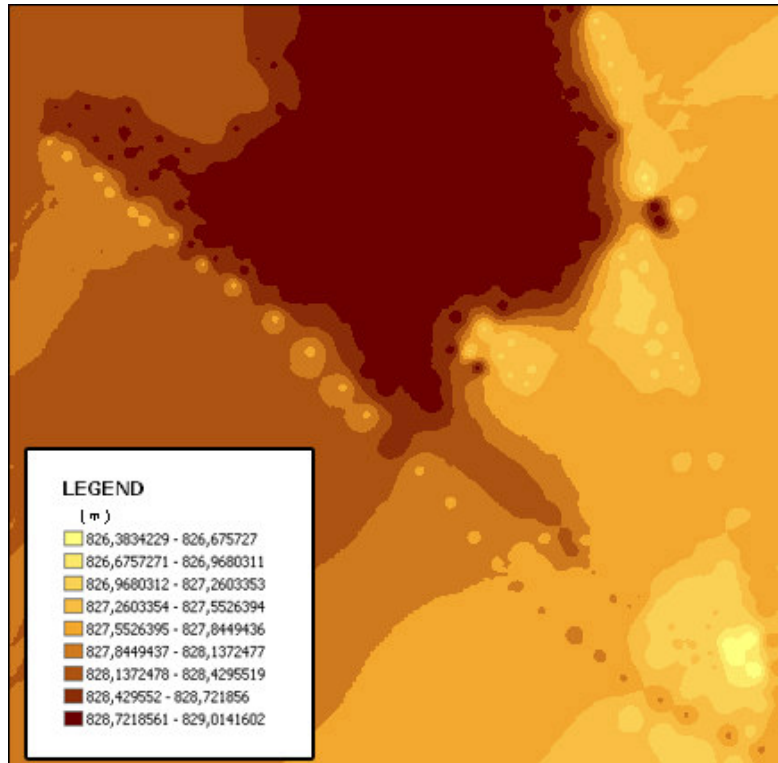
Figure 5-13: Generated DTM
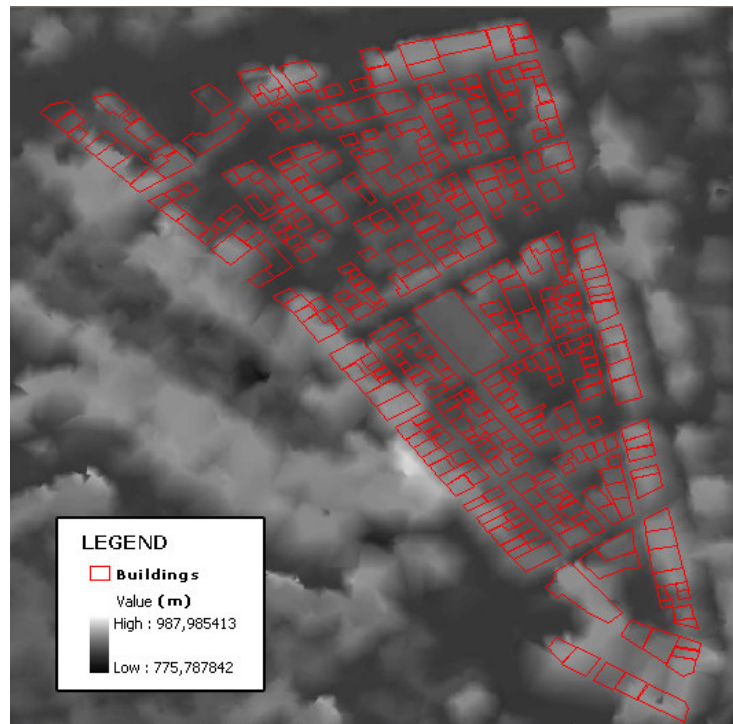
Figure 5-14: Generated DSM with shape file of building polygons

Raster calculation is simply performing mathematical calculations using operators and functions on raster data. Generated DEM and DSM are used as input raster for the calculation. In order to get height values of the buildings, raster data of DSM is subtracted from DEM raster. A new raster data is created as an output of this operation.

Zonal functions take a raster data as input and for each cell or defined zone, calculate some function or statistic using the value of the cell or all cells belonging to the same zone. With Zonal Statistics, building height is calculated for each zone defined by building polygons in shape data, based on difference between DSM and DEM raster. Zonal statistical functions perform operations on a per-zone basis; a single output value is computed for every zone in the input zone dataset.

Between the computable statistics, mean value calculation, which computes average value of each cell belonging to the building polygon, is used in the study. Therefore, the mean value of each cell of the building

polygons gives us the height value of the buildings. Results of the zonal statistic calculation are given in Table A-3 in APPENDIX A.

5.3.3 Obtaining Building Height in Method 3

This section describes the methodology used in obtaining building heights from IKONOS precision stereo satellite images. First, satellite images and used software is explained, and then information about the users who perform measurements are given.

In order to visualize stereo pairs of IKONOS satellite images, commercial of-the-shelf software Stereo Analyst for ERDAS IMAGINE is utilized. ERDAS IMAGINE constitutes a comprehensive software package for analysis and processing of spatial data. This package serves to elaborate, process and use satellite images, aerial photographs, and radar images as well as GIS data.

Stereo Analyst module allows users to perform 3D model generation, interpretation, measurement, visualization, 3D feature collection and stereo editing. In addition, software lets users to access, collect, edit, update image and feature data, collect points for the creation of elevation models, and seamlessly work in conjunction with ArcMap.

In order to get 3D visualization from stereo images, stereo shutter glasses should be used. An example of stereo shutter glasses is displayed in Figure 5-15. Stereo3D with shutter glasses is realized in such a way that 50% of rendered pictures will be displayed to the left, and the other 50% to the right eye. The technique, which is called "time-sequential multiplexing" will alternately display left- and right-eye images every time the computer refreshes (draws) the screen.

Shutter glasses are synchronized to these altering images. There are 2 LCDs, one directly in front of each eye. Each LCD can eye's view to the

screen. When an image for the left eye is drawn on the monitor, the LCD of the right eye will block the right eye's view and the other way round. As a result, 3D stereoscopic representation is achieved.

Figure 5-15: Stereo 3D shutter glasses

The measurements from stereo views were repeated 10 times with the aid of ten different people. The operators are selected from three different experience levels as advance users, moderately experienced users and inexperienced users. Each user is asked to measure height of 359 buildings from the stereo images using stereo 3D shutter glasses, and software.

As seen from the Table 5-4, there is one well experienced user who deals with 3D models for 3 years in her professional work. 5 people selected as moderately experienced user which means that they have at least one experience with stereoscopic measurement or have an idea about it. They are selected from staff of Geodetic and Geographic Information Department of Middle East Technical University. Inexperienced users are people who are not familiar to stereo satellite images and all of them saw stereo pairs at the first time.

The results of these measurements that belong to 10 users are presented in the Table A-2 in APPENDIX A.

Table 5-4: Number of people according to experience level

Number of People	Level
1	Well experienced
5	Moderately experienced
4	Inexperienced

5.4 Uncertainty Analysis of Field Measurements

After completing measurements from the field study, "Error Propagation Law" is utilized, in order to find out accuracy of measured building heights. As specified in the user manual of the range finder device, it has an accuracy of +/- 1 ft (+/- 30 cm) in distance and +/- 0.25 degrees as an inclination. (Range Finder User Manual, 2003) According to these specifications, the error in height measurement is calculated by applying "Error Propagation Law".

The term is seen in many places in the literature with some authors giving its derivations (Leung et al., 2004). According to Heuvelink (1998), since a model is only an approximation of reality, and because the inputs to the model are rare, if ever, exactly known, the output of the model is also likely to deviate from reality. In other words, uncertainties that are contained in the model and its inputs will propagate to the model output. Hence, it becomes important to know how large the uncertainties in the model output are, particularly when the model is used for predictive purposes.

The theory of error propagation can be explained as below;

Consider the following equation:

$$y = g(z_1, z_2, z_3, ... z_n) \qquad \text{(5-1)}$$

Where g is a continuously differentiable function from real numbers into real numbers. Equation (5-1) is a generalized form which is more suited for the analysis that will follow (Heuvelink et al., 1989).

Let U be a function measured quantities X, Y, Z, ..., Q. This can be written as; U = f(X, Y, Z ..... Q) If each independent variable is allowed to change by a small amount dX, dY, dZ .... dQ, then the quantity U will change by an amount dU which is equal to;

$$\partial U = \frac{\partial U}{\partial X} \partial X + \frac{\partial U}{\partial Y} \partial Y + \frac{\partial U}{\partial Z} \partial Z + ... \frac{\partial U}{\partial Q} \partial Q \qquad \textbf{(5-2)}$$

In this equation $\partial U / \partial X$ denotes the partial derivative of U with respect to X, and likewise for the other variables. Applying this to a set of measurements, and by assuming the residuals as small quantities $x_i = dx_i$, $y_i = dy_i$, $z_i = dz_i$ and finally $u_i = du_i$ the equation is written as;

$$u_1 = \frac{\partial U}{\partial X} x_1 + \frac{\partial U}{\partial Y} y_1 + \frac{\partial U}{\partial Z} z_1 + ... \frac{\partial U}{\partial Q} q_1$$

$$u_2 = \frac{\partial U}{\partial X} x_2 + \frac{\partial U}{\partial Y} y_2 + \frac{\partial U}{\partial Z} z_2 + ... \frac{\partial U}{\partial Q} q_2$$

$$u_n = \frac{\partial U}{\partial X} x_n + \frac{\partial U}{\partial Y} y_n + \frac{\partial U}{\partial Z} z_n + ... \frac{\partial U}{\partial Q} q_n \qquad \textbf{(5-3)}$$

If the both sides are squared in equation (5-3), the equation can be written as in (5-4). This equation is the general error propagation law and can be applied to any function (Moffitt and Bossler, 1997).

$$\sigma_u^2 = \left(\frac{\partial U}{\partial X}\right)^2 \sigma_x^2 + \left(\frac{\partial U}{\partial Y}\right)^2 \sigma_y^2 + \left(\frac{\partial U}{\partial Z}\right)^2 \sigma_z^2 + ...\left(\frac{\partial U}{\partial Q}\right)^2 \sigma_q^2 \qquad \textbf{(5-4)}$$

The height measurement instrument used in field study requires users to take three shots to the target. First shot is taken to the surface of the building to measure horizontal distance (s) and the inclination of laser beam (δ). Other two shots are taken to measure inclination of the bottom (β) and the top (α) of the building. After completing three shots, the device automatically calculates the height of the target, and the results are displayed in the LCD.

Figure 5-16 illustrates three shots required for the height routine.

α = Top Angle
β = Base Angle
δ = Horizantal Angle
s = Horizantal Distance
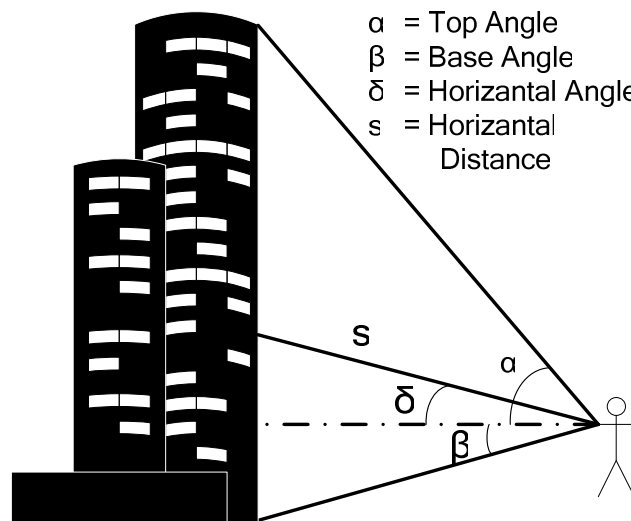
Figure 5-16: Height measurement routine

Equation 5-5 is used to calculate the height of the building.

$$h = s \times \cos(\delta) \times \left[(\tan(\alpha) + \tan(\beta)) \right]$$
(5-5)

According to equation of error propagation law, Equation 5-3 applied on the Equation 5-5 which is used to calculate the height of the building.

$$\sigma^2 h = \begin{bmatrix} \dfrac{\partial h}{\partial \alpha} & \dfrac{\partial h}{\partial \beta} & \dfrac{\partial h}{\partial \delta} & \dfrac{\partial h}{\partial s} \end{bmatrix} \begin{bmatrix} \sigma^2\alpha & 0 & 0 & 0 \\ 0 & \sigma^2\beta & 0 & 0 \\ 0 & 0 & \sigma^2\delta & 0 \\ 0 & 0 & 0 & \sigma^2 s \end{bmatrix} \begin{bmatrix} \dfrac{\partial h}{\partial \alpha} \\ \dfrac{\partial h}{\partial \beta} \\ \dfrac{\partial h}{\partial \delta} \\ \dfrac{\partial h}{\partial s} \end{bmatrix}$$

$$\frac{\partial h}{\partial \alpha} = s \times \cos(\delta) \times \sec^2(\alpha)$$

$$\frac{\partial h}{\partial \beta} = s \times \cos(\delta) \times \sec^2(\beta)$$

$$\frac{\partial h}{\partial \delta} = -s \times \sin(\delta) \times (\tan(\alpha) + \tan(\beta))$$

$$\frac{\partial h}{\partial s} = \cos(\delta) \times (\tan(\alpha) + \tan(\beta))$$

$$\sigma^2 h = (s \times \cos(\delta) \times \sec^2(\alpha) \times \sigma\alpha)^2 +$$
$$(s \times \cos(\delta) \times \sec^2(\beta) \times \sigma\beta)^2 +$$
$$(-s \times \sin(\delta) \times (\tan(\alpha) + \tan(\beta)) \times \sigma\delta)^2 +$$
$$(\cos(\delta) \times (\tan(\alpha) + \tan(\beta)) \times \sigma s)^2$$

Accuracy specification of the measurement device states that, the device has 0,30 meter accuracy on high quality targets and 0,25° accuracy on inclination measurements. In Table 5-5 the error values for different α and β angles are listed. Note that while generating the values in the Table 5-5 "s" is taken as 10m and δ is taken as 0°. The error in the height measurement increases with increasing α and β angles, which is clearly observed from Table 5-5, However also note that increasing α and β angles means that measurements are taken closer to the building, which means "S" is decreasing.

Table 5-5: Error values for different α and β degrees

β \ α	75°	70°	65°	60°	55°	50°	45°	40°	35°	30°
20°	1,392	1,006	0,793	0,654	0,556	0,481	0,421	0,372	0,330	0,293
18°	1,217	0,922	0,741	0,617	0,526	0,455	0,397	0,349	0,308	0,271
16°	1,206	0,910	0,729	0,606	0,514	0,444	0,386	0,338	0,296	0,259
14°	1,194	0,899	0,718	0,594	0,503	0,432	0,375	0,327	0,285	0,248
12°	1,183	0,888	0,707	0,583	0,492	0,421	0,364	0,315	0,274	0,237
10°	1,173	0,877	0,696	0,573	0,481	0,410	0,353	0,305	0,263	0,226
8°	1,162	0,866	0,686	0,562	0,471	0,400	0,342	0,294	0,252	0,215
6°	1,151	0,856	0,675	0,551	0,460	0,389	0,332	0,283	0,242	0,205

In addition to the quality control of measurement instrument and the collected data, there is another problem that provides an opportunity of further improvement. The preparation year of the data, which contains floor number of buildings, is 2002. Thus, some changes have to be made to update the data, which were collected in field study. Hence the floor number data set is updated by using filed study and building height from method 1 are calculated by using updated dataset.

In order to be sure about accuracy analysis with Stereo Images and DEM; and also to avoid confusions in the statistical calculations, 35 buildings has been excluded from the statistical calculations. These 35 buildings have big differences when comparing today's height values and height values in the stereo images from which has an acquisitions year of 2002. Probably these buildings have been constructed and increased their height values. Some of the buildings were reconstructed after 2002 and some of them were added extra floors. The excluded buildings can be seen in the Figure 5-17 with highlighted color.

Figure 5-17: Excluded buildings

Hence to be consistent in all of the methods, 359 buildings in the study area is considered in height error analyses.

As mentioned before, the measurements of 359 buildings in the study area are repeated six times by the help of range finder measurement instrument. The results of the measurements are listed in Table A-1 in Appendix A.

According to the measurement results, the mean, variance and standard deviation are calculated for each building. Using calculated descriptive statistics, standard deviation of the sample mean ($\sigma_{\bar{x}}$), standard error, and confidence limits are obtained with 95% confidence interval (Table A-1 in Appendix A).

The mean values of the measurements for each building are classified according to floor numbers of building. Results of this calculation are displayed in the Table 5-6.

Table 5-6: Mean values of building height measurements in field study

Number of Floors	Number of Buildings	Number of Measurements	Mean
2	70	6 x 70	6,01
3	73	6 x 73	9,30
4	80	6 x 80	11,49
5	35	6 x 35	13,15
6	25	6 x 25	16,06
7	10	6 x 10	19,33
8	25	6 x 25	20,25
9	37	6 x 37	24,71
10	4	6 x 4	26,00

Figure 5-18 represents 95% confidence intervals for the height measurements for each building in the field study. As seen in the legend, the maximum error interval is equal to 1,51 - 3,30 m which are determined for only 9 buildings' (2,5% of 359 buildings in the study area). The minimum error interval is 0 – 0,25 m, which are calculated for 140 buildings. Approximately 75% of the buildings (271 buildings) have an estimated mean error in the 95% confidence limits under 0,50 m.
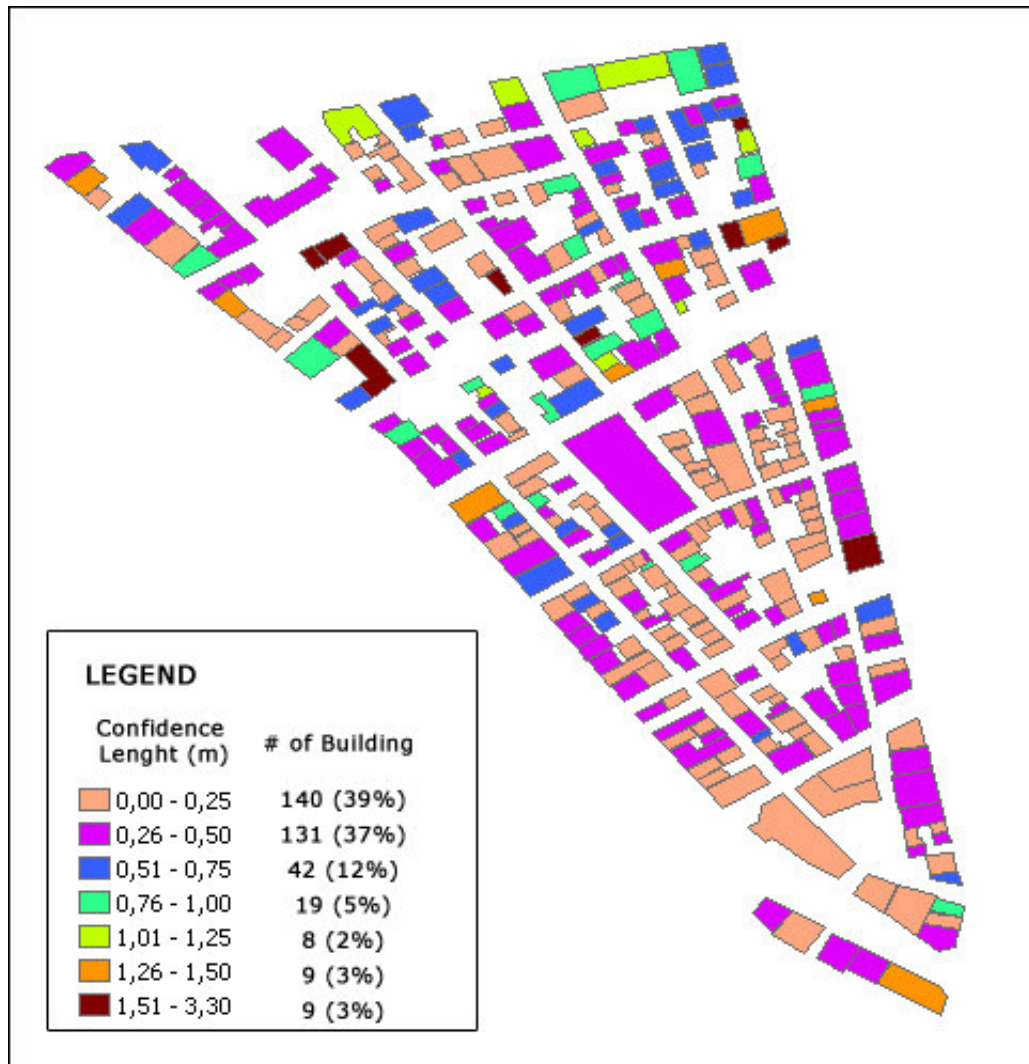
Figure 5-18: Confidence interval length of the field study results

5.5 Analyses of Errors in the three Methods

This section describes the statistical methods used to evaluate the error in the height obtained from number of floors (Method 1), DSM and DEM (Method 2) and satellite images (Method 3) when compared to the reference data, which were acquired from the field study. The methods being used in this case study include descriptive statistics, zonal statistics and analysis with representations of the statistical analysis on maps.

5.5.1 Method 1: Number of Floors

As mentioned in the Chapter 4, obtained data for method 1 is analyzed statistically. First, error value for each building is calculated. In order to find the error value, the mean values of the measured height values in the field study are subtracted from height values that are obtained from number of floors multiplication for each building. Table 5-7 shows calculated descriptive statistics for error. According to these results the mean error is -0,587 meter, standard deviation is found as 1,668 and the length of 95% confidence intervals are calculated as 0,345 with using Equation of (4-7).

Table 5-7: Descriptive statistics for method 1

Number of Measurements (N)	359
Mean Error	-0,587
Std. Deviation (σ)	1,668
Std. Error ($\sigma_{\bar{x}}$)	0,088
%95 Confidence Limits	-0,759 − -0,414
%95 Confidence Length	0,345
Variance	2,781

Furthermore, the descriptive statistics for error value is calculated splitting data according to floor numbers. Table 5-8 presents descriptive statistics according to number of floors, which is located in the first column of the table.

Table 5-8: Descriptive statistics for method 1 according to floor numbers

# of Floors	n	Mean Error	Std. Deviation	Variance	Std. Error	95 % Confidence limits	% 95 Confidence Length
2	70	-1,17	1,69	2,87	0,10	-1,17 ± 0,19	0,40
3	73	-0,29	1,64	2,69	0,10	-0,28 ± 0,18	0,38
4	80	-0,72	1,45	2,09	0,08	-0,71 ± 0,15	0,32
5	35	-0,30	1,60	2,55	0,13	-0,29 ± 0,26	0,53
6	25	-0,04	2,11	4,44	0,21	-0,04 ± 0,41	0,83
7	10	-1,27	1,67	2,79	0,26	-1,26 ± 0,51	1,04
8	25	-0,28	1,69	2,84	0,17	-0,28 ± 0,33	0,66
9	37	-0,44	1,61	2,60	0,13	-0,43 ± 0,25	0,52
10	4	-0,75	1,74	3,04	0,44	-0,75 ± 0,85	1,71

As seen in the Table 5.8, the buildings which have 7 floors have maximum mean error value as -1,27 m, and 10-floored buildings have the maximum confidence length as 1,71 m. However all of the mean values are in acceptable range and minimum mean error value of 0,04 m is achieved in 6 floored buildings. There is not a significant relation between the number of floors and the mean error in the method 1 as seen in the Figure 5-19.

According to Figure 5-19, all the buildings are overestimated with negative mean error values. The reason for that may be the floor number formulation which is based on the regulations of the municipality. According to Equation 4-1, the height value of each building is found by multiplying floor numbers with 3.00 m and summed with 0,5 m. However, this regulation could be unconsidered by the constructors of the buildings and the height value for each floor may be less than 3 m. In addition to this, the old buildings' floor heights were lower than today's buildings' floor heights.
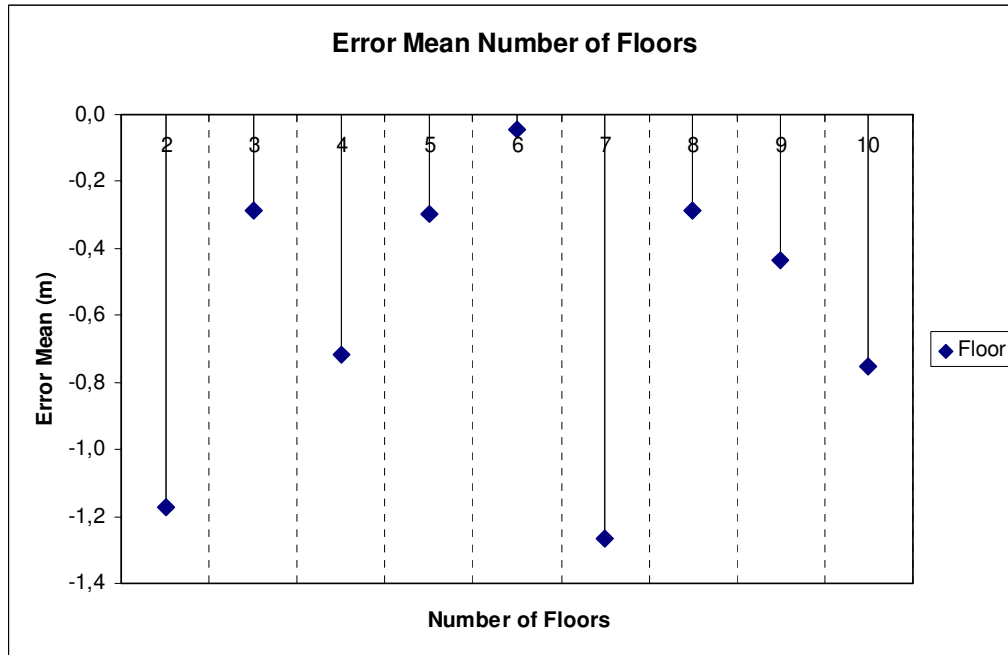
Figure 5-19: Mean error graph for method 1

Figure 5-20 represents spatial distribution of the error values, which are obtaining from Method 1. The error values are grouped and illustrated with different colors on the map. Moreover, Table 5-9 contains mean error ranges which are mapped in Figure 5-20 and numbers of buildings in percentages within each range are listed. According to Table 5-9, most of the buildings have mean error values between -0,50 and 0,50 m, with a percentages of 44%. The values between -2,00 and +2,00 m are considered to be the acceptable level of accuracy, 99,44% of the whole buildings have an mean error value between -2,00 and +2,00 m according to height estimation of Method 1.

Figure 5-20: Spatial distribution of error values in method 1

Table 5-9: Mean error ranges and percentages of buildings for method 1

	Mean Error Ranges (m)	Percentages of Buildings	Comment
	-7,23 - -4,00	2,23%	Overestimated
	-3,99 - -2,00	17,27%	Overestimated
	-1,99 - -0,51	26,18%	Acceptable Level Of Accuracy
	-0,50 – 0,50	31,48%	Acceptable Level Of Accuracy
	0,51 – 2,00	17,83%	Acceptable Level Of Accuracy
	2,01 – 3,87	5,01%	Underestimated

As seen in the Figure 5-20, the error ranges are quite variable and this makes difficult to determine the specific areas which have less or higher error values. In order to explore how the mean error value varies across the study area, "Spatial Moving Average" method is applied to smooth out the mean error in Figure 5-20. The spatial proximity should be defined before applying spatial moving average. Mostly, the general tool of (n x n) spatial proximity matrix W is generated for this purpose. In the matrix, W_{ij} represents each of its elements and Ai and Aj shows a measure of the spatial proximity of areas. As a rule, the choice of W_{ij} depend, upon the sort of data that one is dealing with and the particular mechanisms through which one expects spatial dependence to arise. The Equation 5-6 given by Bailey and Gatrell, (1995) is selected;

$$W_{ij} = \begin{cases} A_j \text{ shares a common boundary } A_i \\ 0 \text{ otherwise} \end{cases} \qquad \textbf{(5-6)}$$

In the generated W matrix, in order to estimate global variations and trends in the values of an attribute (mean error) over the areas is to estimate μ_i by an average (usually weighted) of the values in "neighbouring" areas. The spatial proximity matrix W provides a flexible method of defining a suitable set of weights for neighbouring areas and smoothed estimate is then calculated by using Equation 5-7;

$$\hat{\mu}_i = \frac{\sum_{j=1}^{n} w_{ij} y_j}{\sum_{j=1}^{n} w_{ij}} \qquad \textbf{(5-7)}$$

By applying the Equation 5-7 on error values of the building height values according to criteria defined in Equation 5-6, a smoothed map is generated as seen in the Figure 5-21.

Figure 5-21: Spatial moving average applied to method 1

Figure 5-21 shows spatial moving average applied to mean error values of the building according to Method 1. In Figure 5-21, the areas of the buildings which have minimum and maximum error amounts are defined in zones and labeled. In the zone A, there are buildings which have an error values between -4,00 m and -4,85 m. In Figure 5-22, there is an example building which has 4 floors with its extensions in the roof. However it has error values between 4,00 and 4,85 m which equals approximately 1,5 floors. Probably, during the data collection in the field study the roof extension of the building can not be seen from the basement and were not added to total height value of the building.

Figure 5-22: An example building in zone A

In zones B, C, D, E, and G there are buildings which have error value ranges of 2,00 and 3,87 m which are underestimated. The reason of this error value is the lower floor heights of the buildings. For example, in the zone E, there is a building with 2 floored, which is also represented in the Figure 5-23. When calculating its height according to Equation 4-1, it is found that the height of the building should be 6,50 m. However, it was measured as 5,00 m in the field study with range finder.

Figure 5-23: An example building in zone E

A special case is defined in the zone F, where a building that serves for military purposes is located. It has 8 floors according to database, and as seen in the Figure 5-24, it has 6 floors and plus 2 floors for high entrance. However, this building's floor heights are higher than 3,00 m especially the terrace floor at the top an the entrance floors.

Figure 5-24: An example buildings in zone F

5.5.2 Method 2: DTM and DSM

As mentioned in Section 4.2.2, acquired height value from zonal statistics of calculated DEM is subtracted from mean value of height values collected in the field study in order to find error value for each building. Descriptive statistics of the error values are calculated, which can be observed in the Table 5-10.

Table 5-10: Descriptive statistics for method 2

Number of Measurements (N)	359
Mean Error	1,494
Std. Deviation (σ)	2,13
Std. Error ($\sigma_{\bar{x}}$)	0,112
%95 Confidence Limits	1,274 – 1,714
%95 Confidence Length	0,44
Variance	4,541

Furthermore, the descriptive statistics for error value of DEM data is calculated grouping the data according to the floor numbers. Table 5-11 presents descriptive statistics according to number of floors and in Figure 5-25 line graph of mean error for different floors numbers are presented.

Table 5-11: Descriptive statistics of method 2 according to floor numbers

# of Floors	n	Mean Error	Std. Deviation	Variance	Std. Error	95 % Confidence limits	% 95 Confidence Length
2	70	-1,61	3,99	15,95	0,48	-1,60 ± 0,93	1,87
3	73	-0,54	3,73	13,93	0,44	-0,53 ± 0,85	1,71
4	80	1,04	2,84	8,05	0,32	1,04 ± 0,62	1,24
5	35	1,43	5,06	25,65	0,86	1,43 ± 1,67	3,36
6	25	0,41	3,13	9,83	0,63	0,40 ± 1,22	2,46
7	10	-0,57	6,74	45,49	2,13	-0,56 ± 4,18	8,36
8	25	2,57	4,96	24,63	0,99	2,57 ± 1,94	3,89
9	37	4,08	5,47	29,92	0,90	4,07 ± 1,76	3,53
10	4	0,62	1,79	3,22	0,90	0,61 ± 1,75	3,51
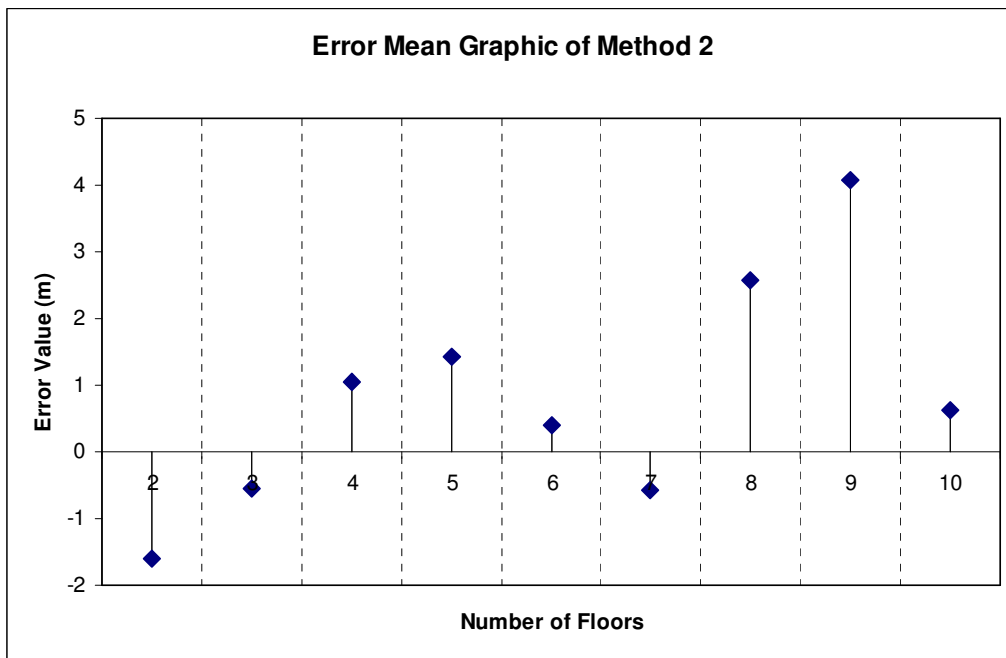
Figure 5-25: Graph of mean error for method 2

According to Table 5-11 and Figure 5-25, the buildings which are 9 floored have maximum mean error and on the contrary the 3, 6, 7 and 10 floored buildings have small mean errors.

Figure 5-26 shows spatial distribution of error values of the building according to Method 2. As seen from the Figure 5-26, the range of the error is changing -17,62 m to 21,08 m and this range is separated into intervals. Each interval is represented with different colors. The light colors show low error values and dark colors show high error values.

In order to explore how the mean error value varies across the study area, "Spatial Moving Average" method is applied, and generated map is illustrated in the Figure 5-27.
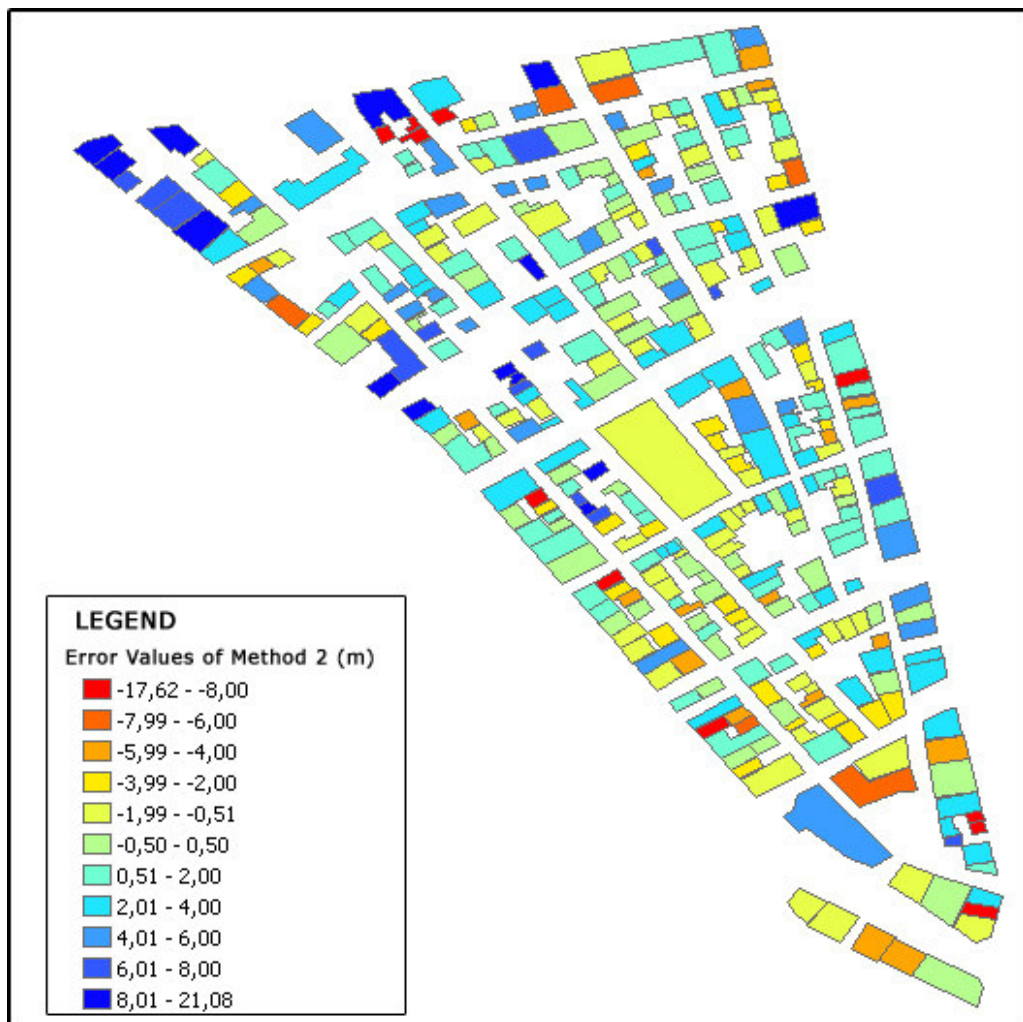
Figure 5-26: Spatial distribution of error in method 2

Moreover, Table 5-12 contains mean error ranges which are mapped in Figure 5-26 and numbers of buildings in percentages in these ranges are listed. According to Table 5-12, %20 of the buildings have mean error values in between +0,50 and +2,00 m. The values in between -2,00 and +2,00 m are considered to be acceptable error levels and totally 50% of the buildings have an mean error value between -2,00 and +2,00 m according to height estimation of Method 2.

Table 5-12: Mean error ranges and percentages of Buildings for method 2

	Mean error Ranges (m)	Percentages of Buildings	Comment
	-17,62 - -8,00	3,06%	Overestimated
	-7,99 - -6,00	1,67%	Overestimated
	-5,99 - -4,00	5,01%	Overestimated
	-3,99 - -2,00	8,64%	Overestimated
	-1,99 - -0,51	18,38%	Acceptable Level Of Accuracy
	-0,50 – 0,50	14,21%	Acceptable Level Of Accuracy
	0,51 – 2,00	19,50%	Acceptable Level Of Accuracy
	2,01 – 4,00	14,48%	Underestimated
	4,01 – 6,00	7,24%	Underestimated
	6,01 – 8,00	3,90%	Underestimated
	8,01 – 21,08	3,90%	Underestimated

Figure 5-27: Spatial moving average applied to method 2

In the Figure 5-27, the locations of the buildings which have minimum and maximum error amounts are defined in zones and labeled. As seen in the legend, blue colored zones represent underestimated calculations in Method 2. In the zone A, there are buildings which have an error value more than 6 m and 8 m to 18 m. These error values are too much and most probably, the reason for these high error values is propagation of errors in DTM and DSM. As seen in the Figure 5-14, the area of zone A has low height values in the generated DSM which is shown in dark color. Zone B, E, F, and E also represent high error values and the reasons of these results are the same with Zone A.

In Zones C, D, I, H, J, and K, there are buildings which have overestimated height values and they are illustrated with orange and red colors as in the legend of the map. The common reason for the high amount of error in these buildings is their location among the surrounding buildings which are quite high. In Figure 5-28, an example to this situation in zone K is illustrated.

Figure 5-28: An example building in zone K

5.5.3 Method 3: Manual Measurement from Stereo Pairs
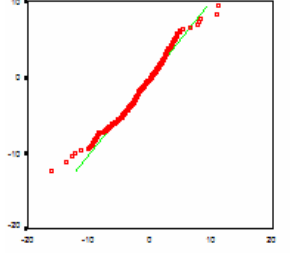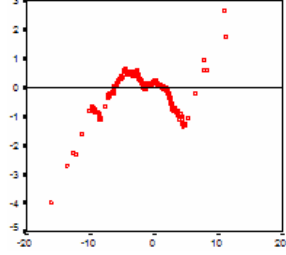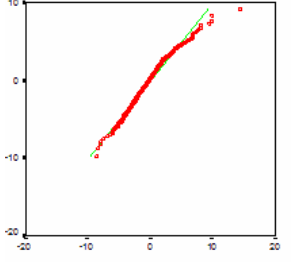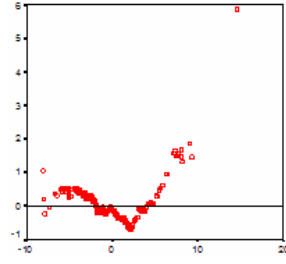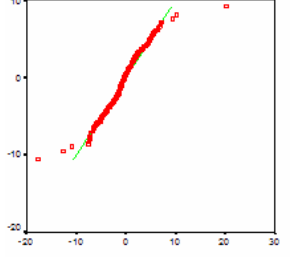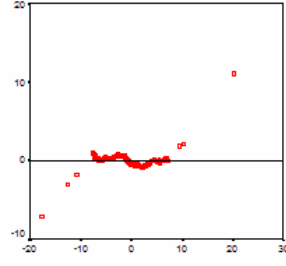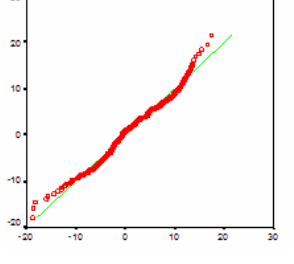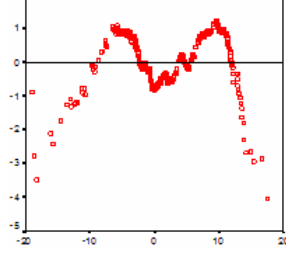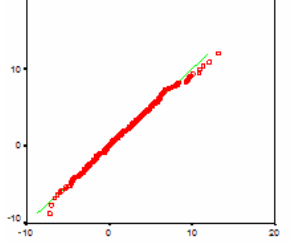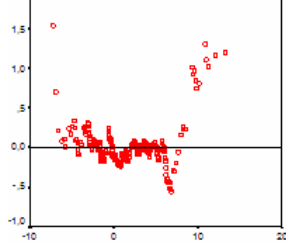
Similar to the previous two methods, in order to evaluate the third method, user measurements are compared with the building height values obtained from the field study. Then descriptive statistics of the user measurements are presented similar to the previous methods, as a whole and per number of floor basis. Also in this method measurements are presented and compared according to the experience level of the users.

Before starting to analyze users' errors, whether users' errors are normally distributed or not, should be checked. Generally statistics such as confidence intervals could only be applied to the normally distributed random variables. For this purpose Q-Q Plots for each user is drawn and presented in the Table 5-13. As can be seen in Table 5-13, most of the user's error are close to normal distribution, except for users 2, 6, 8 and 10. Hence in this study user errors are assumed to have normal distribution

Secondly, several analyses have been performed according to each user's error. User based analyses also contains, descriptive statistics calculations and descriptive statistics according to number of floors so that an idea about error level for each of user can be obtained. The third part of the analysis are comparing user measurement errors with each other by calculating descriptive statistics, analyzing the results with graphics and representing their spatial distribution on maps.

Table 5-13: Q-Q plot for users' errors

User ID	Normal QQ Plot	Detruded Normal QQ Plot
1		
2		

Table 5-13: Q-Q plot for users' errors		
User ID	Normal QQ Plot	Detruded Normal QQ Plot
3		
4		
5		
6		
7		

83

	Table 5-13: Q-Q plot for users' errors	
User ID	Normal QQ Plot	Detruded Normal QQ Plot
8		
9		
10		
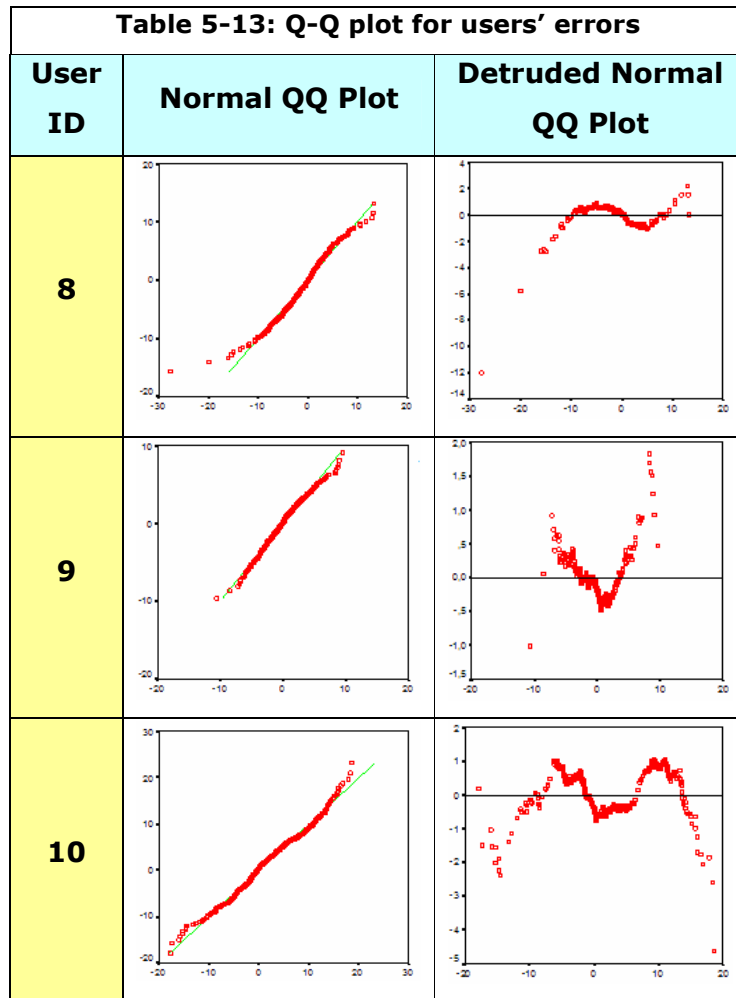
Histogram graphs of the Users are presented in the Appendix B to better visualize and discussed error distribution of the users.

As mentioned before, the measurements of 359 buildings from IKONOS stereo satellite images repeated ten times by the help of ten users. The results of the measurements are listed in the Table A-2 in APPENDIX A.

According to the measurement results, the mean, variance and standard deviation descriptive statistics are calculated for each user which are listed in Table C-1 in APPENDIX C. Table 5-14, Table 5-15, and Table 5-16 lists the mean error distribution of well experienced, moderately experienced and inexperienced users, respectively. Furthermore they are visualized in Figure 5-29, Figure 5-35, and Figure 5-41. By inspecting the

Table 5-14 and Table 5-15 it is clearly observed that users tend to make overestimations. Inexperienced and moderately experienced users' mean error varies between -30 and 20 meter whereas well experienced user's only varies between -6 and 4 meter interval. As expected, well experienced user is making more accurate measurements, however there is not a significant difference between the inexperienced and moderately experienced users.

Table 5-14: Mean error distribution of well experienced users

Mean error Interval		Number of FLOORS									Total
MIN	MAX	2	3	4	5	6	7	8	9	10	
-30,00	-6,01	-	-	-	-	-	-	-	-	-	0
-6,00	-4,01	1	1	-	-	-	1	-	-	-	3
-4,00	-2,01	13	5	6	4	3	4	1	2	1	39
-2,00	-0,51	28	27	18	14	8	3	12	10	-	120
-0,50	0,50	20	29	37	12	5	2	9	13	-	127
0,51	2,00	4	10	17	2	7	-	3	12	2	57
2,01	4,00	4	1	2	3	2	-	-	-	1	13
4,01	6,00	-	-	-	-	-	-	-	-	-	0
6,01	30,00	-	-	-	-	-	-	-	-	-	0
Total		70	73	80	35	25	10	25	37	4	359

Table 5-15: Mean error distribution of moderately experienced users

Mean error Interval		Number of FLOORS									Total
MIN	MAX	2	3	4	5	6	7	8	9	10	
-30,00	-6,01	60	31	36	28	14	8	2	3	1	183
-6,00	-4,01	40	39	24	7	7	4	4	6	-	131
-4,00	-2,01	79	51	44	13	17	6	17	12	-	239
-2,00	-0,51	69	76	71	32	17	4	27	37	-	333
-0,50	0,50	35	62	60	19	9	3	22	27	4	241
0,51	2,00	37	51	56	19	14	8	5	32	4	226
2,01	4,00	23	25	59	16	16	2	9	26	7	183
4,01	6,00	4	16	30	19	9	-	12	8	-	98
6,01	30,00	3	14	20	22	22	15	27	34	4	161
Total		290	334	364	147	111	42	123	182	19	1795

Table 5-16: Mean error distribution of inexperienced users

Mean error Interval		Number of FLOORS									Total
MIN	MAX	2	3	4	5	6	7	8	9	10	
-30,00	-6,01	56	39	39	34	15	8	7	10	-	208
-6,00	-4,01	28	24	25	13	4	2	10	9	1	116
-4,00	-2,01	39	43	37	10	20	10	15	15	1	190
-2,00	-0,51	48	53	53	21	14	5	19	35	6	254
-0,50	0,50	42	39	44	15	16	3	10	14	2	185
0,51	2,00	34	44	49	17	10	3	13	28	3	201
2,01	4,00	21	32	37	18	6	1	6	10	-	131
4,01	6,00	9	4	14	4	7	-	4	3	1	46
6,01	30,00	3	14	22	8	8	8	16	24	2	105
Total		224	253	281	106	85	32	93	138	16	1436

Figure 5-29: Spatial distribution of error values of method 3, well-experienced users results

Error (meter)

1

1

0

-1

-1

-2

-2

-3

2   3   4   5   6   7   8   9   10

Floor Number

◆ Method 3: Well-Experienced Users
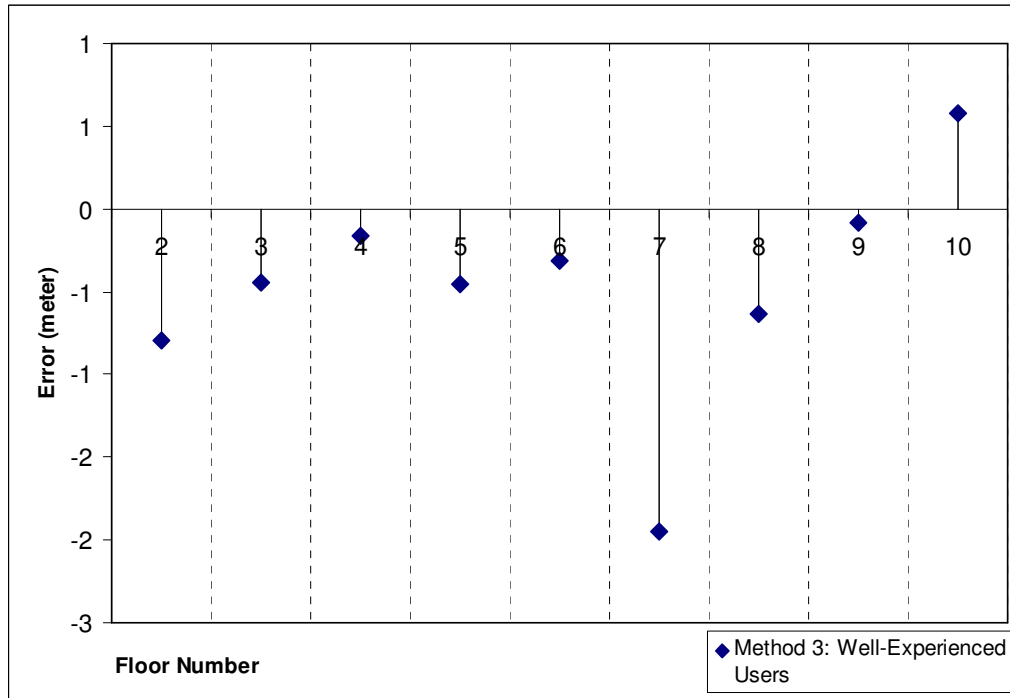
Figure 5-30: Graph of mean error for well-experienced users in method 3

As can be seen in Figure 5-30, the buildings which are 7 floored has maximum mean error and they are overestimated. On the other hand, the buildings that have 2, 3, 4, 5, 6, 8 and 9 have mean error value under 1, 00 m.

Table 5-17 contains mean error ranges which are mapped in Figure 5-31 and numbers of buildings in percentages are listed. According to Table 5-17, most of the buildings have mean error values in between -0,50 and +0,50 m, with a percentage of 36%. The values in between -2,00 and +2,00 m are considered to be acceptable error margin and totally 85% of the buildings have an mean error value between -2,00 and +2,00 m according to well-experienced user in Method 3.

Table 5-17: Mean error ranges and percentages of buildings of well-experienced user for method 3

	Mean error Ranges (m)	Percentages of Buildings	Comment
	-4,85 - -4,00	0,84%	Overestimated
	-3,99 - -2,00	10,86%	Overestimated
	-1,99 - -0,51	33,43%	Acceptable Level Of Accuracy
	-0,50 – 0,50	35,38%	Acceptable Level Of Accuracy
	0,51 – 2,00	15,88%	Acceptable Level Of Accuracy
	2,01 – 3,88	3,62%	Underestimated
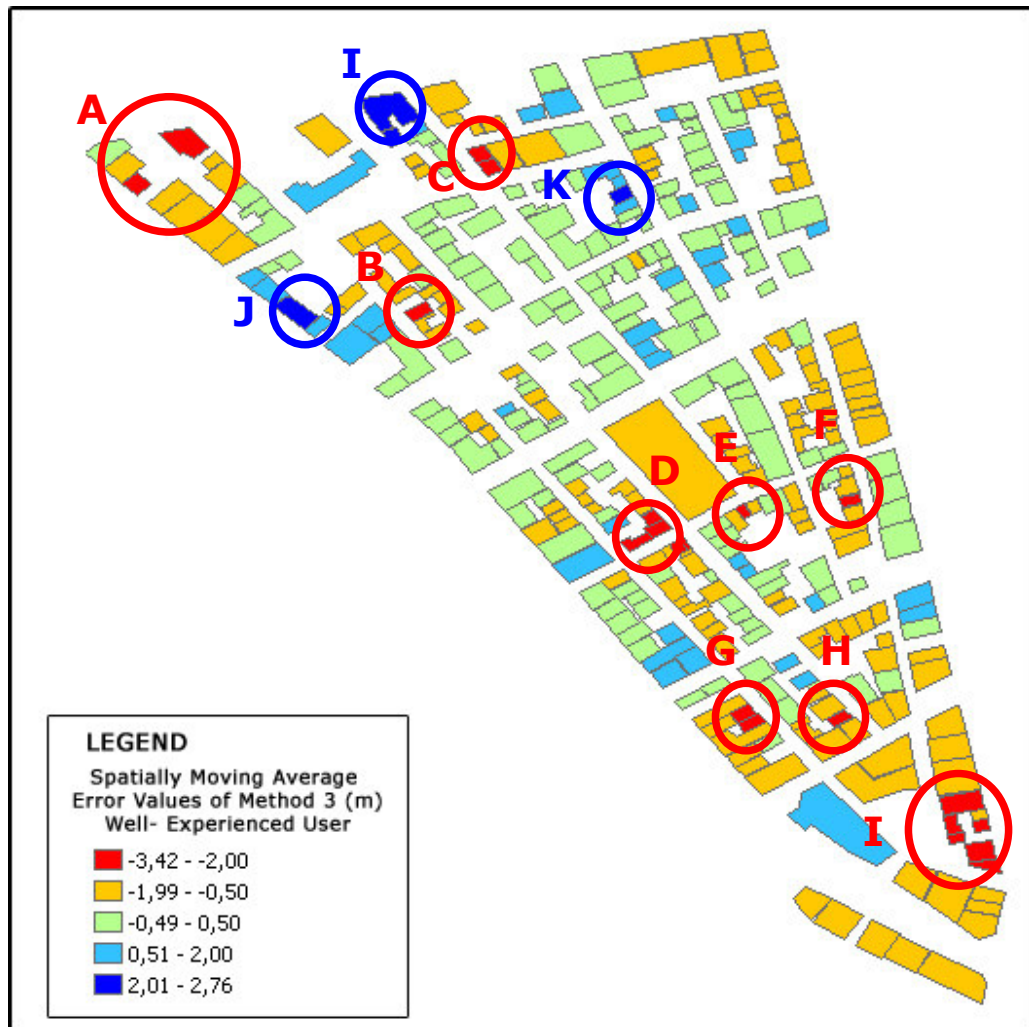
Figure 5-31: Spatial moving average applied for well-experienced user of method 3

In order to explore how the mean error value varies across the study area, "Spatial Moving Average" method is applied, and generated map is illustrated in the Figure 5-31.

The overestimated buildings, which are colored red in the Figure 5-31, and labeled with zones A, B, C, D, E, F, G, H and I are located in different locations. One of them is located at lower right corner, the second one is in the top left corner, and the third one is at the center of the figure. They have error amount value in the ranges of -4,00 and -4,85 m. The

building in the zone A has high error value, because it has a different building structure as seen in Figure 5-32.

Figure 5-32: An example building in zone A

The well- experienced user overestimated the height of the building in zone B, because it has a modified roof structure as seen in the Figure 5-33. As explained in the Methodology chapter, special attention is requested from users about considering roof structures of the buildings. They were asked to make their measurements from the corners or edges of the buildings as exemplified in the Figure 4-5. But as seen in the Figure 5-33, the building has a roof at the edge part of the building and this may misguide the user's measurement.

Figure 5-33: An example building in zone B

The underestimated buildings, which are colored blue in the Figure 5-31, are labeled with Zones I, J and K. Figure 5-34 shows an example building in zone I, which has a mean error value between 2,00 and 2,76 m. The reason for the underestimation may be the error emerged in the measurements in the field study. As seen in the Figure 5-18, this building has a confidence interval of 1,00- 1, 25 m.

Figure 5-34: An example building in zone I

Figure 5-35: Spatial distribution of error values of method 3, moderately experienced users results

Figure 5-35 illustrates the mean error of the measurements performed by moderately experienced users. It is hard to come up with a pattern from the Figure 5-35, but one could say that buildings which are located on the major streets are generally underestimated. Figure 5-2 displays the satellite image of the study area, and major streets can be identified from it.
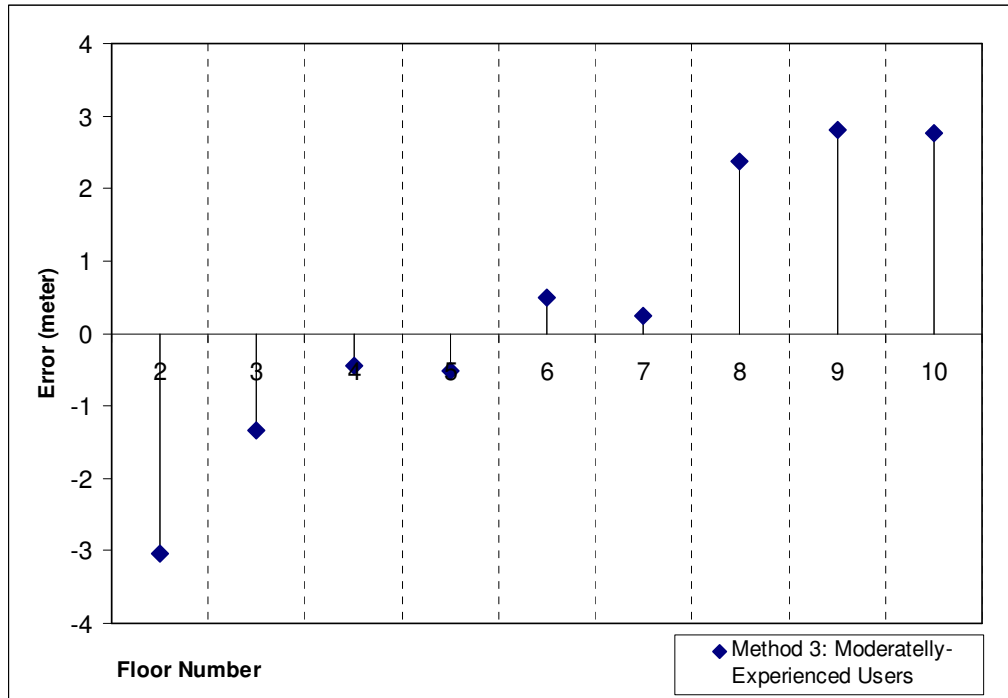
Figure 5-36: Graph of mean error for moderately-experienced users in method 3

In Figure 5-36, the buildings which are 8, 9 and 10 floored have maximum mean error and they are overestimated. On the other hand, the buildings that have 4, 5, 6, 8 and 9 have mean error value under 1,00 m. The buildings up to 5 floored are overestimated and buildings higher than 6 floored are underestimated by moderately-experienced users.

Table 5-18: Mean error ranges and percentages of buildings of moderately-experienced user for method 3

	Mean error Ranges (m)	Percentages of Buildings	Comment
	-17,62 - -8,00	1,95%	Overestimated
	-7,99 - -6,00	3,06%	Overestimated
	-5,99 - -4,00	9,75%	Overestimated
	-3,99 - -2,00	17,55%	Overestimated
	-1,99 - -0,51	18,66%	Acceptable Level Of Accuracy
	-0,50 – 0,50	13,93%	Acceptable Level

			Of Accuracy
	0,51 – 2,00		Acceptable Level Of Accuracy
		12,81%	
	2,01 – 4,00	12,53%	Underestimated
	4,01 – 6,00	5,29%	Underestimated
	6,01 – 8,00	1,95%	Underestimated
	8,01 – 21,08	2,51%	Underestimated

Table 5-18 contains mean error ranges which are mapped in Figure 5-35 and numbers of buildings. According to Table 5-18, the most of the buildings have mean error values in between -2,00 and -0,50 m (19%). The values in between -2,00 and +2,00 m are considered to be acceptable error margin and totally 45% of the buildings have an mean error values between -2,00 and +2,00 m according to height measurement of moderately-experienced user in Method 3.

In order to explore how the mean error value varies across the study area, "Spatial Moving Average" method is applied, and generated map is illustrated in the Figure 5-37.

Figure 5-37, illustrates spatial distribution of the mean error of the measurements performed by moderately-experienced users in the third method. The overestimated buildings, which are colored red in the Figure 5-37, and labeled with Zones F, G, H, and I are located in different locations. They have error value in the ranges of -4,00 and -10,01 m. The building in the zone H has the highest error value; it is illustrated in the Figure 5-38. The reason of this error is because of the two leveled roof structure of the building as seen in the Figure 5-38.
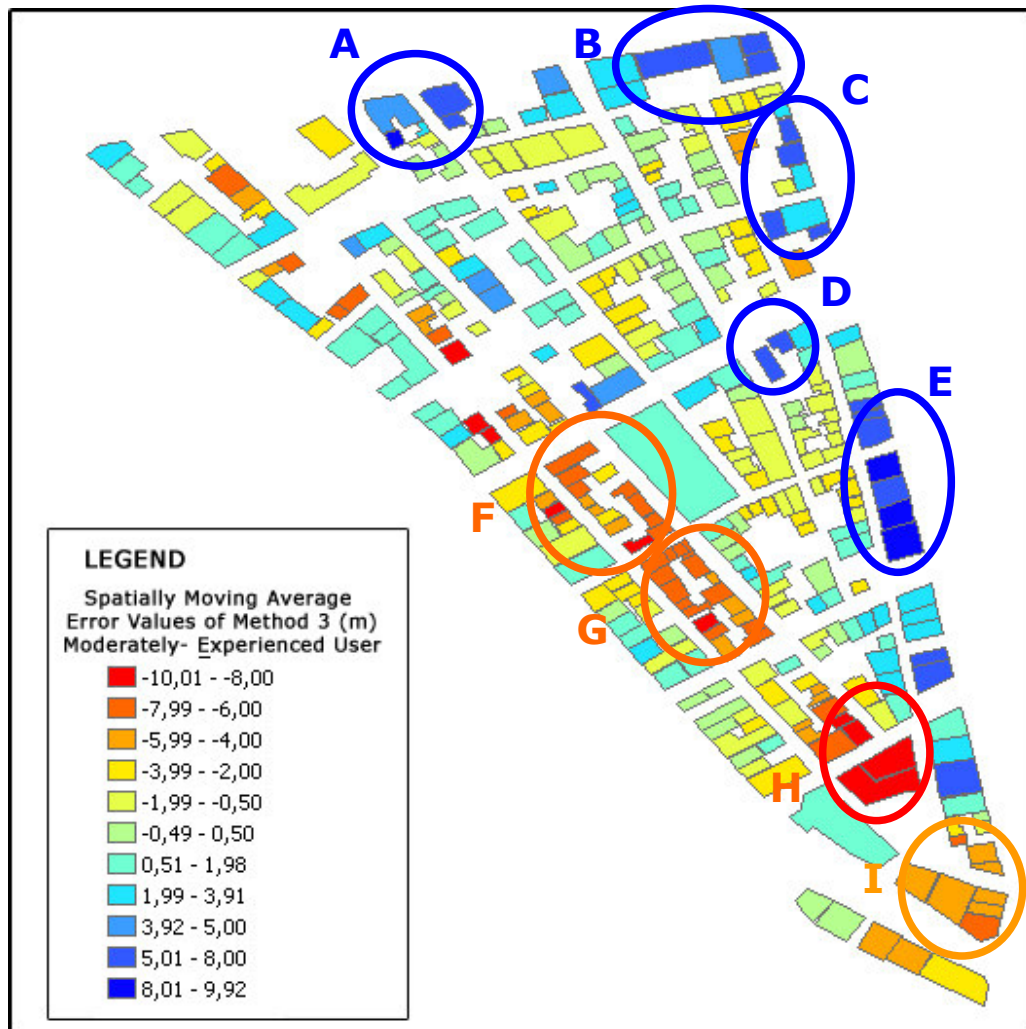
Figure 5-37: Spatial moving average applied for moderately-experienced user of method 3

Figure 5-38: An example building in zone H

95

The underestimated buildings, which are colored blue in Figure 5-37, and labeled with Zones A, B, C, D and E are located in different locations. They have error value in the ranges of 5,00 and 9,42 m. The buildings in the zone E have the highest error value, because they are located so closely to each other as seen in the Figure 5-39 and because of this, user may not distinguish easily the height differences among them.

Figure 5-39: Example buildings in zone E

The Figure 5-40 represents the graph of the mean error values for inexperienced users result in method 3 according to floor numbers of the buildings. As seen in the Figure 5-40, the buildings which are 2 and 5 floored have maximum mean error and they are overestimated. On the other hand, there is no building that has a mean error value under 1, 00 m. The buildings up to 7 floored are overestimated and buildings higher than 8 floored are underestimated by inexperienced users.
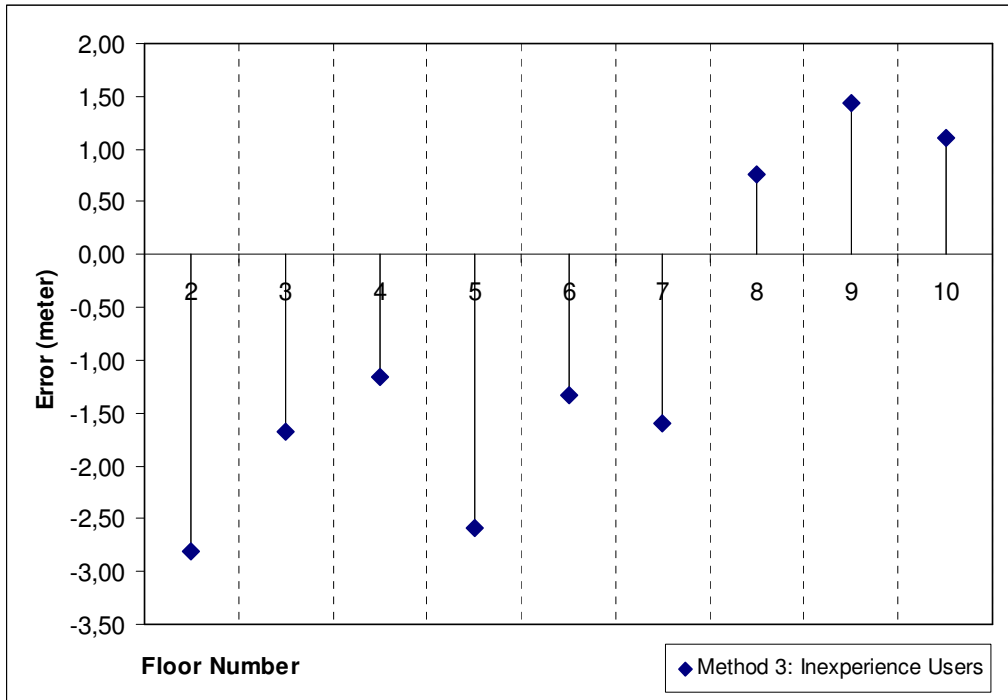
Figure 5-40: Graph of mean error for in-experienced users in method 3

Table 5-19 has mean error ranges which are mapped in Figure 5-41 and numbers of buildings are listed. According to Table 5-19, 23% of buildings have mean error values between -2,00 and -0,50 m. The values in between -2,00 and +2,00 m are considered to be acceptable error margins and totally 49% of the buildings have an mean error value between -2,00 and +2,00 m according to in-experienced user in Method 3.
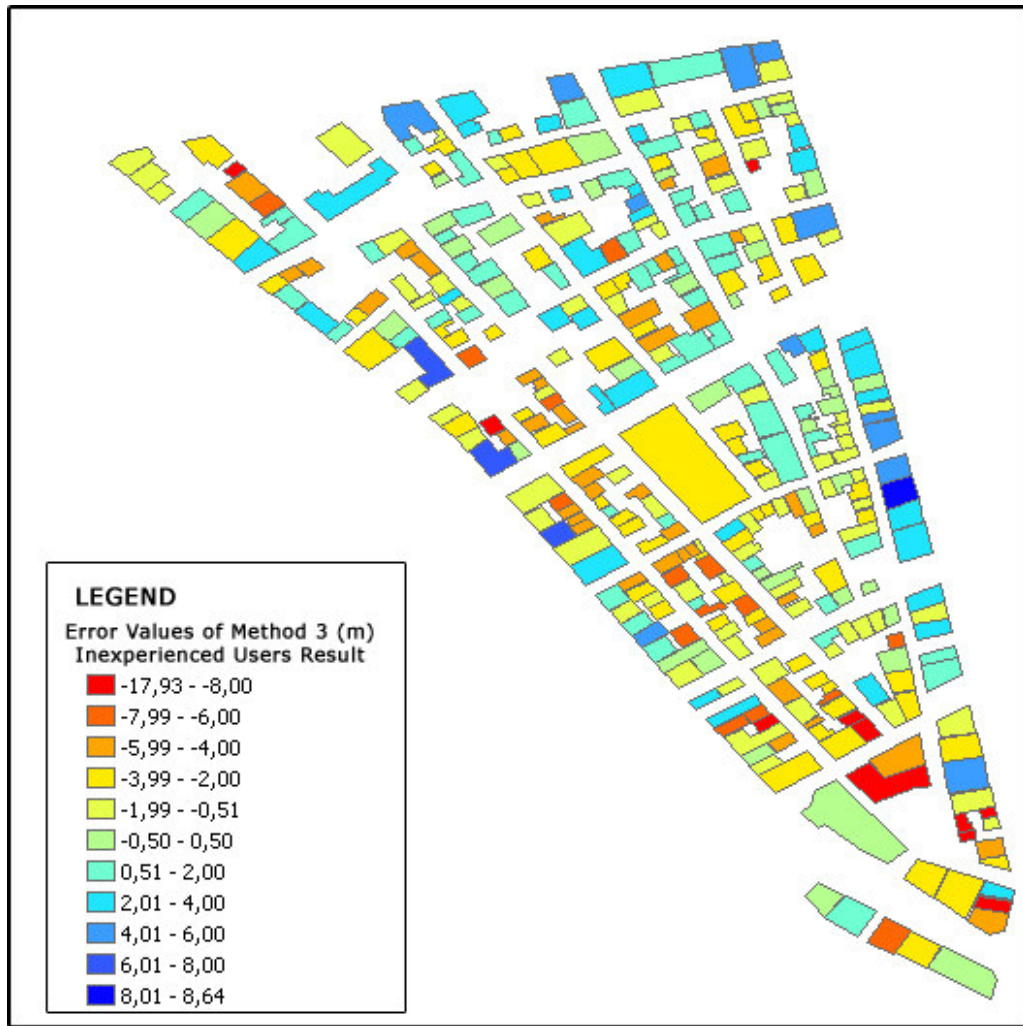
Figure 5-41: Spatial distribution of error values of method 3, In-experienced users results

Table 5-19: Mean error ranges and percentages of buildings of in-experienced user for method 3

	Mean error Ranges (m)	Percentages of Buildings	Comment
	-17,93 - -8,00	3,06%	Overestimated
	-7,99 - -6,00	4,18%	Overestimated
	-5,99 - -4,00	11,70%	Overestimated
	-3,99 - -2,00	18,94%	Overestimated
	-1,99 - -0,51	22,56%	Acceptable Level Of Accuracy
	-0,50 – 0,50	10,03%	Acceptable Level Of Accuracy
	0,51 – 2,00	15,88%	Acceptable Level Of Accuracy
	2,01 – 4,00	9,19%	Underestimated
	4,01 – 6,00	3,34%	Underestimated
	6,01 – 8,00	0,84%	Underestimated
	8,01 – 8,64	0,28%	Underestimated

In order to explore how the mean error value varies across the study area, "Spatial Moving Average" method is applied, and generated map is illustrated in Figure 5-42.

In Figure 5-42, the mean error of the measurements performed by in-experienced users in the third method is given. The zones A, B, C, and D are the underestimated buildings. The building in the zone G has the highest error value; it is illustrated in the photo in Figure 5-44.
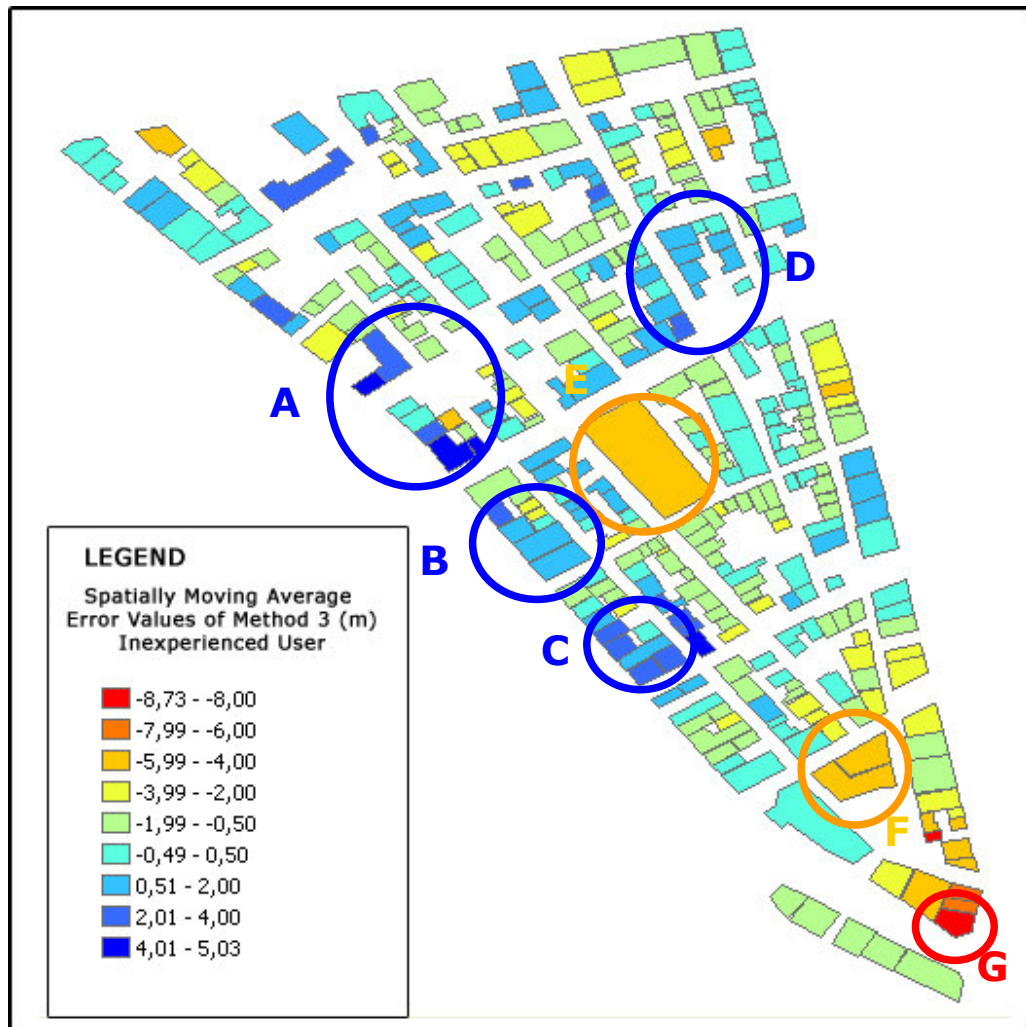
Figure 5-42: Spatial moving average applied for in-experienced user of method 3

Figure 5-43: An example building in zone A

Figure 5-44: An example building in zone G

Figure 5-45: An example building in zone E

Table 5-20 and Table 5-21 list the %95 confidence interval of moderately experienced and inexperienced users, respectively. Furthermore they are visualized in Figure 5-46 and Figure 5-47. As there was only one well-experienced user in this study, confidence interval cannot be constructed. By observing both Table 5-20 and Table 5-21 inexperienced users confidence lengths seems to be shorter than the moderately experienced users. Moderately experienced users only have 3 buildings in the range of 0 to 1,00 m, whereas inexperienced users have 67.

Table 5-20: %95 Confidence interval length distribution of moderately experienced users

%95 Confidance Interval Length		Number of FLOORS									Total
MIN	MAX	2	3	4	5	6	7	8	9	10	
0,00	1,00	-	3	-	-	-	-	-	-	-	3
1,01	2,00	25	35	34	19	12	3	6	15	1	150
2,01	4,00	19	11	9	11	7	4	8	9	-	78
4,01	6,00	4	5	8	2	3	-	1	8	-	31
6,01	8,00	9	13	15	2	1	1	6	3	1	51
8,01	10,00	13	6	14	1	2	2	4	2	2	46
Total		70	73	80	35	25	10	25	37	4	359

Table 5-21: %95 Confidence interval length distribution of inexperienced users

%95 Confidance Interval Length		Number of FLOORS									Total
MIN	MAX	2	3	4	5	6	7	8	9	10	
0,00	1,00	14	13	22	5	6	-	5	2	-	67
1,01	2,00	17	16	16	11	3	5	5	10	3	86
2,01	4,00	21	25	24	7	8	-	7	16	1	109
4,01	6,00	11	8	11	7	2	4	5	5	-	53
6,01	8,00	5	6	4	3	5	-	2	4	-	29
8,01	10,00	2	3	3	2	-	1	1	-	-	12
Total		70	71	80	35	24	10	25	37	4	356

Figure 5-46: %95 confidence interval length distribution of moderately experienced users

It is not possible to observe any relation between %95 confidence lengths of the measurements and the location of the building from Figure 5-46 and Figure 5-47. It seems that all of the ranges are distributed randomly to the different locations of the study area (Figure 5-46 and Figure 5-47).

Figure 5-47: %95 confidence interval length distribution of inexperienced users

5.6 Results and Discussions

In this section, three methods are compared with each other. Figure 5-48 shows the mean errors of each method where as Figure 5-49 shows the 95% confidence intervals of them. The first method achieves acceptable results for low buildings but the mean error of method one increases with the number of floors.
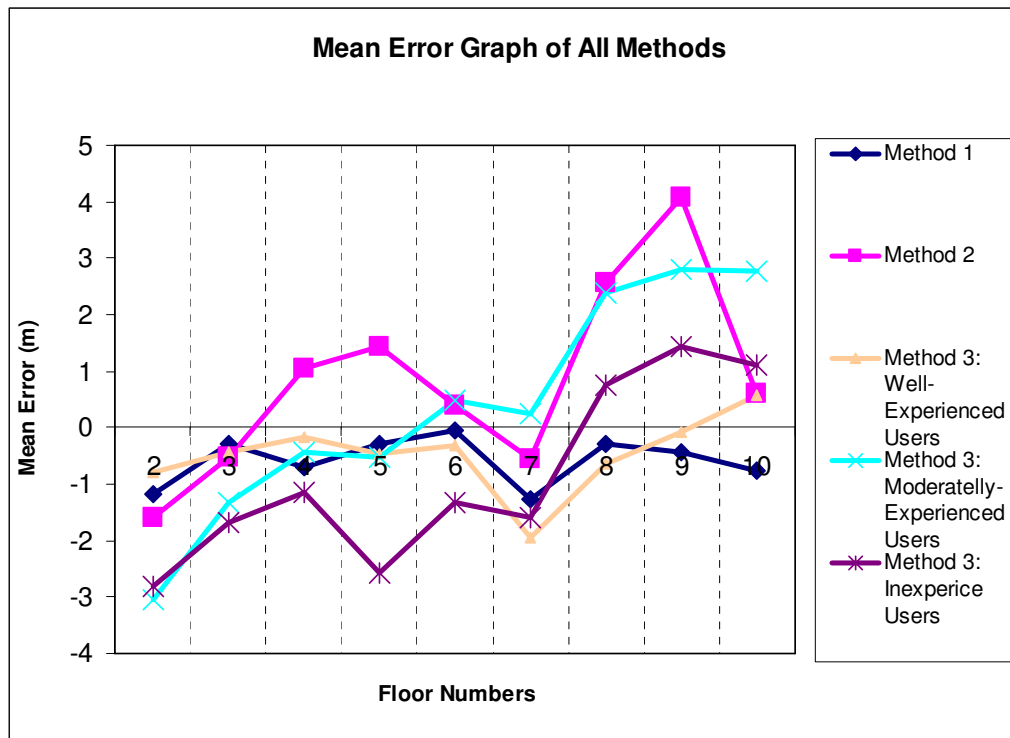
Figure 5-48: Mean error graph of all methods

As seen from the Figure 5-48, method 1 and method 2 mostly give the same results in the 2 and 3 floored buildings. On the other hand, they are opposed to each other in 4, 5, 8, 9 and 10-floored buildings. The maximum error value for the method 1 is found in 7-floored buildings, in 9-floored buildings for method 2 and, for well experienced users in 7-floored, for moderately experienced users in 9-floored and for inexperienced users, 2 floored buildings in method 3.

The well-experienced users of the third method are overestimating up to 9- floored buildings, and then underestimating in the 10– floored building, while they have very close measurement in the 9- floored. On the other hand, moderately experienced users are overestimating up to 5-floored buildings and underestimating after floor number over 5. Inexperienced users curve is very similar to moderately advance users', but the mean error values are different.

As seen in the Figure 5-49, method 2 which is using the generated DSM and DTM for obtaining height values, has the maximum confidence lengths almost in all buildings except 10 floored ones. Moreover, method 2 has the maximum confidence interval length in the 7-floored buildings, and similarly in most of the methods, the confidence interval length is increasing in the buildings which have 7 floors. Method 1 and well experienced users in method 3 have results of minimum confidence interval lengths.
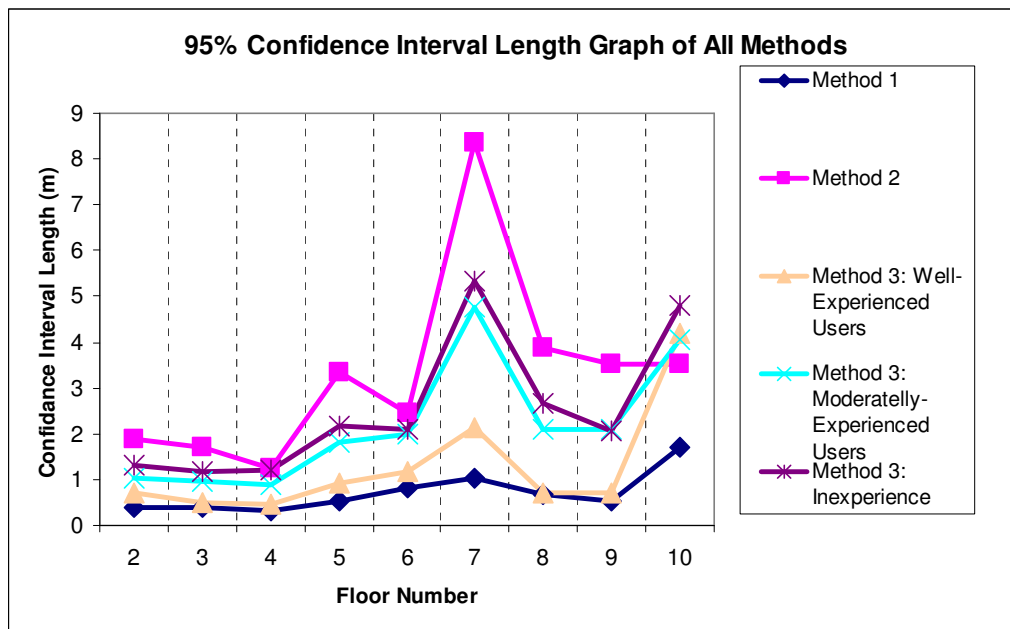
Figure 5-49: 95% confidence interval lengths of all methods

CHAPTER 6

CONCLUSION

6.1 Conclusion

The adopted methodology, which is applying 3 methods for predicting height values of the buildings in the urban environments leads to some considerable results. The conclusions derived from the study are as follows:

Obtaining height values from the field study gives accurate results which are indicated in the section 5.4.1 as approximately 75% of the buildings (271 buildings) have an estimated mean error in the 95% confidence limits less then 0,50 m. However measurements should be repeated several times. Therefore this method is the most time consuming method. Moreover, the study area may not be accessible easily, or accessing to the field may be costly. Also, the measurements should be performed with a professional measurement instruments such as range finders, but purchasing an instrument like a range finder can be costly.

In order to obtain accurate results from Method 1, updated data that contains floor numbers of the buildings should be used. Obtaining accurate height values of the buildings is possible, when updated data is available. The mean error value is found as -0,578 m. as seen in the Table 5-7. However, getting the updated data of floor numbers of the buildings may not be possible all the time. Since, in Turkish municipalities, the databases are not usually updated and retrieving these databases is not possible in all cases. Even if the database is retrieved, it may be out-dated. On the other hand, constructors may not obey the building height codes which are defined in zone regulations of

the municipality, so using the Equation 4-1 may result in high amount of error. In addition to these reasons, using a constant value for floor heights may not give the accurate results, because the different types of buildings may have higher floor heights than defined in the regulations. For example, in Figure 5-21, a building that serves for military purposes which is labeled as in the zone F, is located. It has 8 floors according to database, and as seen in the Figure 5-24, it has 6 floors and plus 2 floors for high entrance. However, this building's floor heights are higher than 3,00 m especially the terrace floor on the top and the entrance floor.

Automatic generation of DSM and DTM from high resolution satellite images is a rapid method for obtaining height values of the human made structures in urban areas. However the accuracy of the used satellite images is very important. In this study, IKONOS Precision Stereo images are used, which has 1 meter horizontal (RMSE) and 2 meter vertical (RMSE) accuracy. As a result of the method 2, 1,495 m is found as mean error and 2,13 as standard deviation values (Table 5-10: Descriptive statistics for method 2) for the height values of the buildings. According to Figure 5-25, the ranges of the error is changing -17,62 m to 21,08 m and these error ranges are too much and most probably, the reason for these high error values is propagation of errors in DTM and DSM. The accuracy achieved in the DTM and DSM generation would be improved with using IKONOS Geo with precise Ground Control Points (GCPs) which are collected from study field. On the other hand, because of the high cost of the satellite images, this method is also described as an expensive method.

In method 3, the reasons of the high amount of error values in some areas are as follows;

• As explained in the Methodology chapter, special attention is requested from users about considering roof structures of the buildings. They were asked to make their measurements from the corners or edges of the buildings as exemplified in the Figure 4-5, but in some cases users are

confused because of the different roof structures. As seen in the example in the Figure 5-33, the building has a roof at the edge part of the building and this misguides the user's measurement.

• In some buildings, the high error results are because of the two leveled roof structure of the buildings. It is illustrated in the Figure 5-39 and Figure 5-45 as an example.

• The buildings which are located so closely to each other may cause high error values in height measurements, because adjacent buildings make difficult to distinguish easily the height differences among them. The buildings labeled as zone E in the Figure 5-37 can be given as an example for this kinds of buildings, they are also illustrated in the Figure 5-39.

• When the results of the users according to their experience levels investigated, it is found that the experience level is very important factor in manual measurements from 3D viewing. If the Figure 5-48 and Table C.1 in APPENDIX C are examined, the mean error values of -0,45 m, -0,60 m and -1,06 m are found as a results of the well-experienced, moderately experienced users and inexperienced users, respectively. The error standard deviations are found as 1, 30 m, 5,48 m, and 5,01 m.

• By inspecting the Table 5-14 and Table 5-15 it is clearly observed that users tend to make overestimations. Inexperienced and moderately experienced users' mean error varies between -30 and 20 meter whereas well experienced users only varies between -6 and 4 meter interval. As expected well experienced user is making more accurate measurements, however there is not a significant difference between the inexperienced and moderately experienced users.

When three methods are compared, results of the method which is obtaining height of buildings from municipality database is found to be the most accurate one if the database is up to date. The second most

accurate method is obtaining building heights from 3D viewing of stereo satellite images by experienced users (Method 3).

In the GIS projects, obtaining height values from the satellite images may used for updating floor numbers of the buildings in the databases.

6.2 Future Work

It is recognized that this research has certain limitations. The directions in which future study would offer considerable rewards are listed as below.

- In this research, satellite images, which has acquisition year of 2002, are used. Up-to-date satellite images could be purchased to get better solutions. Moreover, using IKONOS Geo product with precise GCP's may result in better DTM and DSM, and hence better accuracies.

- For measuring height values from 3D viewing only one experienced user is conciliated, the number of the experienced users could be increased.

- This research focused on evaluating the height values of the buildings under consideration and the accuracy of the predicted 3-D height values. However, the positional accuracy of the predicted 3-D model could also be examined.

REFERENCES

Akçın, H., and Yüceer, K., 2006, Kent Gelişiminde ve Kent Bilgi Sistemlerinin Oluşumunda 3 Boyutlu Mülkiyet.

Amrhein, C. G., and Schut, P., 1990, Data quality standards and geographic information systems, Proc., National Conf. "GIS for the 1990's, Canadian Institute of Surveying and Mapping, Canada, pp. 918–930.

Bailey, T.C., and Gatrell, A.C., 1995, Interactive Spatial Data Analysis, Harlow Essex, England: Longman Scientific & Technical; New York

Baltsavias, E, Pateraki, P.M., and Zhang, L., 2001, Radiometric and Geometric Evaluation of IKONOS Geo Images and Their Use for 3D Building Modeling. Proc. Joint International Archives of the Photogrammetry, Remote Sensing Workshop on "High Resolution Mapping from Space 2001", 19-21 September, Hannover, Germany.

Burrough, P. A., 1986, Principles of Geographical information Systems for Land Resources Assessment, Oxford: University Press.

Burrough, P. A., and McDonnell, R. A., 1998, Principles of Geographical Information Systems, Oxford University Press, New York.

Cai, H., 2003, Accuracy Evaluation Of a 3D Spatial Modeling Approach To Model Linear Objects And Predict Their Lengths, PhD Thesis.

Clode, S.P., Rottensteiner, F., and Hinz S., 2005, Improving City Model Determination by Using Road Detection from LIDAR Data, International Archives of the Photogrammetry, Remote Sensing, Vol. 36, Part 3/w24, Vienna, Austria pp. 29-30.

Chong, A. K., 1997, A Field Check Sampling Procedure to Evaluate the Positional Accuracy of Digital Database, Proceedings of ASPRS/ACSM, Volume 2, Annual Convention and Exposition of Technical Papers, Seattle, Washington.

Davis, T.J., and Keller, C.P., 1997, Modelling uncertainty in natural resource analysis using fuzzy sets and Monte Carlo simulation: slope stability prediction, International Journal of Geographical Information Systems, Vol. 11, Issue 5.

Di, K., Ma, R., and Li.,R., 2002, Geometric Processing of IKONOS Geo Stereo Imagery for Coastal Mapping Applications, Journal of Photogrammetric Engineering & Remote Sensing.

Ehlschlaeger, C.R., and Goodchild, M.F., 1994, Uncertainty in Spatial Data: Defining, Visualizing, and Managing Data Errors, Proceedings of LIS/GIS '94 Annual Conference, pp. 246-253.

Eskişehir Büyükşehir Belediyesi İmar Yönetmeliği, 2004, Belediye Meclisi.

Evans, B.J., 1997, Dynamic display of spatial data reliability: does it benefit the map user?, Computers & Geosciences, Vol. 23, No. 4, pp. 409–422.

Förstner, W., 1999, 3D-City models: Automatic and semi-automatic acquisition methods, Proceedings Photogrammetric Week '99, H. Wichmann Verlag, Heidelberg, pp. 291-304.

Fraser, C.S., Baltsavias. E., and Gruen, A., 2002, Processing of IKONOS Imagery for Submitter 3D Positioning and Building Extraction, International Archives of the Photogrammetry, Remote Sensing Journals of Photogrametry and Remote Sensing 1209.

Fuchs, C., Gülch, E. and W. Förstner , 1998, OEEPE Survey on 3D-City Models, OEEPE Publication, No. 35, Frankfurt, pp. 9-124.

Goodchild, M. F.,1991a, Issues of quality and uncertainty, Advances in cartography, J. C. Muller, ed., Elsevier, New York, pp.113–139.

Goodchild, M. F., 1991b, Issues of quality and uncertainty, Proc., State of Indiana Geographic Information System Conf., Indiana University GIS Alliance, Indianapolis, pp.17–53.

Goodchild, M. F., 1998, Geographic Information Systems and Disaggregate Transportation Planning, Geographical Systems, Vol. 5, pages 19-44, 1998.

Grün, A., 2000, Semi-automated Approaches to Site Recording and Modeling, International Archives of the Photogrammetry, Remote Sensing, Vol. 33, Amsterdam.

Haala, N., and Brenner, C., 1997, Generation of 3D City Models from Airbonne Laser Scanning Data, Proc. 3rd Earsel Workshop on LIDAR Remote Sensing on Land and Sea, Tallinn, Estonia, pp. 105-112.

Haala, N., and Brenner, C., 1999, Extraction of Buildings and Trees in Urban Environments, Journal of Photogrammetry & Remote Sensing, Issue 54, pp. 130-137.

Heuvelink, G.B.M., 1998, Error Propagation in Environmental Modelling with GIS, London: Taylor & Francis.

Heuvelink, G.B.M., Burrough, P.A., and Stein, A., 1989, Propagation of errors in spatial modeling with GIS, International Journal of Geographical Information Systems, Vol. 3, pp. 303–322.

Hong, G., and Zhang, Y., 2004, The Effects of Different Types of Wavelets on Image Fusion, International Archives of Photogrammetric and Remote Sensing, 35: pp.915-920.

Huertas, A., and Nevatia, R., 1988, Detecting Buildings in Aerial Images, Computer Vision, Graphics and Image Processing, Vol. 41, pp. 131-152.

Hu, X., and Tao, C. V., 2003, Automatic Extraction of Main-Road Centerlines from IKONOS and Quick-Bird Imagery Using Perceptual Grouping, Proceedings of ASPRS Annual Convention 2003, 5-9 May, Anchorage, Alaska.

International Organization for Standardization (ISO), 2003, Geographic Information – Quality Evaluation Procedures.

Jacobsen K., 2004, DTM Generation by SPOT5 HRS, International Archives of the Photogrammetry, Remote Sensing, 35(B1): pp. 439-444.

Kim,J.R., and Muller, J.P., 2002, 3D Reconstruction from very high resolution satellite stereo and its application to object identification, International Archieves of Photogrammetry and Remote Sensing.

Kraak, M.J., and Ormerling, F.J., 1996, Cartography, Visualization of Spatial Data, England: Addison Wesley Longman Limited.

Lawless, J., 2001, Urban Roof Morphology Extraction using Random Sampling of LIDAR Data, Master's Thesis, University Collage London.

Lee, D. S., Shan, J., and Bethel, J. S., 2002, Class-Guided Building Extraction from IKONOS Imagery, Photogrammetric Engineering and Remote Sensing, 69(2): pp.143-150.

Lee, T.Y., and Kim, T., 2005, Reconstruction of 3D Building Structures from IKONOS Images Through Monoscopic Line and Shadow Analysis, Asian Association on Remote Sensing, Section 36.

Leica Photogrammetry Suite OrthoBASE & OrthoBASE Pro User's Guide, 2003, Leica Geosystems GIS & Mapping, LLC.

Leung, Y., Ma, J. H., and Goodchilds, M. F., 2004, A general framework for error analysis in measurement-based GIS Part 1: The basic measurement-error model and related concepts, Journal of Geographical Systems, Vol. 6, pp. 325–354

Liow, Y.T., and Pavlidis, T., 1990, Use of Shadows for Extracting Buildings in Aerial Images, Comput. Vision Graphics Image Process, Vol.49, pp.242-277.

Maas, H. G., and Vosselman, G., (1999), Two Algorithms for extracting building models from raw Laser altimetry data, International Archives of the Photogrammetry, Remote Sensing 54 pp.153-163.

METU 2003, GEOE 528 Lecture Notes.

METU 2007, GGIT 537 Lecture Notes.

OrthoBASE Pro User's Guide, 2003, Leica Geosystems GIS & Mapping, LLC.

Range Finder User Manual, 2005, Laser Technology Inc., Second Edition.

Rasdorf, W., Cai, H., Tilley, C., Brun, S., and Robson, F., 2001, Accuracy assessment of road length measurement using DEM., J. Transp. Eng.

Shettigara, V.K., and Sumerling, G.M., 1998, Height Determination of Extended Objects Using Shadows in SPOT Images, Photogrammetric Engineering & Remote Sensing, Vol. 64, No. 1, pp. 3544.

Shiode, N.,2001, 3D Urban Models: Recent developments in the digital modeling of urban environments in three-dimensions, GeoJournal 52, pp.263-269.

Smith, S.L., 2003, Advanced Spatial Analysis, The CASA book of GIS, ESRI, California, pp.171-190.

Stoter, J.E., van Oosterom, P.J.M., Ploeger, H.D. and Aalders, H.J.G.L., 2004. Conceptual 3D Cadastral Model Applied in Several Countries. In: Proceedings of the International Federation of Surveyors (FIG) Working Week, Athens, Greece.

Suveg I., and Vosselman, G., 2003, Reconstruction of 3D Building Models from Aerial Images and Maps, ISPRS Journal of Photogrammetry and Remote Sensing, Vol. 58, pp. 202-224.

Tao, G., and Yasuoka, Y., 2002, Combining High Resolution Satellite Imagery and Airborne Laser Scanning Data for Generating Bareland DEM in Urban Areas, International Archives of the Photogrammetry, Remote Sensing and Spatial Information Sciences, Vol.34, No.5/W3.

Toutin, T., 2004, Comparison of Stereo-Extracted DTM from Different High-Resolution Sensors: SPOT-5 EROS-A IKONOS-II, and QuickBird. IEEE Transactions on Geoscience and Remote Sensing, 42(10): pp. 2121-2119.

Zhang, L., and Gruen, A., 2004, Automatic DSM Generation from Linear Array Imagery Data, International Archives of the Photogrammetry, Remote Sensing, 35(B3): pp. 128-133.

Zlatanova, S., and Tempfli, K., 2000, Modeling for 3D GIS; Spatial Analysis and Visualization Through The WEP International Archives of the Photogrammetry, Remote Sensing, Vol. 33, Amsterdam.

Wilneff, J., Poon, J., and Fraser, C., 2005, Single-Image High-Resolution Satellite Data for 3D Information Extraction, International Archives of the Photogrammetry, Remote Sensing, Hannover, Germany, Vol. 36.

Web 1: http://www.sieurasia.com/showpage.aspx?id=145. Last accessed November 15, 2007.

Web 2:

http://www.opticsplanet.net/rangefinders1.html. Last accessed
November 15, 2007.

Web 3:

http://en.wikipedia.org/wiki/Digital_terrain_model. Last accessed
November 15, 2007.

Web 4:

www.en.wikipedia.org. Last accessed November 15, 2007.

Web 5:
http://www.une.edu.au/WebStat/unit_materials/c4_descriptive_statistics
/determine_skew_kurt.html, Last accessed November 15, 2007.
Web 6:

http://www.integralgis.com/pdf/LIDAR.pdf. Last accessed 15 Nov,2007,
Last accessed November 15, 2007.

Web 7: http://www.geolas.com/Pages/laser.html. Last accessed
November 15, 2007.

APPENDIX A

BUILDING HEIGHT MEASUREMENTS

Table A-1: Range finder measurements in study field

FID	LASER1	LASER2	LASER3	LASER4	LASER5	LASER6	LASER_MEAN	LSR_VAR	LSR_STD
1	15.50	15.90	16.00	16.10	16.20	16.10	15.97	.06	.25
2	12.00	12.40	12.30	12.40	12.10	12.20	12.23	.03	.16
3	12.80	12.90	12.70	12.80	12.90	12.80	12.82	.01	.08
4	9.90	9.80	10.00	10.00	10.00	9.90	9.93	.01	.08
5	10.20	10.50	10.50	10.50	10.50	10.50	10.45	.02	.12
6	6.20	6.90	6.90	7.00	6.90	6.90	6.80	.09	.30
7	17.50	17.20	17.30	17.50	17.40	17.50	17.40	.02	.13
8	14.50	14.70	14.60	14.60	14.70	14.40	14.58	.01	.12
9	8.20	8.40	8.30	8.30	8.30	8.30	8.30	.00	.06
10	25.70	25.80	26.20	26.10	26.40	26.20	26.07	.07	.27
11	6.30	6.50	6.50	6.50	6.60	6.50	6.48	.01	.10
12	12.80	13.40	13.30	13.30	13.60	13.10	13.25	.07	.27
13	12.90	12.60	12.70	12.90	12.80	13.00	12.82	.02	.15
14	3.50	3.60	3.50	3.60	3.50	3.60	3.55	.00	.05
15	26.20	25.50	25.60	25.60	25.70	25.70	25.72	.06	.25
16	25.20	25.20	25.20	25.30	25.40	25.50	25.30	.02	.13
17	25.70	25.50	25.50	25.60	25.70	25.60	25.60	.01	.09
18	8.50	9.00	9.10	8.90	9.00	9.10	8.93	.05	.23
19	9.10	9.40	9.30	9.50	9.50	9.50	9.38	.03	.16
20	14.50	14.70	14.60	14.60	14.70	14.40	14.58	.01	.12
21	14.10	14.10	14.10	14.10	14.30	14.30	14.17	.01	.10
22	3.60	3.60	3.40	3.30	3.30	3.30	3.42	.02	.15
23	9.70	9.70	9.80	9.90	9.60	9.60	9.72	.01	.12
24	25.20	25.20	24.50	25.20	24.70	25.20	25.00	.10	.32
25	11.80	11.80	11.70	11.80	12.00	11.80	11.82	.01	.10
26	13.40	13.40	13.50	13.50	13.50	13.50	13.47	.00	.05
27	4.20	4.20	4.20	4.20	4.20	4.20	4.20	.00	.00
28	12.60	13.00	12.80	12.80	12.90	12.90	12.83	.02	.14
29	17.30	17.40	17.10	17.50	17.10	17.20	17.27	.03	.16
30	24.29	26.20	26.10	25.80	25.90	26.00	25.71	.51	.71
31	25.20	25.10	25.20	25.10	24.70	25.40	25.12	.05	.23
32	25.40	26.60	26.40	26.10	26.50	26.60	26.27	.21	.46
33	17.50	17.70	17.60	17.70	17.70	17.50	17.62	.01	.10
34	14.80	15.00	14.80	15.00	14.80	14.90	14.88	.01	.10
35	28.30	28.40	28.30	28.40	28.40	28.40	28.37	.00	.05
36	19.00	19.80	19.60	19.80	19.70	19.50	19.57	.09	.30
37	19.50	19.40	19.40	19.60	19.30	19.60	19.47	.01	.12
38	9.50	9.70	9.70	9.70	9.70	9.70	9.67	.01	.08
39	13.20	13.20	13.30	13.10	13.50	13.50	13.30	.03	.17
40	9.60	9.50	9.80	9.70	9.60	9.70	9.65	.01	.10
41	23.50	23.70	23.80	23.50	23.80	23.70	23.67	.02	.14
42	24.90	25.00	24.60	25.10	24.70	24.90	24.87	.03	.19
43	22.10	22.00	22.00	21.90	22.40	21.90	22.05	.03	.19

Table A-1: Range finder measurements in study field

FID	LASER1	LASER2	LASER3	LASER4	LASER5	LASER6	LASER_ MEAN	LSR_ VAR	LSR_ STD
44	7.00	7.10	6.90	7.00	7.00	6.90	6.98	.01	.08
45	12.40	12.70	12.70	12.60	12.60	12.60	12.60	.01	.11
46	16.60	16.80	16.70	16.60	16.60	16.80	16.68	.01	.10
47	9.50	9.30	9.40	9.40	9.50	9.30	9.40	.01	.09
48	15.90	16.00	16.00	15.90	15.80	15.70	15.88	.01	.12
49	17.10	16.80	16.80	17.10	17.40	17.10	17.05	.05	.23
50	23.00	23.10	23.00	23.30	22.80	23.00	23.03	.03	.16
51	24.60	25.10	25.00	24.60	25.00	24.60	24.82	.06	.24
52	13.80	13.80	13.90	13.70	14.00	14.00	13.87	.01	.12
53	7.30	7.30	7.40	7.20	7.40	7.40	7.33	.01	.08
54	10.30	10.00	10.10	9.90	10.10	10.00	10.07	.02	.14
55	15.70	15.30	15.90	15.40	15.70	15.70	15.62	.05	.22
56	6.40	6.40	6.40	6.40	6.40	6.40	6.40	.00	.00
57	6.70	6.60	6.70	6.80	6.70	6.70	6.70	.00	.06
58	7.50	7.60	7.60	7.60	7.60	7.60	7.58	.00	.04
59	6.50	6.90	7.00	7.00	7.00	7.00	6.90	.04	.20
60	10.00	10.30	10.20	10.10	10.20	10.10	10.15	.01	.10
61	13.60	13.20	13.30	13.60	13.30	13.40	13.40	.03	.17
62	16.40	16.40	16.30	16.10	16.00	16.20	16.23	.03	.16
63	10.70	10.70	11.00	11.10	11.20	10.70	10.90	.05	.23
64	13.60	13.30	13.10	13.40	13.30	13.00	13.28	.05	.21
65	15.50	15.90	16.00	16.10	16.20	16.10	15.97	.06	.25
66	3.40	3.30	3.40	3.30	3.40	3.30	3.35	.00	.05
67	12.50	12.70	12.70	12.50	12.80	12.90	12.68	.03	.16
68	12.00	12.70	12.60	12.50	12.70	12.90	12.57	.09	.31
69	13.30	13.30	13.20	13.30	13.20	13.10	13.23	.01	.08
70	24.40	24.40	24.40	24.50	24.50	24.40	24.43	.00	.05
71	25.70	25.70	25.90	26.10	26.30	25.70	25.90	.06	.25
72	26.40	25.90	26.20	26.00	26.40	26.50	26.23	.06	.24
73	26.40	26.60	26.40	26.40	26.70	26.40	26.48	.02	.13
74	25.40	25.20	25.20	25.60	25.10	25.50	25.33	.04	.20
75	23.20	22.80	22.90	23.00	22.80	22.80	22.92	.03	.16
76	22.90	23.10	23.20	23.00	23.30	23.30	23.13	.03	.16
77	25.20	25.20	25.50	25.30	25.40	25.10	25.28	.02	.15
78	25.00	25.00	24.90	25.10	24.80	25.20	25.00	.02	.14
79	25.60	25.50	25.70	25.70	25.70	25.70	25.65	.01	.08
80	27.00	27.90	27.50	27.20	27.50	27.40	27.42	.09	.31
81	9.20	9.60	9.40	9.50	9.70	9.70	9.52	.04	.19
82	25.90	26.70	26.60	26.50	26.00	25.70	26.23	.17	.42
83	25.90	25.70	25.80	25.70	25.80	26.00	25.82	.01	.12
84	16.50	16.90	17.10	16.90	17.00	16.90	16.88	.04	.20
85	16.50	16.90	17.00	16.90	17.00	16.90	16.87	.03	.19
86	14.90	14.70	14.60	14.50	14.80	14.70	14.70	.02	.14
87	6.40	6.90	6.90	6.80	6.90	7.00	6.82	.05	.21
88	26.80	26.90	26.30	26.60	27.00	26.60	26.70	.06	.25
89	24.10	24.00	23.50	23.90	24.00	24.40	23.98	.09	.29
90	23.20	24.90	24.90	24.90	25.00	25.20	24.68	.54	.74
91	21.60	21.30	21.40	21.30	21.40	21.40	21.40	.01	.11
92	23.40	23.60	23.50	23.70	23.50	23.90	23.60	.03	.18
93	9.40	9.90	10.00	9.70	9.60	9.70	9.72	.05	.21
94	24.40	24.80	24.60	24.80	24.90	25.50	24.83	.14	.37

Table A-1: Range finder measurements in study field

FID	LASER1	LASER2	LASER3	LASER4	LASER5	LASER6	LASER_MEAN	LSR_VAR	LSR_STD
95	12.00	10.00	9.60	10.00	10.00	9.90	10.25	.76	.87
96	5.30	5.20	5.30	5.20	5.30	5.20	5.25	.00	.05
97	6.20	6.80	6.90	6.70	6.60	6.60	6.63	.06	.24
98	4.60	4.60	4.50	4.50	4.60	4.50	4.55	.00	.05
99	6.40	6.40	6.50	6.50	6.50	6.50	6.47	.00	.05
100	9.20	9.10	8.90	8.80	8.90	9.00	8.98	.02	.15
101	6.30	5.80	5.80	5.90	6.10	5.90	5.97	.04	.20
102	6.30	5.80	5.80	5.80	5.80	5.80	5.88	.04	.20
103	23.20	24.90	25.30	24.80	24.90	24.90	24.67	.55	.74
104	9.80	10.30	10.20	10.30	10.40	10.30	10.22	.05	.21
105	8.90	9.20	9.10	9.10	9.20	9.00	9.08	.01	.12
106	6.20	6.10	6.30	6.30	6.10	6.20	6.20	.01	.09
107	6.20	6.30	6.40	6.30	6.20	6.30	6.28	.01	.08
108	5.90	5.60	5.70	5.60	5.70	5.60	5.68	.01	.12
109	9.00	8.60	8.70	8.70	8.60	8.80	8.73	.02	.15
110	9.00	9.60	9.80	9.50	9.80	9.80	9.58	.10	.31
111	11.40	11.50	11.00	11.30	11.40	11.10	11.28	.04	.19
112	4.50	4.60	4.60	4.70	4.70	4.60	4.62	.01	.08
113	6.30	6.70	6.80	6.90	6.70	6.70	6.68	.04	.20
114	26.90	26.90	27.00	27.10	26.70	27.50	27.02	.07	.27
115	9.10	11.20	11.10	11.20	11.30	11.10	10.83	.73	.85
116	22.10	23.30	23.50	23.50	23.30	23.30	23.17	.28	.53
117	11.50	12.30	12.30	12.30	12.30	12.30	12.17	.11	.33
118	9.60	8.80	8.70	8.70	8.70	8.70	8.87	.13	.36
119	11.70	12.00	12.20	12.10	12.10	12.10	12.03	.03	.18
120	6.10	6.50	6.60	6.60	6.60	6.70	6.52	.05	.21
121	11.50	11.60	11.60	11.40	11.50	11.60	11.53	.01	.08
122	11.50	11.60	11.50	11.60	11.60	11.50	11.55	.00	.05
123	10.10	10.00	10.60	10.10	10.00	10.00	10.13	.05	.23
124	12.00	9.70	9.90	9.50	9.70	9.40	10.03	.96	.98
125	11.40	11.40	11.10	11.30	11.50	11.20	11.32	.02	.15
126	11.40	11.20	11.20	11.20	11.20	11.30	11.25	.01	.08
127	10.40	10.70	10.70	10.60	10.60	10.70	10.62	.01	.12
128	11.70	12.70	12.70	12.60	12.70	12.40	12.47	.15	.39
129	11.60	12.30	12.20	12.30	12.20	12.50	12.18	.09	.31
130	12.10	12.60	12.30	12.70	12.50	12.50	12.45	.05	.22
131	8.80	9.40	9.30	9.50	9.20	9.20	9.23	.06	.24
132	9.00	9.00	9.00	9.00	8.90	9.10	9.00	.00	.06
133	12.00	12.70	12.80	12.70	12.80	12.80	12.63	.10	.31
134	5.90	6.30	6.30	6.30	6.30	6.50	6.27	.04	.20
135	6.40	6.60	6.40	6.50	6.60	6.60	6.52	.01	.10
136	11.50	9.40	9.40	9.40	9.40	9.40	9.75	.73	.86
137	6.60	6.50	6.60	6.50	6.40	6.70	6.55	.01	.10
138	9.80	10.30	10.20	10.30	10.20	10.20	10.17	.03	.19
139	8.40	9.40	9.40	9.40	9.40	9.40	9.23	.17	.41
140	8.50	9.00	9.10	8.90	9.00	9.00	8.92	.05	.21
141	6.00	6.50	6.50	6.60	6.50	6.50	6.43	.05	.22
142	11.70	12.00	11.90	11.80	11.80	11.80	11.83	.01	.10
143	11.00	12.30	12.30	12.60	12.10	12.10	12.07	.31	.55
144	9.40	9.60	9.60	9.60	9.60	9.60	9.57	.01	.08
145	12.10	11.60	11.60	11.40	11.30	11.60	11.60	.08	.28

Table A-1: Range finder measurements in study field

FID	LASER1	LASER2	LASER3	LASER4	LASER5	LASER6	LASER_MEAN	LSR_VAR	LSR_STD
146	12.20	12.30	12.30	12.00	12.20	12.20	12.20	.01	.11
147	10.60	10.30	10.10	10.00	10.30	10.10	10.23	.05	.22
148	5.20	5.30	5.20	5.30	5.30	5.30	5.27	.00	.05
149	7.30	7.70	7.60	7.60	7.70	7.50	7.57	.02	.15
150	9.90	10.80	10.80	10.70	10.60	10.40	10.53	.12	.34
151	12.00	11.80	12.00	12.00	11.80	11.80	11.90	.01	.11
152	3.70	3.60	3.70	3.60	3.60	3.60	3.63	.00	.05
153	4.00	3.90	4.00	3.80	3.90	3.90	3.92	.01	.08
154	23.30	24.20	24.10	24.00	24.20	23.70	23.92	.13	.35
155	25.10	26.50	26.20	26.70	26.40	26.60	26.25	.35	.59
156	12.20	12.60	12.30	12.50	12.50	12.10	12.37	.04	.20
157	6.60	6.60	6.60	6.50	6.40	6.50	6.53	.01	.08
158	25.10	26.30	26.70	25.40	26.40	25.70	25.93	.39	.63
159	11.70	13.20	13.20	13.10	13.20	13.00	12.90	.35	.59
160	12.40	13.00	12.90	12.80	12.80	12.90	12.80	.04	.21
161	8.80	9.60	9.60	9.60	9.70	9.60	9.48	.11	.34
162	11.80	12.20	12.50	12.60	12.30	12.30	12.28	.08	.28
163	3.00	3.10	3.10	3.00	3.10	3.20	3.08	.01	.08
164	12.70	13.20	13.30	13.40	13.20	13.20	13.17	.06	.24
165	12.40	13.00	12.80	12.90	13.10	12.90	12.85	.06	.24
166	6.30	6.40	6.40	6.50	6.30	6.40	6.38	.01	.08
167	9.00	9.80	9.80	9.80	9.80	9.90	9.68	.11	.34
168	11.30	11.60	11.50	11.60	11.40	11.50	11.48	.01	.12
169	11.20	11.90	11.80	12.10	12.00	12.10	11.85	.12	.34
170	11.80	12.40	12.40	12.40	12.40	12.30	12.28	.06	.24
171	12.20	12.60	12.50	12.60	12.50	12.40	12.47	.02	.15
172	5.60	6.00	6.10	6.00	6.00	6.00	5.95	.03	.18
173	10.90	10.80	10.80	10.80	10.80	10.80	10.82	.00	.04
174	16.70	14.90	15.00	14.60	14.60	14.90	15.12	.63	.79
175	10.80	10.90	10.80	11.00	11.00	10.90	10.90	.01	.09
176	11.70	12.80	12.60	12.70	12.60	12.70	12.52	.17	.41
177	8.00	8.30	7.60	7.60	8.30	7.60	7.90	.12	.35
178	3.20	3.40	3.30	3.40	3.40	3.40	3.35	.01	.08
179	11.60	11.60	12.00	11.90	11.30	11.70	11.68	.06	.25
180	11.20	11.30	11.30	11.20	11.40	11.40	11.30	.01	.09
181	2.30	2.40	2.50	2.40	2.50	2.50	2.43	.01	.08
182	8.80	8.10	8.80	8.90	9.00	9.10	8.78	.13	.35
183	8.80	9.20	9.50	9.00	9.40	8.80	9.12	.09	.30
184	11.20	11.80	11.70	11.80	11.90	11.80	11.70	.06	.25
185	12.90	12.50	12.90	12.90	12.80	13.20	12.87	.05	.23
186	9.40	10.20	10.20	10.00	9.90	9.50	9.87	.12	.34
187	3.80	3.80	3.80	3.70	3.60	3.80	3.75	.01	.08
188	9.00	9.70	8.80	9.10	9.20	9.30	9.18	.09	.31
189	11.60	11.60	11.90	12.40	11.80	11.90	11.87	.09	.29
190	9.70	9.80	9.70	9.90	9.40	9.40	9.65	.04	.21
191	6.10	6.50	6.50	6.50	6.00	5.90	6.25	.08	.28
192	23.80	23.90	23.20	24.40	23.70	22.80	23.63	.31	.56
193	24.70	25.50	24.80	25.50	25.00	25.00	25.08	.12	.34
194	24.40	23.50	23.00	23.20	23.40	23.50	23.50	.23	.48
195	9.20	9.10	9.10	9.30	9.30	9.50	9.25	.02	.15
196	11.20	12.10	11.40	11.60	11.70	11.50	11.58	.09	.31

Table A-1: Range finder measurements in study field

FID	LASER1	LASER2	LASER3	LASER4	LASER5	LASER6	LASER_MEAN	LSR_VAR	LSR_STD
197	9.10	8.80	9.00	9.20	8.80	9.20	9.02	.03	.18
198	12.90	12.40	11.90	12.20	12.20	12.60	12.37	.12	.35
199	15.70	14.90	15.80	15.60	15.30	15.50	15.47	.11	.33
200	25.20	25.00	24.20	25.20	24.40	24.80	24.80	.18	.42
201	13.00	11.80	10.00	12.00	12.20	11.50	11.75	.99	1.00
202	22.70	22.20	23.30	23.70	23.00	23.90	23.13	.40	.63
203	19.70	20.40	20.30	19.40	20.60	20.80	20.20	.29	.54
204	7.00	7.10	6.90	6.80	6.50	7.50	6.97	.11	.33
205	7.40	7.10	6.90	6.90	6.90	7.10	7.05	.04	.20
206	24.30	26.30	25.90	25.30	26.30	25.20	25.55	.60	.77
207	14.40	17.00	17.10	17.00	17.10	17.10	16.62	1.18	1.09
208	8.40	9.20	5.30	5.30	5.40	7.90	6.92	3.18	1.78
209	8.60	8.90	9.20	9.10	9.10	9.10	9.00	.05	.22
210	7.20	7.40	7.40	7.40	7.40	7.40	7.37	.01	.08
211	9.30	9.20	9.20	9.30	9.50	9.20	9.28	.01	.12
212	15.30	15.60	15.60	15.50	15.60	15.60	15.53	.01	.12
213	19.40	19.40	19.80	19.40	19.80	19.40	19.53	.04	.21
214	20.70	20.70	20.70	20.70	20.70	20.70	20.70	.00	.00
215	9.50	9.50	9.20	9.50	9.50	9.50	9.45	.02	.12
216	15.80	15.90	15.80	15.90	15.90	15.90	15.87	.00	.05
217	17.30	17.60	17.60	17.70	17.70	17.90	17.63	.04	.20
218	15.80	16.20	16.00	15.80	16.10	16.10	16.00	.03	.17
219	17.80	18.80	18.80	18.70	18.90	18.80	18.63	.17	.41
220	13.50	14.30	14.10	14.20	14.20	14.20	14.08	.09	.29
221	11.50	12.40	12.40	12.20	12.30	12.20	12.17	.11	.34
222	13.90	14.00	14.10	14.30	13.80	14.10	14.03	.03	.18
223	11.50	12.80	12.80	12.70	12.80	13.10	12.62	.32	.56
224	17.00	18.00	17.80	18.10	17.60	17.70	17.70	.15	.39
225	9.40	9.20	9.20	9.20	9.20	9.40	9.27	.01	.10
226	9.10	9.80	9.60	9.60	9.60	9.60	9.55	.06	.23
227	9.40	10.20	10.20	10.30	10.20	10.00	10.05	.11	.33
228	6.50	6.60	6.60	6.70	6.70	6.60	6.62	.01	.08
229	3.80	4.10	4.20	4.10	4.10	4.00	4.05	.02	.14
230	2.80	3.40	3.50	3.40	3.40	3.40	3.32	.07	.26
231	8.80	9.20	9.40	9.30	9.20	9.40	9.22	.05	.22
232	8.90	9.30	9.40	9.50	9.50	9.50	9.35	.05	.23
233	8.60	9.50	9.60	9.30	9.70	9.60	9.38	.17	.41
234	6.90	9.60	9.60	9.60	9.60	9.60	9.15	1.21	1.10
235	17.30	19.50	19.20	18.70	18.80	18.70	18.70	.57	.76
236	8.80	10.30	10.40	10.20	10.20	10.20	10.02	.36	.60
237	12.30	13.70	13.70	13.80	13.60	13.50	13.43	.32	.56
238	14.50	14.90	14.90	14.90	15.00	15.10	14.88	.04	.20
239	11.50	11.30	11.70	11.40	11.60	11.60	11.52	.02	.15
240	11.50	12.60	12.60	12.50	12.60	12.60	12.40	.20	.44
241	13.80	13.80	13.90	13.80	13.80	13.90	13.83	.01	.08
242	11.50	12.50	12.60	12.90	12.70	12.70	12.48	.25	.50
243	8.70	8.70	9.00	9.10	9.00	8.90	8.90	.03	.17
244	10.60	10.90	10.70	10.50	10.60	10.60	10.65	.02	.14
245	17.30	16.70	17.10	17.10	17.00	16.80	17.00	.05	.22
246	6.70	7.10	7.30	7.40	7.20	7.20	7.15	.06	.24
247	14.50	15.30	14.60	15.10	15.00	15.10	14.93	.10	.31

Table A-1: Range finder measurements in study field

FID	LASER1	LASER2	LASER3	LASER4	LASER5	LASER6	LASER_ MEAN	LSR_ VAR	LSR_ STD
248	10.40	11.10	11.10	11.00	11.10	11.10	10.97	.08	.28
249	26.20	26.00	26.00	25.80	26.30	25.80	26.02	.04	.20
250	14.80	14.90	14.70	14.90	14.80	15.00	14.85	.01	.10
251	9.70	9.80	9.70	9.70	9.70	9.80	9.73	.00	.05
252	25.10	26.60	26.50	27.00	26.60	26.90	26.45	.47	.69
253	5.90	6.80	6.80	7.00	7.00	6.90	6.73	.17	.42
254	9.00	9.80	9.80	9.80	9.80	9.80	9.67	.11	.33
255	10.20	10.50	10.40	10.30	10.40	10.30	10.35	.01	.10
256	24.50	24.50	23.90	24.40	24.30	24.40	24.33	.05	.23
257	24.10	24.20	24.10	24.00	24.10	23.90	24.07	.01	.10
258	8.80	9.90	10.00	9.50	9.40	9.90	9.58	.21	.45
259	15.30	15.60	15.60	15.40	15.40	15.60	15.48	.02	.13
260	10.60	10.30	10.70	10.80	10.60	10.60	10.60	.03	.17
261	14.50	14.90	14.80	14.90	14.60	15.00	14.78	.04	.19
262	10.50	10.70	10.50	10.60	10.60	10.60	10.58	.01	.08
263	10.10	10.20	10.10	10.20	10.30	10.10	10.17	.01	.08
264	5.60	5.60	5.70	5.80	5.70	5.70	5.68	.01	.08
265	12.60	13.50	13.60	13.50	13.50	13.50	13.37	.14	.38
266	9.70	10.00	10.00	10.00	10.10	10.10	9.98	.02	.15
267	11.80	11.80	11.80	11.70	11.80	11.70	11.77	.00	.05
268	23.40	23.80	23.70	23.50	23.70	23.80	23.65	.03	.16
269	6.60	6.80	6.70	6.70	6.70	6.70	6.70	.00	.06
270	5.20	5.50	5.50	5.50	5.50	5.50	5.45	.01	.12
271	6.90	6.70	6.80	6.90	6.80	6.80	6.82	.01	.08
272	9.20	9.90	9.90	10.00	9.80	9.90	9.78	.09	.29
273	6.50	7.00	6.90	7.00	7.00	6.90	6.88	.04	.19
274	6.10	6.50	5.90	6.00	6.50	6.40	6.23	.07	.27
275	13.70	13.70	13.70	13.70	13.60	13.60	13.67	.00	.05
276	11.60	12.30	11.80	11.70	11.40	11.40	11.70	.11	.33
277	4.90	5.30	5.10	5.20	5.30	5.20	5.17	.02	.15
278	7.80	7.90	7.80	7.90	7.80	7.90	7.85	.00	.05
279	9.30	9.50	9.40	9.30	9.50	9.40	9.40	.01	.09
280	26.00	26.00	25.80	25.80	25.90	25.90	25.90	.01	.09
281	9.80	9.80	9.90	10.10	10.00	9.90	9.92	.01	.12
282	13.70	13.30	13.70	13.30	13.40	13.50	13.48	.03	.18
283	13.90	14.00	13.80	13.80	13.80	13.80	13.85	.01	.08
284	13.50	13.50	13.50	13.30	13.50	13.50	13.47	.01	.08
285	5.10	5.50	5.50	5.50	5.50	5.50	5.43	.03	.16
286	11.20	11.40	11.50	11.40	11.30	11.50	11.38	.01	.12
287	11.80	11.20	11.70	11.70	11.70	11.70	11.63	.05	.22
288	9.60	9.90	9.80	9.90	9.80	9.80	9.80	.01	.11
289	8.50	8.80	8.80	8.90	8.80	8.80	8.77	.02	.14
290	9.10	9.40	9.30	9.40	9.40	9.40	9.33	.01	.12
291	10.00	10.20	10.10	10.10	10.00	10.10	10.08	.01	.08
292	10.30	10.40	10.30	10.30	10.30	10.30	10.32	.00	.04
293	13.50	13.60	13.60	13.50	13.60	13.60	13.57	.00	.05
294	13.10	13.20	13.20	13.10	13.10	13.20	13.15	.00	.05
295	11.50	11.50	11.50	11.50	11.50	11.50	11.50	.00	.00
296	9.40	9.40	9.60	9.50	9.40	9.40	9.45	.01	.08
297	5.30	5.60	5.70	6.30	6.40	6.30	5.93	.21	.46
298	4.80	5.10	5.00	5.10	5.00	5.10	5.02	.01	.12

Table A-1: Range finder measurements in study field

FID	LASER1	LASER2	LASER3	LASER4	LASER5	LASER6	LASER_ MEAN	LSR_ VAR	LSR_ STD
299	4.80	5.10	5.00	5.10	5.00	5.10	5.02	.01	.12
300	4.80	5.30	5.20	5.20	5.20	5.20	5.15	.03	.18
301	6.10	7.00	7.00	7.00	7.00	7.00	6.85	.14	.37
302	12.30	13.30	13.10	13.30	13.30	13.30	13.10	.16	.40
303	10.00	10.10	10.10	10.20	10.20	10.00	10.10	.01	.09
304	15.80	16.20	15.90	15.80	15.90	15.80	15.90	.02	.15
305	7.30	7.30	7.30	7.30	7.30	7.30	7.30	.00	.00
306	9.90	11.10	11.30	11.20	11.10	11.30	10.98	.29	.54
307	13.40	13.50	13.40	13.60	13.40	13.40	13.45	.01	.08
308	14.80	14.70	15.00	14.80	14.80	14.70	14.80	.01	.11
309	12.10	12.80	12.60	12.70	12.50	12.70	12.57	.06	.25
310	9.40	9.20	9.40	9.50	9.50	9.20	9.37	.02	.14
311	4.40	4.50	4.40	4.50	4.50	4.50	4.47	.00	.05
312	4.40	4.50	4.50	4.50	4.50	4.50	4.48	.00	.04
313	8.30	8.30	8.20	8.30	8.30	8.30	8.28	.00	.04
314	7.30	7.40	7.10	7.30	7.30	7.40	7.30	.01	.11
315	12.60	12.50	12.60	12.60	12.40	12.40	12.52	.01	.10
316	6.60	6.30	6.50	6.50	6.50	6.50	6.48	.01	.10
317	10.50	10.10	10.00	10.10	10.10	10.10	10.15	.03	.18
318	6.60	6.90	6.80	6.70	6.80	6.70	6.75	.01	.10
319	9.60	9.70	9.60	9.50	9.60	9.60	9.60	.00	.06
320	10.10	10.10	10.20	10.10	10.10	10.10	10.12	.00	.04
321	10.50	10.50	10.60	10.50	10.50	10.50	10.52	.00	.04
322	8.40	8.60	8.70	8.70	8.70	8.70	8.63	.01	.12
323	3.70	3.60	3.60	3.60	3.60	3.60	3.62	.00	.04
324	4.50	4.80	4.90	4.90	4.90	4.90	4.82	.03	.16
325	5.50	7.50	7.40	7.00	7.60	7.60	7.10	.66	.81
326	25.50	26.00	25.80	24.60	26.90	26.70	25.92	.70	.84
327	11.00	11.10	11.00	10.90	11.00	11.10	11.02	.01	.08
328	25.50	25.40	25.50	25.10	25.50	25.30	25.38	.03	.16
329	27.10	27.10	27.20	27.90	27.30	27.20	27.30	.09	.30
330	6.20	6.20	6.30	6.30	6.30	6.30	6.27	.00	.05
331	4.40	4.60	4.60	4.60	4.60	4.60	4.57	.01	.08
332	5.10	5.60	5.50	5.60	5.60	5.60	5.50	.04	.20
333	3.20	3.30	3.40	3.30	3.40	3.40	3.33	.01	.08
334	27.30	27.40	27.80	27.40	27.30	27.30	27.42	.04	.19
335	6.30	6.70	6.70	6.70	6.70	6.70	6.63	.03	.16
336	26.00	25.70	25.80	26.10	25.80	25.90	25.88	.02	.15
337	9.90	10.00	10.00	10.10	9.90	10.20	10.02	.01	.12
338	25.20	25.60	25.20	25.20	25.40	25.20	25.30	.03	.17
339	6.00	6.10	6.00	6.10	6.10	6.10	6.07	.00	.05
340	6.00	6.10	6.00	6.10	6.10	6.10	6.07	.00	.05
341	9.30	9.60	9.60	9.60	9.60	9.60	9.55	.01	.12
342	9.60	9.60	9.60	9.60	9.60	9.60	9.60	.00	.00
343	9.90	11.20	11.10	11.10	11.10	11.10	10.92	.25	.50
344	9.60	10.20	9.80	9.60	9.90	9.90	9.83	.05	.23
345	10.10	10.10	10.20	10.30	10.40	10.30	10.23	.01	.12
346	9.50	9.70	9.80	9.80	9.90	9.90	9.77	.02	.15
347	24.10	24.10	23.70	24.10	23.80	24.30	24.02	.05	.22
348	9.30	9.70	9.40	9.40	9.60	9.70	9.52	.03	.17
349	8.70	9.00	9.20	9.20	9.10	9.30	9.08	.05	.21

Table A-1: Range finder measurements in study field

FID	LASER1	LASER2	LASER3	LASER4	LASER5	LASER6	LASER_ MEAN	LSR_ VAR	LSR_ STD
350	17.30	17.00	16.80	16.70	17.10	17.60	17.08	.11	.33
351	22.80	24.40	24.90	24.80	24.80	24.70	24.40	.64	.80
352	17.30	17.30	16.90	17.20	17.30	17.30	17.22	.03	.16
353	25.20	25.60	25.20	25.20	25.40	25.20	25.30	.03	.17
354	11.60	11.90	11.90	12.00	11.80	11.90	11.85	.02	.14
355	7.10	7.10	7.20	7.10	7.10	7.10	7.12	.00	.04
356	6.50	6.40	6.40	6.50	6.50	6.60	6.48	.01	.08
357	9.10	9.10	9.30	9.20	9.20	9.20	9.18	.01	.08
358	7.20	7.30	7.20	7.20	7.20	7.20	7.22	.00	.04
359	26.20	26.60	25.80	26.00	25.40	26.20	26.03	.17	.41

Table A-2: User measurements from stereo image pairs

FID	SI1_ USR1	SI1_ USR2	SI1_ USR3	SI1_ USR4	SI1_ USR5	SI1_ USR6	SI1_ USR7	SI1_ USR8	SI1_ USR9	SI1_ USR10
1	19,47	21,54	21,11	19,25	18,76	29,01	27,35	16,60	21,11	18,68
2	24,92	24,92	12,71	13,32	22,76	15,96	24,95	27,51	30,75	15,87
3	26,22	12,72	12,72	29,63	26,76	15,96	14,44	22,48	26,86	15,88
4	12,06	15,82	15,82	12,00	14,15	13,91	21,14	28,21	14,65	16,57
5	16,62	19,04	19,04	12,00	15,48	29,73	27,15	28,21	15,54	16,57
6	24,98	15,12	15,12	26,46	26,75	15,96	31,71	21,64	26,86	15,87
7	8,36	10,25	19,14	11,03	9,45	24,90	21,19	17,44	10,05	28,72
8	13,44	19,14	15,92	13,18	13,44	24,90	18,19	6,54	14,47	28,72
9	25,92	25,67	25,67	25,69	28,71	12,50	29,50	27,17	29,13	13,94
10	28,24	25,67	25,67	25,69	27,38	11,81	31,00	32,68	26,49	9,04
11	25,09	24,86	24,86	25,14	24,71	17,99	27,99	26,80	28,68	9,04
12	24,68	26,47	26,47	25,15	24,72	18,00	28,75	23,45	29,42	18,84
13	25,60	26,98	26,98	28,01	25,22	17,13	27,75	23,96	29,56	13,22
14	14,87	14,41	14,41	14,83	12,73	7,68	18,98	14,72	15,85	12,10
15	15,68	4,77	4,77	16,72	14,06	15,94	17,48	16,69	17,69	11,49
16	15,68	4,77	4,77	18,14	14,07	12,50	18,98	25,13	18,79	12,11
17	5,45	4,76	4,76	5,19	7,41	4,93	7,74	16,69	7,05	9,03
18	13,53	5,57	5,57	13,55	11,41	13,19	13,73	13,38	13,66	10,27
19	13,52	5,56	5,56	13,54	11,40	13,87	16,72	13,37	14,75	10,25
20	27,73	26,37	26,37	28,72	25,42	26,96	36,95	20,80	27,30	27,26
21	12,04	10,39	10,39	15,91	12,73	27,62	10,72	12,76	13,29	12,10
22	9,25	12,80	12,80	9,51	7,41	27,62	17,48	5,83	7,06	28,02
23	14,91	19,23	19,23	11,26	11,40	15,93	9,97	20,09	15,86	28,02
24	17,95	16,02	16,02	18,54	11,40	26,26	16,73	18,41	18,46	28,02
25	15,68	14,41	14,41	16,79	14,07	27,63	15,98	11,70	15,49	11,49
26	9,25	11,99	11,99	9,16	11,40	27,62	15,22	11,70	10,72	28,02
27	8,91	9,59	9,59	8,90	11,41	15,94	9,22	8,35	5,59	19,69
28	13,53	17,63	17,63	13,42	11,41	10,44	17,48	14,07	13,29	12,12
29	13,52	5,56	17,62	13,41	11,40	10,43	16,72	14,06	13,28	11,64
30	13,53	14,41	14,41	13,42	11,40	5,62	15,98	5,83	13,29	10,26
31	13,52	14,40	14,40	13,41	11,40	3,55	13,72	5,82	14,75	11,40
32	8,91	8,78	8,78	8,90	7,41	15,94	12,22	10,02	11,02	19,69
33	9,69	10,39	10,39	9,50	7,41	15,93	12,97	9,48	10,28	19,69
34	9,69	10,39	10,39	9,50	7,41	15,94	15,23	10,02	11,01	19,69
35	11,34	16,74	16,74	11,18	13,98	15,85	9,89	9,10	10,64	27,94
36	10,12	9,59	9,59	10,65	10,07	15,94	9,97	3,31	13,22	19,69
37	10,12	9,59	9,59	10,65	14,07	15,94	8,47	3,31	13,22	19,69
38	9,69	11,19	11,19	9,91	10,07	12,49	12,97	10,02	9,55	19,69
39	12,15	7,38	7,38	12,95	13,47	15,34	19,13	11,10	10,78	17,87
40	13,66	12,81	7,18	13,55	8,74	15,94	15,23	15,90	14,68	18,47

Table A-2: User measurements from stereo image pairs

FID	SI1_USR1	SI1_USR2	SI1_USR3	SI1_USR4	SI1_USR5	SI1_USR6	SI1_USR7	SI1_USR8	SI1_USR9	SI1_USR10
41	9,26	2,36	2,36	9,78	16,73	15,94	14,48	13,42	8,73	19,69
42	24,68	7,98	7,98	24,68	6,09	15,94	12,98	24,55	25,53	18,47
43	14,22	7,98	7,98	14,23	14,07	25,00	13,73	14,73	12,71	18,47
44	17,96	16,83	16,83	18,21	16,73	15,94	19,74	13,42	18,46	19,69
45	17,95	11,20	11,20	17,73	16,73	15,94	20,48	16,69	17,13	19,69
46	17,74	17,24	11,20	17,53	16,73	15,94	17,48	13,38	18,46	19,69
47	9,10	8,19	8,19	9,46	10,81	11,90	12,38	10,86	16,98	19,10
48	15,24	15,24	8,78	24,67	10,07	12,49	14,47	24,28	25,53	21,53
49	10,44	10,44	8,78	10,05	11,40	12,49	12,97	12,10	17,57	19,69
50	24,68	21,65	21,65	24,88	22,05	25,00	27,24	14,73	30,39	18,47
51	25,34	2,36	2,36	27,96	21,97	16,55	24,16	26,72	26,17	15,08
52	25,34	25,40	25,40	27,96	21,97	11,73	28,66	25,88	26,16	6,46
53	7,52	10,80	10,80	7,40	6,00	12,41	3,13	11,61	7,26	7,12
54	11,31	-0,72	-0,72	11,25	6,00	12,42	13,64	3,23	9,78	13,86
55	10,31	4,65	4,65	10,57	8,66	11,73	15,14	2,39	10,20	12,64
56	7,94	3,71	3,71	6,11	9,26	12,32	12,74	2,99	7,86	13,24
57	6,29	1,41	1,41	6,44	5,26	8,20	4,47	5,50	6,59	8,91
58	6,28	11,39	11,39	5,77	5,26	8,19	4,47	5,50	6,59	8,91
59	6,28	11,39	11,39	6,44	5,26	8,19	6,73	5,50	6,59	8,91
60	28,08	23,69	23,69	28,02	26,56	12,32	26,25	18,92	25,50	3,96
61	25,93	23,69	23,69	25,79	26,55	5,44	26,25	18,92	26,34	12,61
62	26,64	27,13	27,13	30,86	28,09	29,02	24,95	26,57	32,16	18,67
63	17,83	18,29	18,29	15,82	20,10	26,94	18,19	19,36	25,97	18,68
64	13,97	15,63	15,63	16,48	12,11	26,94	23,44	10,19	14,92	27,24
65	27,18	27,60	27,60	27,48	26,75	26,95	24,49	26,56	27,73	27,25
66	26,63	28,26	28,26	29,02	24,08	29,02	31,70	30,49	30,39	27,87
67	26,63	22,94	22,94	26,33	26,75	29,02	21,94	23,32	27,30	18,68
68	8,54	8,54	22,28	25,67	26,09	28,37	22,79	29,84	27,08	18,02
69	22,93	27,64	27,64	22,31	23,46	29,72	22,65	29,05	21,73	19,39
70	22,94	27,65	27,65	22,65	22,14	29,73	21,90	29,06	24,39	19,40
71	13,71	6,36	6,36	14,02	14,15	16,66	18,89	28,21	15,09	16,57
72	16,17	18,96	18,96	16,27	13,44	26,95	22,84	14,93	18,46	16,24
73	6,02	4,95	4,95	6,53	4,66	15,01	6,13	10,05	5,16	10,79
74	6,61	5,54	5,54	7,11	5,25	15,60	5,97	5,50	6,59	8,91
75	5,69	4,95	4,95	5,51	8,65	11,72	9,88	6,12	4,73	12,63
76	5,69	4,95	4,95	5,51	8,65	11,72	5,38	6,78	4,73	10,78
77	7,98	8,24	8,24	8,54	12,65	12,41	10,63	11,61	6,67	8,25
78	11,71	7,70	7,70	12,59	12,65	8,29	8,38	14,97	12,30	10,15
79	11,71	7,70	7,70	12,25	4,66	13,10	6,13	14,97	13,98	15,17
80	10,21	7,15	7,15	9,83	8,66	11,73	9,89	10,71	10,20	12,02
81	7,70	6,05	6,05	7,33	7,33	14,48	9,14	9,40	8,10	13,00
82	7,70	6,05	6,05	7,33	8,66	14,48	8,39	12,46	8,52	13,61
83	5,18	6,05	6,05	5,65	7,33	14,48	9,13	3,23	5,58	9,32
84	7,70	6,05	6,05	8,68	7,33	14,48	12,14	3,51	7,68	10,12
85	12,08	7,70	7,70	12,05	12,65	8,06	12,89	14,97	13,37	13,01
86	9,50	7,70	7,70	6,66	12,65	9,67	15,14	4,91	7,26	10,12
87	12,40	12,64	12,64	12,59	12,65	8,28	15,89	11,62	12,18	10,15
88	10,09	13,19	13,19	13,26	12,65	8,28	15,14	4,90	13,76	17,52
89	13,07	13,75	13,75	13,00	12,65	8,29	15,90	13,33	12,19	17,53
90	12,74	9,90	9,90	12,99	12,65	14,47	18,14	12,67	11,00	12,29
91	12,80	9,96	9,96	13,73	12,71	14,54	15,20	12,74	11,06	12,35
92	12,80	9,96	9,96	13,06	12,71	14,54	15,20	13,39	11,07	12,35
93	13,69	16,49	16,49	12,05	12,65	9,67	18,15	14,97	13,37	10,12
94	11,39	16,49	16,49	11,65	12,65	9,67	15,15	12,68	12,19	8,69
95	10,77	11,55	11,55	10,84	13,98	24,92	15,14	10,06	7,85	23,90
96	8,84	10,44	10,44	8,68	11,32	24,92	12,89	10,05	6,67	23,90
97	9,32	10,44	10,44	9,01	11,32	24,91	9,13	8,09	9,43	25,12
98	12,21	11,00	11,00	12,05	11,32	24,92	12,14	20,85	13,77	20,59
99	13,65	14,84	14,84	13,53	8,66	24,92	11,39	20,85	13,76	20,59
100	13,65	15,94	15,94	13,87	13,98	22,93	12,14	11,62	12,18	23,65
101	9,65	14,85	14,85	13,88	13,99	22,94	15,90	14,98	13,37	23,66
102	7,49	8,25	8,25	7,81	8,66	21,94	6,88	2,39	3,52	23,65

Table A-2: User measurements from stereo image pairs

FID	SI1_USR1	SI1_USR2	SI1_USR3	SI1_USR4	SI1_USR5	SI1_USR6	SI1_USR7	SI1_USR8	SI1_USR9	SI1_USR10
103	7,88	8,25	8,25	7,47	8,66	21,94	9,14	2,39	3,52	23,65
104	7,88	8,25	8,25	7,81	8,66	21,94	10,64	2,39	3,52	23,65
105	7,88	8,25	8,25	7,81	8,66	21,94	6,88	2,39	3,52	15,17
106	6,41	6,09	6,09	5,95	8,15	21,43	9,38	6,91	6,16	22,53
107	6,41	10,49	10,49	5,95	5,49	18,46	13,13	6,91	4,59	23,14
108	6,89	9,38	9,38	6,96	5,48	18,45	10,12	-7,35	4,98	23,14
109	13,62	12,14	12,14	13,56	5,49	24,41	7,12	5,62	12,07	23,14
110	6,67	12,14	12,14	6,49	5,49	24,41	4,87	5,62	7,35	30,13
111	10,26	12,14	12,14	8,51	8,15	24,41	10,13	-1,47	7,74	30,13
112	10,25	11,03	11,03	8,50	8,14	24,40	6,37	-1,48	8,92	30,12
113	14,28	6,09	6,09	10,33	8,15	24,41	10,88	9,43	13,25	24,61
114	8,82	8,29	8,29	8,98	8,15	24,37	8,63	7,58	7,56	20,08
115	10,88	8,29	8,29	11,34	8,15	24,37	14,64	7,58	9,40	23,14
116	2,24	2,24	5,85	11,90	8,71	7,02	6,20	1,25	5,96	3,71
117	12,18	9,39	9,39	12,01	12,14	18,45	11,63	13,47	10,13	23,14
118	9,30	9,39	9,39	9,93	13,48	24,41	17,64	10,21	10,13	30,13
119	24,09	9,39	9,39	24,69	16,14	24,41	25,15	23,96	23,70	30,13
120	13,62	9,94	9,94	13,29	14,80	24,41	24,39	-5,67	14,16	24,61
121	24,59	21,99	21,99	24,52	19,31	24,92	25,65	25,04	26,04	30,63
122	22,95	22,54	22,54	23,18	24,63	24,92	26,41	16,66	21,27	23,65
123	24,59	17,59	17,59	24,19	17,98	24,92	19,65	8,26	22,37	23,65
124	24,59	25,28	25,28	24,52	24,63	18,96	22,65	25,12	26,77	23,65
125	24,60	25,29	25,29	24,86	24,63	18,97	31,67	23,82	22,74	23,65
126	24,60	26,94	26,94	24,19	24,63	24,88	24,16	25,88	24,94	20,59
127	25,92	29,72	29,72	26,93	26,54	3,71	30,75	19,75	25,91	4,57
128	27,29	25,87	25,87	27,61	26,55	3,72	25,50	26,37	25,92	4,58
129	25,93	25,87	25,87	28,21	29,21	6,67	23,99	24,40	25,91	7,67
130	17,79	25,87	25,87	18,04	19,90	3,72	24,74	20,60	17,93	7,67
131	12,69	25,87	25,87	13,51	37,19	9,65	11,97	11,30	12,05	9,44
132	24,94	25,88	25,88	25,52	27,88	11,64	27,00	23,12	26,34	10,95
133	18,36	19,28	19,28	18,10	21,22	10,64	17,23	16,40	17,09	9,45
134	10,42	11,58	11,58	10,28	9,24	6,67	10,47	11,37	14,15	6,43
135	7,86	8,29	8,29	10,96	9,25	6,68	7,48	6,34	7,85	7,67
136	6,43	8,29	8,29	7,93	9,25	6,68	7,48	6,34	7,01	7,67
137	10,42	12,68	12,68	10,96	9,25	8,65	11,23	8,01	14,15	10,76
138	10,42	12,68	12,68	10,28	9,24	9,65	8,97	8,01	12,88	9,94
139	10,42	12,68	12,68	10,95	9,25	6,67	11,98	8,01	12,47	10,76
140	10,43	11,04	11,04	10,28	9,25	7,67	10,48	14,72	10,79	9,95
141	10,43	11,04	11,04	10,28	9,25	9,66	9,73	8,02	10,37	9,95
142	15,22	16,57	16,57	15,34	12,96	4,08	20,88	13,11	14,64	2,84
143	19,07	19,32	19,32	18,78	12,96	6,06	18,62	18,14	19,68	2,84
144	24,19	19,86	19,86	21,21	23,61	6,06	24,63	24,10	23,46	4,34
145	10,90	13,23	13,23	10,62	9,25	-0,27	12,73	7,17	10,79	6,43
146	10,90	13,23	13,23	10,62	9,24	8,66	8,22	7,17	11,20	6,43
147	10,30	12,64	12,64	10,03	8,65	15,00	10,63	10,05	8,51	12,02
148	10,30	12,64	12,64	9,68	8,65	15,00	11,38	10,77	9,35	5,83
149	10,16	10,99	10,99	11,37	8,65	14,00	6,87	8,25	9,35	15,11
150	10,81	13,83	13,83	10,56	14,29	11,01	14,12	2,21	9,60	14,71
151	14,99	12,72	12,72	15,07	15,62	7,04	18,62	13,11	15,90	8,83
152	16,51	16,57	16,57	16,42	15,62	9,03	19,38	18,15	15,48	9,76
153	7,60	9,39	9,39	7,85	7,91	11,62	8,22	7,17	10,78	15,08
154	7,60	9,39	9,39	7,85	6,58	5,69	6,72	7,17	8,26	12,61
155	9,11	10,44	10,44	9,48	8,65	11,03	8,38	9,93	8,51	9,31
156	9,71	11,04	11,04	10,08	6,59	5,69	8,22	10,53	7,43	8,19
157	9,71	11,04	11,04	10,08	6,59	11,63	9,73	10,53	7,43	9,91
158	12,98	8,83	8,83	12,84	18,55	8,65	19,47	13,25	13,23	13,82
159	9,98	11,07	11,07	10,08	6,30	25,88	11,86	11,00	9,58	29,36
160	9,84	11,08	11,08	9,75	6,31	23,86	11,12	3,89	8,77	29,37
161	10,69	11,08	11,08	11,10	6,31	23,87	13,37	9,69	8,36	29,37
162	15,00	13,28	13,28	14,81	14,30	22,91	12,62	10,60	14,10	26,92
163	6,74	6,68	6,68	6,72	7,64	25,88	11,87	-0,31	5,90	26,92
164	10,35	14,30	14,30	10,44	8,66	21,95	10,64	0,71	11,02	24,27

127

Table A-2: User measurements from stereo image pairs

FID	SI1_USR1	SI1_USR2	SI1_USR3	SI1_USR4	SI1_USR5	SI1_USR6	SI1_USR7	SI1_USR8	SI1_USR9	SI1_USR10
165	11,38	14,30	14,30	10,98	12,66	24,89	14,40	4,91	10,21	20,60
166	14,50	14,30	14,30	14,62	12,65	24,89	9,89	4,91	11,02	24,27
167	8,66	7,74	7,74	8,78	12,14	24,37	6,37	4,39	6,41	20,08
168	16,48	11,08	11,08	16,15	14,29	25,88	8,12	10,60	12,87	26,92
169	12,42	11,08	11,08	12,99	14,29	25,88	12,62	10,60	11,64	26,92
170	9,33	11,08	11,08	9,42	11,63	20,93	8,12	10,60	9,59	23,25
171	24,80	18,22	18,22	25,05	23,61	23,86	28,39	28,21	25,02	29,37
172	7,18	18,21	18,21	6,85	11,62	23,86	11,86	7,72	7,19	29,36
173	9,84	12,17	12,17	9,75	16,95	25,88	11,86	9,69	10,49	29,36
174	11,38	12,17	12,17	12,11	16,95	25,88	26,89	0,53	10,50	26,92
175	13,58	12,17	12,17	16,15	14,29	25,88	8,86	11,00	9,59	26,92
176	12,98	12,17	12,17	12,78	16,95	25,88	26,89	0,53	12,33	26,92
177	24,80	23,88	23,88	24,37	23,61	23,85	23,88	22,13	25,01	29,36
178	24,80	21,42	21,42	24,38	18,28	25,88	26,89	-7,02	23,92	26,92
179	24,80	17,11	17,11	24,72	23,61	25,88	28,39	20,67	25,39	26,92
180	25,01	26,55	26,55	25,26	23,82	24,07	21,84	28,42	27,79	19,78
181	24,09	11,56	11,56	24,04	26,27	10,02	28,49	22,34	24,14	9,41
182	14,31	11,56	11,56	14,20	8,97	19,94	24,73	14,93	15,32	18,32
183	9,18	9,71	9,71	8,40	8,96	20,92	11,16	5,56	8,69	20,80
184	9,18	10,94	10,94	9,75	6,31	4,08	13,43	5,56	9,06	8,85
185	4,21	6,63	6,63	4,56	6,30	11,99	9,65	5,10	2,41	14,44
186	7,68	6,63	6,63	8,06	6,30	18,92	11,16	4,72	6,37	14,44
187	9,06	6,63	6,63	8,40	6,31	18,92	10,41	9,69	9,63	16,12
188	9,05	11,55	11,55	8,40	6,30	15,95	11,16	9,03	7,76	16,11
189	9,05	8,48	8,48	8,40	6,30	15,95	13,42	8,92	9,63	13,32
190	12,70	12,78	12,78	12,17	6,30	11,01	11,91	13,61	13,12	15,81
191	12,14	12,78	12,78	12,51	6,30	15,94	15,68	13,61	11,25	16,67
192	13,08	8,48	8,48	13,86	6,31	15,95	14,18	12,96	12,19	16,68
193	12,14	7,86	7,86	11,50	6,30	9,02	14,93	7,24	11,72	8,29
194	16,60	4,17	4,17	11,19	3,64	11,01	8,90	15,63	15,69	15,81
195	1,52	11,47	11,47	1,12	7,63	12,98	17,19	9,75	2,17	15,00
196	8,36	11,47	11,47	8,46	8,96	11,00	17,93	9,75	8,46	4,38
197	9,13	14,98	14,98	9,75	7,64	9,03	14,18	13,95	8,46	13,32
198	12,99	14,98	14,98	12,17	7,64	9,03	14,93	7,24	11,96	13,88
199	9,91	11,48	11,48	10,36	12,96	12,00	12,67	7,24	11,96	9,41
200	14,15	15,56	15,56	10,36	12,96	12,00	16,44	8,08	13,13	13,88
201	12,22	15,55	15,55	13,11	12,95	9,02	15,68	8,07	12,89	13,87
202	15,69	10,89	10,89	16,83	7,63	11,99	26,23	17,30	15,31	9,41
203	25,35	24,31	24,31	25,45	7,64	12,00	28,50	24,86	24,51	4,94
204	27,27	24,88	24,88	25,18	32,91	9,02	25,47	23,17	24,14	9,41
205	24,57	23,72	23,72	23,50	24,94	14,96	27,74	24,86	23,78	13,88
206	23,80	14,98	14,98	24,51	24,94	9,03	24,72	21,48	24,51	14,70
207	11,83	14,38	14,38	11,83	7,63	11,00	17,17	13,94	12,81	13,31
208	9,16	6,81	6,81	9,54	6,30	11,00	14,16	3,88	9,39	7,17
209	4,33	9,15	9,15	3,48	6,31	10,02	11,91	3,88	3,81	7,17
210	9,78	10,31	10,31	9,54	8,96	10,01	14,16	12,27	11,49	8,84
211	9,01	8,56	8,56	8,20	8,96	9,02	15,67	14,79	9,39	12,76
212	8,76	9,15	9,15	8,20	8,97	9,02	11,91	14,79	10,09	7,73
213	11,88	12,05	12,05	13,78	12,95	9,02	16,42	5,55	11,49	9,96
214	11,79	13,23	13,23	11,10	12,96	9,03	14,17	12,31	11,03	6,61
215	11,79	13,23	13,23	10,76	10,29	9,02	11,91	10,34	12,89	8,29
216	11,79	13,23	13,23	12,65	12,96	9,03	14,92	13,11	11,03	7,73
217	12,82	13,23	13,23	13,93	10,30	9,03	14,17	11,44	11,96	9,97
218	4,23	13,23	13,23	10,77	10,30	9,03	7,40	10,35	4,04	8,30
219	13,22	14,39	14,39	12,92	11,63	9,03	14,17	5,56	13,35	10,53
220	10,22	14,39	14,39	13,93	10,30	9,03	14,92	11,44	11,96	9,97
221	13,22	14,39	14,39	12,31	11,63	8,04	14,92	5,56	12,19	10,52
222	5,35	6,23	6,23	9,54	6,30	10,02	14,16	0,53	6,13	9,96
223	24,57	11,48	11,48	25,52	18,28	7,05	23,97	24,02	27,10	8,29
224	8,36	5,06	5,06	8,13	6,30	7,05	7,39	7,24	8,69	11,64
225	8,36	8,56	8,56	8,20	6,30	7,05	5,88	8,07	8,00	7,73
226	21,12	9,73	9,73	23,77	18,28	7,05	25,48	8,08	24,07	9,97

128

Table A-2: User measurements from stereo image pairs

FID	SI1_USR1	SI1_USR2	SI1_USR3	SI1_USR4	SI1_USR5	SI1_USR6	SI1_USR7	SI1_USR8	SI1_USR9	SI1_USR10
227	12,63	3,31	3,31	9,68	11,63	11,01	17,93	14,79	11,26	22,00
228	9,38	10,31	10,31	9,68	11,62	19,90	11,15	10,99	8,92	22,00
229	11,55	11,48	11,48	5,15	11,63	9,03	14,17	12,31	9,40	8,97
230	11,91	12,06	12,06	10,43	8,96	11,00	11,15	14,79	12,89	8,29
231	7,21	12,06	12,06	10,43	8,96	8,03	12,66	14,79	5,90	8,29
232	11,21	12,06	12,06	4,39	8,97	9,03	12,66	10,34	13,12	8,85
233	6,55	7,40	7,40	8,17	11,63	9,03	11,16	5,11	7,07	6,61
234	10,28	8,56	8,56	8,93	11,63	7,05	13,41	9,69	10,33	9,41
235	9,82	14,40	14,40	8,93	11,63	4,09	11,92	11,44	9,64	1,03
236	10,28	14,39	14,39	8,92	11,63	8,04	11,91	11,00	9,63	1,02
237	12,15	14,98	14,98	11,95	11,63	12,00	18,68	5,57	11,49	7,18
238	11,23	14,98	14,98	8,93	11,63	12,00	11,16	5,57	12,20	7,18
239	12,02	15,56	15,56	14,23	11,62	10,01	17,17	8,91	13,28	8,29
240	12,02	7,98	7,98	14,99	11,63	8,03	21,69	7,24	11,21	6,06
241	26,13	27,22	27,22	21,80	22,27	9,02	23,95	23,17	28,02	10,52
242	2,94	2,15	2,15	0,60	3,64	11,01	3,63	5,11	1,64	6,06
243	5,74	5,65	5,65	4,38	10,30	12,98	5,14	8,38	4,44	16,79
244	9,23	6,81	6,81	8,93	10,30	3,09	4,36	8,38	6,08	3,76
245	16,59	12,64	12,64	19,50	11,62	10,01	16,41	10,58	15,68	21,99
246	16,60	15,56	15,56	19,51	11,63	10,02	16,43	21,51	15,69	14,71
247	9,07	13,81	13,81	10,44	11,63	9,02	11,91	10,59	9,63	22,00
248	8,80	13,81	13,81	19,51	11,63	10,02	7,39	10,59	9,86	14,71
249	7,89	8,56	8,56	8,92	11,62	17,93	11,15	13,11	6,83	17,30
250	10,25	10,32	10,32	8,17	11,63	17,93	18,69	13,12	8,47	17,31
251	7,90	8,56	8,56	8,93	11,93	17,93	11,16	-1,15	6,14	17,31
252	3,98	4,48	4,48	4,39	11,62	5,07	8,90	-1,15	3,80	16,26
253	3,01	4,48	4,48	4,39	3,64	5,07	7,39	-1,15	1,94	16,26
254	11,21	9,73	9,73	10,43	8,96	8,03	10,40	5,56	10,32	11,05
255	9,07	9,73	9,73	10,43	3,64	10,01	8,14	5,56	7,99	11,05
256	9,07	9,15	9,15	8,17	11,63	8,04	8,90	8,38	7,54	6,36
257	8,68	7,98	7,98	7,42	11,63	10,02	11,16	7,24	8,93	2,20
258	8,68	9,15	9,15	9,68	11,63	9,03	11,16	7,24	9,63	10,54
259	11,42	11,48	11,48	9,68	7,64	8,04	17,18	4,73	10,10	6,36
260	6,33	6,81	6,81	5,90	7,64	11,01	8,15	4,72	6,13	14,18
261	8,69	9,73	9,73	8,93	11,63	14,97	15,68	7,25	7,66	12,11
262	7,51	9,73	9,73	10,44	11,63	11,01	12,67	10,60	6,60	14,19
263	15,33	12,65	12,65	15,75	10,30	13,98	18,69	13,96	12,85	14,19
264	7,11	4,48	4,48	8,17	10,29	15,94	9,65	13,95	5,84	11,57
265	12,60	9,15	9,15	8,17	10,30	15,95	16,43	8,38	10,05	12,62
266	11,24	18,47	18,47	11,96	14,29	3,09	10,37	12,31	1,61	3,76
267	24,61	18,48	18,48	23,33	23,61	0,13	23,91	26,54	22,61	7,93
268	17,68	9,15	9,15	22,53	15,63	9,02	20,19	9,69	18,47	13,47
269	9,16	11,48	11,48	9,68	11,63	9,02	6,64	9,69	9,05	13,47
270	9,16	13,22	13,22	9,68	11,63	18,93	11,15	11,43	9,80	20,44
271	9,16	3,90	3,90	8,17	8,97	9,04	9,65	-2,83	9,43	13,14
272	8,27	7,98	7,98	8,92	8,97	2,10	11,16	5,56	7,92	2,71
273	17,67	6,22	6,22	16,48	15,62	9,01	19,43	14,27	16,58	10,54
274	14,04	10,89	10,89	13,45	8,96	9,02	18,68	15,62	12,06	12,61
275	14,55	12,65	12,65	13,46	15,63	24,86	18,63	18,15	14,25	26,45
276	11,94	14,40	14,40	13,46	15,62	22,91	16,38	6,41	12,38	26,45
277	13,42	14,98	14,98	12,70	15,62	22,91	16,37	18,15	12,61	26,45
278	13,42	5,64	5,64	11,19	14,29	24,88	14,87	18,15	11,21	16,27
279	13,05	5,64	5,64	10,43	14,29	24,88	15,62	16,46	11,91	28,78
280	13,05	5,64	5,64	14,20	14,29	24,85	18,62	13,61	11,91	28,78
281	16,03	7,98	7,98	14,96	15,62	24,85	16,37	17,30	16,57	26,44
282	7,45	9,14	9,14	8,92	6,30	22,90	8,86	7,72	9,11	26,44
283	7,46	10,31	10,31	8,93	6,31	24,88	6,61	6,42	6,32	26,45
284	16,50	21,39	21,39	11,94	15,62	22,90	12,62	6,40	15,40	26,44
285	11,59	11,47	11,47	11,94	15,61	22,90	14,86	11,65	13,07	26,44
286	25,27	13,22	13,22	11,94	24,93	22,90	14,86	6,40	24,64	26,44
287	26,21	23,15	23,15	22,52	24,95	24,86	31,40	26,07	26,12	27,22
288	11,21	23,14	23,14	28,55	15,62	24,88	13,37	11,66	22,86	28,78

129

Table A-2: User measurements from stereo image pairs

FID	SI1_USR1	SI1_USR2	SI1_USR3	SI1_USR4	SI1_USR5	SI1_USR6	SI1_USR7	SI1_USR8	SI1_USR9	SI1_USR10
289	25,98	24,58	24,58	23,95	26,38	26,29	32,83	27,50	27,55	28,65
290	26,32	14,27	24,18	23,55	25,98	25,92	28,68	23,38	27,15	29,82
291	12,68	2,16	2,16	15,73	14,30	24,89	14,13	9,76	11,69	27,23
292	11,82	2,14	2,14	12,71	8,96	4,07	14,87	11,43	12,61	3,75
293	9,16	4,48	4,48	5,91	8,97	1,12	8,15	13,12	9,35	2,20
294	6,49	9,14	9,14	8,17	8,97	11,00	10,40	8,08	7,65	13,14
295	9,30	9,13	9,33	9,69	8,97	9,21	9,48	9,18	9,39	9,00
296	12,26	10,89	10,89	13,47	8,97	6,06	10,40	8,08	12,84	13,14
297	5,61	3,90	3,90	3,62	8,97	8,03	1,37	8,08	1,66	8,45
298	11,38	10,90	10,90	7,42	8,97	9,03	11,91	8,92	11,68	12,10
299	11,38	10,90	10,90	14,99	8,97	8,03	10,40	8,92	10,75	8,45
300	10,60	6,23	6,23	12,71	8,96	9,02	11,90	8,91	9,81	9,49
301	13,22	6,23	6,23	12,71	8,96	7,05	14,17	13,95	13,07	4,28
302	11,82	12,64	12,64	12,72	8,97	7,05	14,13	13,95	12,15	8,45
303	7,46	4,48	4,48	9,68	10,30	24,89	6,62	5,57	6,78	2,19
304	12,05	6,23	6,23	11,19	8,97	18,91	11,12	8,92	11,91	2,19
305	12,05	6,23	6,23	11,19	8,96	18,91	14,13	17,30	14,71	2,19
306	12,05	7,98	7,98	9,69	8,97	18,92	12,63	17,31	12,12	24,09
307	7,08	6,81	6,81	7,41	6,30	24,88	9,61	8,92	7,71	27,22
308	11,56	13,23	13,23	11,20	6,31	24,89	11,87	8,92	10,98	27,23
309	7,22	13,23	13,23	8,93	7,64	24,89	13,37	8,92	6,78	2,19
310	11,56	12,64	12,64	8,93	8,97	18,91	12,62	8,92	10,97	2,19
311	11,56	4,48	4,48	11,19	8,96	18,91	11,12	7,24	9,79	13,14
312	10,64	3,31	3,31	-0,16	8,97	5,06	8,87	12,27	9,32	3,76
313	10,64	3,31	3,31	9,69	8,97	22,91	11,88	12,27	9,56	24,09
314	10,64	3,31	3,31	11,96	8,97	5,06	12,63	12,27	10,95	7,40
315	12,38	6,23	6,23	14,24	7,64	10,02	11,17	4,73	12,28	12,62
316	7,49	3,90	3,90	8,93	7,64	11,01	11,92	5,11	5,62	3,76
317	5,04	3,90	3,90	4,38	7,64	11,01	12,67	5,11	2,28	11,05
318	2,59	3,31	3,31	4,38	4,97	11,99	6,64	3,79	1,61	10,01
319	3,99	3,31	3,31	4,38	4,97	11,99	5,13	3,79	3,95	11,05
320	3,24	3,31	3,31	21,80	4,97	11,99	6,64	3,79	1,61	11,05
321	24,61	2,15	2,15	21,81	23,61	9,03	23,15	25,40	24,88	9,49
322	10,18	9,08	9,08	10,20	5,49	15,48	13,89	6,08	7,73	17,83
323	8,09	3,90	3,90	9,69	4,97	25,88	6,61	6,40	6,49	7,93
324	10,29	4,48	4,48	7,41	7,63	18,90	8,86	2,20	4,90	2,18
325	8,30	9,73	9,73	9,68	11,63	18,91	12,63	2,21	8,29	13,14
326	22,22	16,14	16,14	23,28	24,93	18,90	35,92	35,75	21,34	13,13
327	6,69	11,47	11,47	8,92	8,96	7,04	8,11	0,53	7,94	3,75
328	3,22	3,22	11,47	3,63	8,96	5,05	9,62	0,53	5,28	3,75
329	6,69	8,56	8,56	6,66	8,96	22,90	10,37	3,04	7,28	24,08
330	6,69	6,81	6,81	6,66	8,96	22,90	6,61	2,20	7,28	24,08
331	6,15	9,14	9,14	5,90	10,30	7,05	5,86	5,56	6,28	22,52
332	6,15	9,14	9,14	5,90	10,30	25,87	10,37	5,56	4,95	22,52
333	23,30	13,81	13,81	21,05	18,28	7,05	23,15	23,18	26,28	22,52
334	8,30	8,56	8,56	6,65	12,96	25,87	10,37	25,69	9,94	7,92
335	15,93	14,39	14,39	10,45	15,62	25,88	19,39	18,15	17,16	7,93
336	17,24	14,39	14,39	20,29	12,96	25,87	17,14	17,55	17,89	7,93
337	26,52	21,98	21,98	27,11	23,61	25,87	29,92	25,70	27,09	7,93
338	14,71	13,22	13,22	13,47	14,28	25,87	19,39	18,14	15,31	28,25
339	7,24	13,22	13,22	6,65	6,30	25,87	16,38	5,76	7,22	25,65
340	12,31	13,23	13,23	11,96	14,29	19,91	17,89	27,37	9,80	28,26
341	27,38	9,73	9,73	26,34	28,93	19,90	23,15	27,37	25,98	31,91
342	23,72	18,47	18,47	22,55	23,60	19,90	26,15	22,33	25,98	23,04
343	24,26	20,22	20,22	22,55	23,60	21,90	26,16	25,82	25,98	23,04
344	22,25	22,64	21,64	19,53	23,61	19,90	23,16	23,18	22,30	22,21
345	22,27	24,89	24,89	21,05	23,61	19,91	22,40	18,15	21,20	28,26
346	28,24	30,13	30,13	24,07	23,61	25,87	33,68	29,99	27,09	25,65
347	28,65	30,13	30,13	27,85	23,60	25,87	33,67	18,14	28,18	28,25
348	24,93	26,45	25,73	26,23	22,76	28,13	25,83	27,03	27,03	26,23
349	25,80	27,24	25,91	27,47	26,74	26,94	30,95	23,28	14,92	27,24
350	8,92	8,92	8,92	5,26	14,15	6,66	8,89	8,92	15,09	6,57

Table A-2: User measurements from stereo image pairs

FID	SI1_USR1	SI1_USR2	SI1_USR3	SI1_USR4	SI1_USR5	SI1_USR6	SI1_USR7	SI1_USR8	SI1_USR9	SI1_USR10
351	9,69	10,19	7,19	11,56	15,29	12,00	8,19	7,21	5,56	10,07
352	15,24	15,24	8,78	24,67	12,65	12,49	14,47	24,28	25,53	21,53
353	15,24	14,39	15,43	16,24	8,98	17,48	15,24	14,90	16,17	13,12
354	4,03	4,57	3,41	2,58	8,97	4,57	3,41	6,33	6,33	4,03
355	9,32	10,99	7,19	11,66	11,62	10,48	7,19	7,77	7,77	11,66
356	25,31	24,15	26,86	27,44	6,30	25,41	26,52	24,86	25,97	27,42
357	11,24	14,39	15,43	16,24	10,29	11,48	15,24	14,90	16,17	13,12
358	13,24	14,39	15,43	16,24	24,93	11,48	15,24	14,90	16,17	13,12
359	4,46	2,99	2,14	4,88	8,97	2,16	5,19	5,74	6,62	5,26

Table A-3: DSM segmentation statistical results

FID	MEAN	STD	DEM_ERR		FID	MEAN	STD	DEM_ERR
1	17,96	3,47	-0,34		181	16,83	3,62	8,72
2	21,53	6,81	2,14		182	18,94	1,28	-2,32
3	24,61	4,51	0,26		183	9,24	0,72	-0,24
4	7,29	2,94	2,38		184	8,10	1,92	-1,18
5	7,22	2,53	6,08		185	6,15	1,63	-2,80
6	26,41	1,84	-4,36		186	5,75	1,82	2,15
7	13,37	5,52	-6,39		187	8,14	0,64	3,16
8	13,74	2,52	-1,14		188	8,46	0,72	-1,09
9	22,97	2,79	3,26		189	5,56	1,15	3,72
10	23,34	2,52	3,14		190	7,24	1,47	6,19
11	21,74	1,52	4,16		191	12,37	1,10	-0,85
12	24,09	2,06	0,34		192	13,96	0,71	1,16
13	22,41	4,42	4,89		193	10,30	2,77	1,98
14	16,75	1,05	-3,47		194	15,48	1,20	-0,60
15	12,87	1,79	3,10		195	4,08	0,83	-1,65
16	15,93	0,87	0,04		196	7,27	1,62	1,91
17	9,33	0,75	-5,98		197	9,79	0,41	-0,54
18	12,35	1,66	0,33		198	12,04	0,95	-0,46
19	14,18	0,38	-1,95		199	14,90	1,10	-5,88
20	24,30	5,77	4,07		200	14,21	0,70	-1,84
21	13,28	1,70	-2,38		201	14,59	0,45	-2,84
22	9,55	0,95	-3,15		202	19,71	2,21	-4,24
23	14,73	1,58	0,89		203	19,37	5,29	5,71

Table A-3: DSM segmentation statistical results								
FID	MEAN	STD	DEM_ ERR		FID	MEAN	STD	DEM_ ERR
24	17,26	2,38	-0,58		204	24,01	2,60	0,79
25	12,32	3,79	3,91		205	23,12	2,92	0,51
26	9,07	0,63	-2,37		206	24,07	2,10	-0,57
27	8,62	1,02	-1,04		207	8,07	2,00	3,80
28	13,84	0,59	-1,27		208	8,07	1,27	1,80
29	13,88	0,46	-1,06		209	5,51	0,89	-1,76
30	9,80	2,95	3,43		210	7,68	2,03	1,97
31	13,52	0,52	-3,59		211	9,99	0,50	-1,21
32	11,04	0,53	-4,14		212	9,61	0,69	-0,49
33	12,14	1,17	-1,99		213	9,95	1,57	1,73
34	11,73	0,46	-1,28		214	11,43	1,48	0,42
35	13,01	1,49	-1,63		215	7,22	2,44	4,48
36	10,36	0,42	-0,29		216	11,78	0,69	1,09
37	10,38	1,10	-3,58		217	9,25	0,62	3,03
38	11,09	0,80	-3,76		218	7,74	0,82	-4,66
39	12,21	0,56	1,26		219	12,61	2,26	0,19
40	11,80	1,48	1,60		220	11,65	1,01	-2,17
41	9,75	1,29	-0,35		221	8,83	1,88	4,07
42	20,75	6,09	2,28		222	7,55	1,14	-1,30
43	14,03	2,07	-0,16		223	21,52	3,64	1,61
44	18,34	0,49	-2,46		224	10,57	1,36	-3,60
45	15,78	5,16	1,27		225	13,43	4,02	-6,38
46	17,59	1,81	-0,19		226	21,44	1,84	-1,24
47	11,54	2,58	-6,11		227	12,71	1,38	-0,31
48	24,41	1,85	-9,83		228	9,43	0,44	4,40
49	12,89	2,96	-4,59		229	11,19	0,68	-0,29
50	23,48	1,99	1,34		230	5,21	2,42	7,26
51	20,71	5,18	5,21		231	6,50	2,22	-0,55
52	23,83	3,80	1,55		232	11,86	0,68	0,66
53	4,32	0,85	2,78		233	8,24	0,74	-1,86
54	10,20	2,13	0,82		234	10,44	0,50	-0,76
55	7,15	2,49	1,48		235	12,48	1,05	0,69

	Table A-3: DSM segmentation statistical results							
FID	MEAN	STD	DEM_ ERR		FID	MEAN	STD	DEM_ ERR
56	5,76	0,84	0,51		236	11,19	0,54	0,29
57	4,08	0,63	0,49		237	12,33	1,03	-0,26
58	4,12	0,63	1,38		238	12,92	0,51	-0,07
59	4,50	0,49	-1,17		239	12,08	2,13	-0,48
60	20,55	5,67	6,87		240	19,32	4,25	-6,95
61	24,05	4,03	1,83		241	14,80	7,11	11,13
62	25,64	3,29	0,07		242	1,56	2,31	4,97
63	23,20	4,30	-5,93		243	4,92	1,11	0,35
64	17,95	1,56	-5,12		244	9,83	1,88	-2,26
65	26,70	3,89	-0,63		245	14,22	3,07	3,41
66	26,75	2,45	-1,63		246	16,64	2,46	2,06
67	22,83	2,46	3,44		247	9,26	0,69	0,12
68	24,10	2,68	-17,62		248	10,54	0,46	-0,52
69	18,90	3,20	0,67		249	9,81	0,88	-0,66
70	17,32	3,74	2,15		250	9,87	1,62	0,18
71	22,94	1,76	-13,29		251	5,43	1,18	1,19
72	16,04	3,74	-1,16		252	2,72	0,90	1,33
73	2,66	1,18	3,82		253	4,25	0,78	-0,93
74	4,65	0,73	1,98		254	9,44	0,54	1,38
75	3,91	0,41	-0,29		255	9,10	1,01	0,12
76	5,52	0,53	-0,70		256	8,91	0,86	0,32
77	7,07	2,07	0,23		257	9,65	0,62	0,52
78	11,21	1,53	1,36		258	8,20	1,79	1,37
79	10,04	1,32	2,48		259	6,85	1,99	4,98
80	7,58	1,12	2,57		260	0,67	0,84	5,60
81	5,80	0,71	3,57		261	9,73	1,30	-0,81
82	6,71	1,03	0,04		262	6,13	2,25	0,30
83	5,34	0,39	-0,87		263	10,65	1,42	1,55
84	6,25	0,50	-1,77		264	8,10	1,34	-1,58
85	12,52	1,18	3,38		265	8,23	2,19	2,00
86	7,84	1,00	-0,54		266	19,80	3,15	-9,27
87	11,80	0,45	-0,17		267	20,87	6,89	3,05

Table A-3: DSM segmentation statistical results								
FID	MEAN	STD	DEM_ ERR		FID	MEAN	STD	DEM_ ERR
88	13,15	0,45	-4,38		268	18,08	2,67	-0,38
89	11,83	2,44	1,62		269	10,69	0,44	-1,42
90	14,30	0,74	0,50		270	8,63	1,64	0,92
91	14,24	0,52	-0,99		271	6,65	1,96	2,70
92	10,80	3,58	2,02		272	5,91	2,73	3,32
93	12,34	1,05	-0,84		273	16,09	3,85	2,54
94	12,17	0,45	-1,19		274	7,08	2,56	7,00
95	11,12	2,02	-1,32		275	11,00	0,90	3,85
96	11,24	0,72	-1,91		276	10,54	1,56	-0,81
97	12,21	0,46	-2,13		277	8,80	1,74	3,37
98	13,35	0,45	-3,03		278	6,30	1,52	7,73
99	13,63	0,44	-0,06		279	3,34	1,40	9,28
100	12,81	1,05	0,34		280	2,92	1,41	9,56
101	9,70	1,39	-0,25		281	12,68	1,19	4,32
102	6,72	0,81	-0,79		282	8,62	0,88	-1,47
103	2,11	2,53	2,91		283	7,03	0,57	1,87
104	2,94	2,11	2,08		284	14,80	2,31	0,13
105	3,97	1,99	1,18		285	12,25	0,96	-1,28
106	5,60	1,48	1,10		286	24,97	3,31	1,05
107	6,14	0,44	-0,69		287	7,66	4,85	19,36
108	8,07	1,44	-1,84		288	15,58	4,05	-4,93
109	11,82	0,65	1,85		289	22,99	4,42	3,04
110	10,78	0,97	-5,61		290	26,05	1,08	-0,33
111	7,87	0,65	-0,02		291	7,37	2,37	4,66
112	9,20	1,00	0,72		292	10,36	1,67	2,09
113	13,92	1,58	-0,44		293	1,43	3,34	8,32
114	19,43	3,60	-12,61		294	5,45	2,33	1,10
115	12,96	2,90	-3,18		295	9,83	2,09	-0,83
116	9,37	1,50	-5,82		296	8,53	3,78	4,10
117	11,62	1,51	0,08		297	2,20	1,63	3,05
118	12,91	1,91	-3,51		298	12,79	0,31	-1,47
119	21,12	6,10	4,78		299	8,84	2,53	2,41

			Table A-3: DSM segmentation statistical results				
FID	**MEAN**	**STD**	**DEM_ ERR**		**FID**	**MEAN**	**STD**	**DEM_ ERR**
120	17,92	3,20	-4,07		300	12,36	0,33	-1,74
121	26,79	1,26	-1,46		301	11,15	2,55	1,32
122	23,67	2,85	-0,75		302	12,27	0,85	-0,09
123	24,80	3,11	-1,67		303	5,82	0,78	0,70
124	24,86	2,92	0,42		304	10,01	0,33	2,16
125	24,28	3,87	0,72		305	8,15	1,81	3,38
126	24,76	2,41	0,89		306	9,62	1,33	1,93
127	24,20	1,76	1,10		307	5,96	1,37	0,72
128	23,32	2,44	1,98		308	4,12	0,72	7,16
129	23,55	2,87	0,85		309	4,32	0,64	0,30
130	22,26	3,18	-5,04		310	5,57	1,24	4,01
131	22,78	1,52	-11,86		311	3,27	1,30	5,60
132	22,60	4,36	1,42		312	8,32	3,14	1,93
133	14,02	3,36	3,06		313	10,74	1,48	-0,61
134	10,61	0,54	-0,59		314	8,41	3,59	1,62
135	9,18	1,11	-3,11		315	6,40	1,33	5,50
136	10,74	0,57	-4,67		316	4,79	1,30	1,84
137	8,34	0,95	1,21		317	3,07	0,83	1,48
138	12,12	2,41	-2,29		318	17,36	2,60	-10,89
139	9,33	0,73	0,90		319	12,81	2,64	-9,18
140	12,41	2,04	-2,89		320	21,49	2,28	-17,57
141	10,39	0,82	-1,31		321	16,38	6,37	9,87
142	11,48	5,59	4,05		322	4,63	1,65	4,89
143	18,18	4,19	1,35		323	6,63	2,88	2,35
144	18,98	3,89	1,72		324	3,99	4,49	6,84
145	6,27	2,46	3,33		325	10,39	3,44	-1,66
146	4,49	1,52	5,28		326	22,75	3,24	0,42
147	7,09	1,85	2,51		327	16,03	4,71	-6,95
148	9,41	1,77	0,71		328	9,44	2,45	-3,24
149	7,73	2,54	2,79		329	2,97	1,70	2,71
150	13,52	1,98	-4,07		330	5,22	1,53	1,06
151	12,95	3,66	2,92		331	6,95	1,32	-0,98

Table A-3: DSM segmentation statistical results								
FID	MEAN	STD	DEM_ ERR		FID	MEAN	STD	DEM_ ERR
152	13,56	3,94	2,44		332	10,93	2,11	-5,05
153	10,68	2,15	-3,56		333	19,96	4,94	4,71
154	9,79	0,91	-3,31		334	13,66	2,09	-3,44
155	9,21	0,40	-0,93		335	16,97	1,00	-0,09
156	9,92	1,86	-0,74		336	12,81	4,00	4,06
157	10,21	0,79	-2,99		337	24,07	4,90	2,16
158	12,94	1,54	-1,09		338	13,68	3,02	1,02
159	7,81	1,48	1,77		339	9,66	2,37	-2,84
160	7,41	2,48	3,17		340	10,83	2,30	-1,11
161	10,62	1,73	-0,45		341	13,55	3,59	11,28
162	5,63	1,75	9,15		342	2,52	1,62	21,08
163	5,42	0,78	0,26		343	9,59	2,01	15,09
164	9,15	1,56	0,95		344	13,85	2,52	7,55
165	10,53	1,19	-3,68		345	16,54	8,40	7,44
166	11,72	0,64	1,38		346	16,25	8,67	9,57
167	8,70	2,17	-1,82		347	20,13	9,09	6,57
168	1,12	0,57	14,36		348	23,17	3,25	2,13
169	7,04	2,53	6,33		349	26,64	2,62	-1,04
170	12,71	1,34	-2,73		350	16,99	1,70	-8,06
171	23,56	4,27	2,89		351	4,50	2,95	4,88
172	18,29	2,06	-11,56		352	9,85	0,88	4,73
173	12,26	2,64	-2,59		353	8,57	0,80	5,60
174	9,35	2,74	1,00		354	1,96	1,05	1,46
175	3,49	1,05	7,11		355	12,55	2,35	-2,83
176	11,62	4,83	0,15		356	5,60	2,89	19,40
177	23,89	1,21	0,44		357	5,78	2,85	6,04
178	22,76	2,21	1,31		358	21,19	3,04	-7,72
179	22,31	5,27	1,34		359	2,00	1,13	2,20
180	27,18	1,80	0,24					

APPENDIX B

HISTOGRAM AND NORMAL DISTRIBUTION GRAPHS

Table B-1: Histogram graphs of users' error distribution

User ID	Histogram graph	Graph Comment
1	Std. Dev = 2,64 Mean = -,4 N = 359,00	The error is distributed symmetrically around the mean value; however, it is peaked at close to the mean values, which results in a higher Kurtosis.
2	Std. Dev = 3,57 Mean = -1,3 N = 359,00	The left tail is longer than the right tails; the mass of the distribution is concentrated on the right side of the figure, which is the reason for high value of Kurtosis.

Table B-1: Histogram graphs of users' error distribution
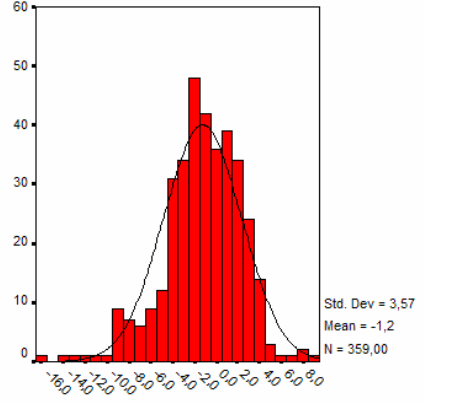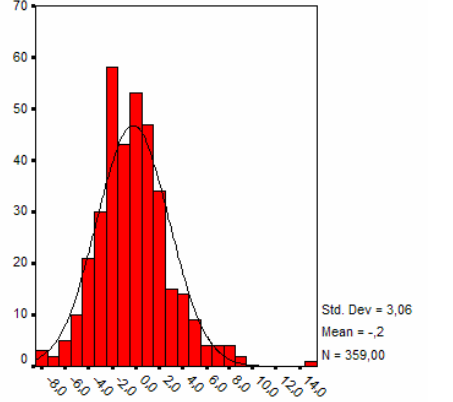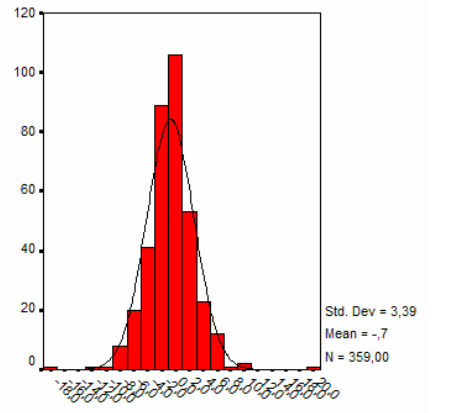
User ID	Histogram graph	Graph Comment
3	Std. Dev = 3,57 Mean = -1,2 N = 359,00	This figure is very similar to the previous one; the error is asymmetrically distributed around the mean, more towards the right side.
4	Std. Dev = 3,06 Mean = -,2 N = 359,00	The right tail is obviously longer than the left one, if the outliner were to be removed one would obtain better normal distribution graph.
5	Std. Dev = 3,39 Mean = -,7 N = 359,00	The error distribution of this user has the highest value of Kurtosis among all users. The Y-axis scaled up-to 120, whereas in all other graphs Y-Axis is either 60 or 70. The right tail of the distribution is longer that the left one.
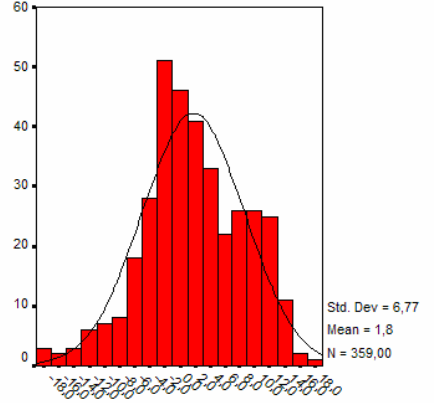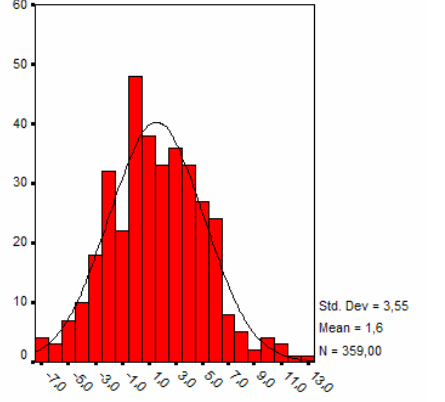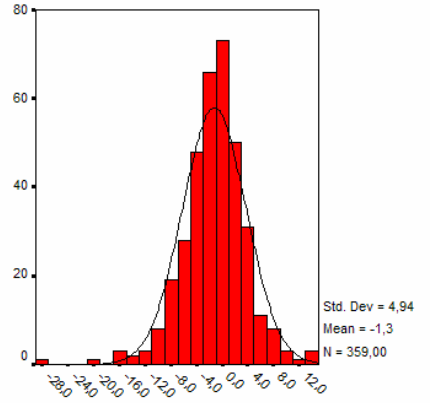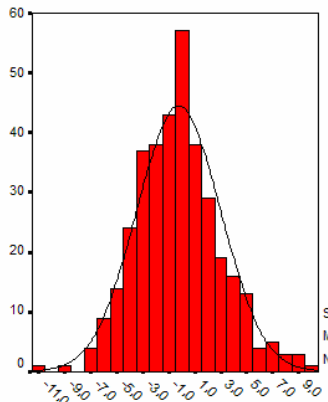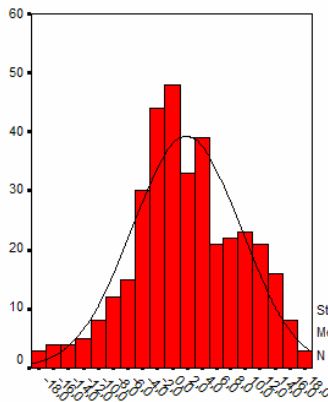
138

Table B-1: Histogram graphs of users' error distribution

User ID	Histogram graph	Graph Comment
6	Std. Dev = 6,77 Mean = 1,8 N = 359,00	The error distribution of this user is very similar to normal distribution. In fact all of the errors are between the +/- 3 Std Dev of the mean.
7	Std. Dev = 3,55 Mean = 1,6 N = 359,00	The error distribution of this user is very similar to normal distribution.
8	Std. Dev = 4,94 Mean = -1,3 N = 359,00	The tail to the left is a bit longer than to the right. If errors lower than -16.3 were to be removed, one would obtain a better-skewed graph. As similar to previous graphs, the distribution is peaked closer to the mean.

Table B-1: Histogram graphs of users' error distribution

User ID	Histogram graph	Graph Comment
9	Std. Dev = 3,22 Mean = -,3 N = 359,00	The left tail of the distribution is a bit longer than the right tail, and the distribution peaks around the mean.
10	Std. Dev = 7,29 Mean = 1,9 N = 359,00	The error distribution of this user is very similar to normal distribution

APPENDIX C

DESCRIPTIVE STATISTICS

Table C-1: User based descriptive statistics of the mean error

Users ID	N	Mean error	Error Std. Dev.	Variance	Standard Error	95 % Confidence limits	% 95 Confidence Length
1	359	-0,4475	1,305	1.703	0,069	(-0,582) - (-0,312)	0,270
2	359	0,4883	4,945	24.456	0,261	(-0,023) - (0,999)	1,023
3	359	0,4323	5,048	25.481	0,266	(-0,089) - (0,954)	1,044
4	359	-0,559	2,693	7.252	0,142	(-0,837) - (-0,280)	0,557
5	359	-2,759	9,24	85.381	0,488	(-3,714) - (-1,802)	1,912
6	359	-2,625	8,786	77.191	0,464	(-3,534) - (-1,716)	1,818
7	359	-2,421	3,960	15.684	0,209	(-2,830) - (-2,011)	0,819
8	359	0,459	5,248	27.535	0,277	(-0,083) - (1,001)	1,086
9	359	-0,613	3,013	9.078	0,159	(-0,924) - (-0,301)	0,623
10	359	-0,108	4,057	16.459	0,214	(-0,527) - (0,311)	0,839

Table C-2: Descriptive statistics of well-experienced users according to floor number

User ID		2	3	4	5	6	7	8	9	10
1	N Statistic	70	73	80	35	25	10	25	37	4
	Mean Statistic	-0,795	-0,441	-0,161	-0,452	-0,316	-1,945	-0,636	-0,088	0,583
	Std. Error	0,184	0,130	0,116	0,237	0,302	0,543	0,179	0,184	1,073
	Std. Deviation	1,538	1,107	1,033	1,402	1,508	1,717	0,893	1,119	2,146
	Variance	2,366	2,366	2,366	2,366	2,366	2,366	2,366	2,366	2,366
	Conf Limit	-0,794 ± 0,043	-0,440 ± 0,029	-0,160 ± 0,025	-0,452 ± 0,078	-0,316 ± 0,118	-1,945 ± 0,336	-0,636 ± 0,069	-0,087 ± 0,059	0,5825 ± 1,051
	Conf Length	0,086	0,059	0,051	0,157	0,236	0,673	0,140	0,119	2,104

Table C-3: Descriptive statistics of moderately experienced users according to floor number

User ID		2	3	4	5	6	7	8	9	10
2	N Statistic	70	73	80	35	25	10	25	37	4
	Mean Statistic	-1,823	-0,509	0,127	1,663	2,065	1,618	3,261	2,976	3,090
	Std. Error	0,421	0,458	0,457	0,744	1,088	2,063	1,104	1,201	1,859
	Std. Deviation	3,526	3,912	4,089	4,403	5,442	6,524	5,518	7,305	3,717
	Variance	12,429	15,304	16,718	19,385	29,616	42,563	30,452	53,365	13,820
	Conf Limit	-1,823 ± 0,098	-0,509 ± 0,105	0,1265 ± 0,100	1,6625 ± 0,246	2,0648 ± 0,426	1,618 ± 1,278	3,2612 ± 0,432	2,9759 ± 0,386	3,09 ± 1,821

Table C-3: Descriptive statistics of moderately experienced users according to floor number

User ID		2	3	4	5	6	7	8	9	10
	N Statistic	70	73	80	35	25	10	25	37	4
	Conf Length	0,197	0,210	0,200	0,493	0,853	2,557	0,865	0,774	3,643
3	Mean Statistic	-2,054	-0,524	0,003	2,133	1,968	1,965	3,261	2,691	3,090
	Std. Error	0,396	0,448	0,448	0,770	1,220	2,803	1,104	1,179	1,859
	Std. Deviation	3,313	3,825	4,005	4,556	6,100	8,864	5,518	7,171	3,717
	Variance	10,978	14,633	16,038	20,760	37,206	78,577	30,452	51,423	13,820
	Conf Limit	-2,053± 0,092	-0,523± 0,102	0,0029± 0,098	2,1331± 0,255	1,968± 0,478	1,965± 1,737	3,2612± 0,432	2,6905± 0,379	3,09± 1,821
	Conf Length	0,186	0,205	0,196	0,510	0,956	3,475	0,865	0,760	3,643
4	Mean Statistic	-1,473	-0,512	-0,199	-0,795	-0,619	-2,082	-0,851	0,480	0,998
	Std. Error	0,361	0,242	0,340	0,539	0,534	2,359	0,329	0,514	0,536
	Std. Deviation	3,024	2,065	3,039	3,189	2,668	7,458	1,643	3,126	1,072
	Variance	9,147	4,263	9,237	10,169	7,119	55,627	2,698	9,770	1,149
	Conf Limit	-1,472± 0,084	-0,511± 0,055	-0,199± 0,074	-0,795± 0,178	-0,619± 0,209	-2,082± 1,461	-0,851± 0,128	0,48± 0,165	0,9975± 0,525
	Conf Length	0,169	0,111	0,149	0,357	0,418	2,924	0,258	0,331	1,050
5										

Table C-3: Descriptive statistics of moderately experienced users according to floor number

User ID		2	3	4	5	6	7	8	9	10
	N Statistic	70	73	80	35	25	10	25	37	4
	Mean Statistic	-2,143	-0,944	0,642	1,161	1,256	-2,659	1,021	1,442	1,088
	Std. Error	0,292	0,481	0,320	0,794	0,667	2,151	1,173	0,648	3,140
	Std. Deviation	2,444	4,109	2,863	4,696	3,336	6,801	5,863	3,944	6,280
	Variance	5,972	16,883	8,196	22,054	11,128	46,254	34,379	15,552	39,436
	Conf Limit	-2,143±0,068	-0,943±0,110	0,642±0,070	1,1605±0,262	1,2564±0,261	-2,659±1,332	1,0212±0,459	1,4418±0,208	1,0875±3,077
	Conf Length	0,137	0,221	0,140	0,526	0,523	2,666	0,919	0,418	6,154
	Mean Statistic	-7,721	-4,181	-2,754	-6,765	-2,216	2,342	5,195	6,492	5,533
	Std. Error	0,867	0,814	0,754	1,317	1,661	3,908	1,614	1,345	3,472
6	Std. Deviation	7,251	6,953	6,748	7,791	8,306	12,358	8,071	8,180	6,944
	Variance	52,577	48,344	45,539	60,701	68,986	152,712	65,135	66,911	48,224
	Conf Limit	-7,720±0,203	-4,180±0,186	-2,754±0,165	-6,764±0,436	-2,215±0,651	2,342±2,422	5,1952±0,632	6,4924±0,433	5,5325±3,402
	Conf Length	0,406	0,373	0,331	0,873	1,302	4,844	1,265	0,867	6,805

Table C-4: Descriptive statistics of inexperienced users according to floor number

User ID		2	3	4	5	6	7	8	9	10
	N Statistic	70	73	80	35	25	10	25	37	4
7	Mean Statistic	-3,058	-2,351	-2,133	-2,810	-2,583	-3,374	-2,103	-1,788	0,663
	Std. Error	0,411	0,348	0,397	0,989	0,840	2,178	0,810	0,683	1,676
	Std. Deviation	3,435	2,971	3,552	5,852	4,199	6,888	4,049	4,154	3,351
	Variance	11,802	8,825	12,616	34,245	17,634	47,438	16,390	17,256	11,232
	Conf Limit	-3,057± 0,096	-2,350± 0,079	-2,133± 0,087	-2,81± 0,327	-2,583± 0,329	-3,374± 1,349	-2,103± 0,317	-1,787± 0,220	0,6625± 1,642
	Conf Length	0,192	0,160	0,174	0,655	0,658	2,700	0,635	0,440	3,284
8	Mean Statistic	-0,066	0,151	0,794	0,696	-0,559	-2,885	2,356	1,495	-0,210
	Std. Error	0,479	0,574	0,571	0,980	0,946	2,882	1,572	0,742	0,745
	Std. Deviation	4,011	4,907	5,104	5,795	4,731	9,113	7,859	4,515	1,490
	Variance	16,089	24,078	26,047	33,588	22,384	83,044	61,762	20,388	2,221
	Conf Limit	-0,066± 0,112	0,1510± 0,131	0,7936± 0,125	0,696± 0,324	-0,558± 0,370	-2,885± 1,786	2,3564± 0,616	1,4945± 0,239	-0,21± 0,730
	Conf Length	0,225	0,263	0,250	0,649	0,742	3,572	1,232	0,478	1,460
9										
	Mean Statistic	-0,530	-0,228	-0,244	-0,253	-1,423	-4,368	-0,905	-0,478	0,250

Table C-4: Descriptive statistics of inexperienced users according to floor number

		2	3	4	5	6	7	8	9	10
	Std. Error	0,270	0,262	0,248	0,556	0,645	1,944	0,445	0,412	0,523
	Std. Deviation	2,257	2,242	2,217	3,290	3,224	6,146	2,226	2,506	1,045
	Variance	5,094	5,026	4,916	10,823	10,394	37,776	4,957	6,281	1,093
	Conf Limit	-0,530± 0,063	-0,227± 0,060	-0,244± 0,054	-0,252± 0,184	-1,422± 0,252	-4,368± 1,204	-0,904± 0,174	-0,477± 0,132	0,25± 0,512
	Conf Length	0,126	0,120	0,109	0,368	0,506	2,409	0,349	0,266	1,024
10	Mean Statistic	-7,573	-4,250	-3,027	-7,973	-0,758	4,248	3,700	6,496	3,703
	Std. Error	0,907	0,883	0,915	1,215	1,599	3,195	1,848	1,488	4,805
	Std. Deviation	7,590	7,543	8,188	7,189	7,994	10,103	9,240	9,054	9,609
	Variance	57,614	56,893	67,043	51,675	63,901	102,075	85,383	81,970	92,335
	Conf Limit	-7,573± 0,212	-4,250± 0,202	-3,026± 0,200	-7,973± 0,402	-0,758± 0,626	4,248± 1,980	3,7± 0,724	6,4962± 0,479	3,7025± 4,708
	Conf Length	0,425	0,405	0,401	0,805	1,253	3,960	1,449	0,959	9,417

Table C-5: Mean error values of all methods according to number of floors

Methods		Number of Floors								
		2	**3**	**4**	**5**	**6**	**7**	**8**	**9**	**10**
Method 1		0.51	-0.13	0.13	-1.79	0.07	-0.57	-2.67	-4.28	
Method 2		-1.61	-0.54	1.04	1.43	0.41	-0.57	2.57	4.08	0.62
Method 3	**Advance**	-0.79	-0.44	-0.16	-0.45	-0.32	-1.95	-0.64	-0.09	0.58
	Moderately	-3.04	-1.33	-0.44	-0.52	0.49	0.24	2.38	2.82	2.76
	Inexperience	-2.81	-1.67	-1.15	-2.59	-1.33	-1.59	0.76	1.43	1.10

Table C-6: Standard error values of all methods according to number of floors

Methods		Number of Floors								
		2	**3**	**4**	**5**	**6**	**7**	**8**	**9**	**10**
Method 1		0.23	0.32	0.38	0.85	0.59	0.52	1.07	1.09	0.59
Method 2		0.48	0.44	0.32	0.86	0.63	2.13	0.99	0.90	0.90
Method 3	**Advance**	0.18	0.13	0.12	0.24	0.30	0.54	0.18	0.18	1.07
	Moderately	0.26	0.24	0.23	0.46	0.51	1.21	0.54	0.54	1.03
	Inexperience	0.33	0.30	0.30	0.56	0.53	1.36	0.68	0.53	1.22

Table C-7: 95% confidence lengths of all methods according to number of floors

Methods		Number of Floors								
		2	**3**	**4**	**5**	**6**	**7**	**8**	**9**	**10**
Method 1		0.91	1.25	1.48	3.34	2.31	2.04	4.18	4.26	2.29
Method 2		1.87	1.71	1.24	3.36	2.46	8.36	3.89	3.53	3.51
Method 3	**Advance**	0.72	0.51	0.45	0.93	1.18	2.13	0.70	0.72	4.21
	Moderately	1.02	0.96	0.88	1.80	2.00	4.76	2.10	2.10	4.04
	Inexperience	1.31	1.18	1.19	2.18	2.09	5.34	2.67	2.06	4.79